Addis Ababa Science and Technology University

College of Architecture and Civil Engineering

COMPARATIVE STUDY ON LOAD CARRYING CAPACITY OF UNDER REAMED AND FRICTION PILE USING FINITE ELEMENT BASED SOFTWARE:

CASE OF SELECTED SITE IN ADDIS ABABA

BY

Ephrem Feleke Haile

October, 2017

Addis Ababa, Ethiopia

Addis Ababa Science and Technology University

Addis Ababa, Ethiopia

Comparative study on load carrying capacity of Under-Reamed and Friction Pile using Finite Element Based Software:

Case of Selected Site in Addis Ababa

A thesis submitted to the department of civil engineering, College of Architecture and Civil Engineering in partial fulfilment of the requirement for the Degree in Master of Science in Civil Engineering (Major in Geotechnical Engineering)

BY

Ephrem Feleke Haile

Advisor: Dr Addis allem Zeleke

October, 2017

Addis Ababa, Ethiopia

ADDIS ABABA SCIENCE AND TECHNOLOGY UNIVERSITY

APPROVED BY BOARDS OF EXAMINERS

Approval Page

This MSc thesis entitled with ***''Comparative study on load carrying capacity of Under-Reamed and Friction Pile using Finite Element Based Software: Case of Selected Site in Addis Ababa''*** has been approved by the following examiners in partial fulfilment of the requirement for the Degree of Masters of Science in Geotechnical Engineering.

Date of Défense: October 4, 2017

Dr – Addis allem Zeleke	_____	_____
Advisor	***Signature***	***Date***
Dr – Mesay Daniel	_____	_____
Internal Examiner	***Signature***	***Date***
Dr – Argaw Asha	_____	_____
External Examiner	***Signature***	***Date***
Dr – Melaku Sisay	_____	_____
ERA PG Program Coordinator	***Signature***	***Date***
Dr – Brook Abate	_____	_____
Dean, Collage of Architecture & Civil Engineering	***Signature***	***Date***
Mr. Simon G/Egziabheer	_____	_____
Head, Civil Engineering Department	***Signature***	***Date***

DECLARATION

I hereby declare that all information in this document has been obtained and presented in accordance with academic rules and ethical conduct. I also declare that, as required by these rules and conduct, I have fully cited and referenced all material and results that are not original to this work.

EPHREM FELEKE HAILE

Addis Ababa Science and Technology University

October, 2017

ACKNOWLEDGMENT

The Achievement of this thesis has come through the overwhelming help of many people. I wish to express my sincere gratitude to all those who offered their kind cooperation and guidance throughout this thesis work.

Foremost, I would like to express my sincerely gratitude to my advisor Dr- Addis allem Zeleke for the continuous support on my research work. His guidance helped me in all the time of research and writing of this thesis.

I would also sincerely thank Mr. Yoseph Mebrehatu General Manager of May Real Estate Development plc. for his support to begin this study and for giving me all the motivation, enthusiasm and fatherly advice throughout my study period.

I wish to express my sincere thanks to Mr. Ephrem head of structural design department at MH consulting for providing me with the necessary data used in this study. I would also like to thank Mr. Lamesgen from Construction and Design S.Co. for providing me the necessary data and software for this research.

In addition, I, would Like to thank my lecturers at AASTU and Guest lecturers from other universities for their valuable guidance. You all definitely provide me with the tool that I need to choose and the right path I should follow to successful completion of this thesis.

Finally, my deep and sincere gratitude to my family for their love, help and support selflessly encouraging me and this journey would not have been possible if not for them, and I want to thank my friends and colleagues.

Thank You Very Much Every one!

Ephrem Feleke

ABSTRACT

Analysis and interaction of soil considering different pile foundation types and their comparative relationship is a study breach that leads to future uncertainty, thus research is essential to properly carry out the performance of those piles constructed nowadays. This implies the type of piles such as under-reamed and friction pile. When structures are erected on a soil stratum because of the applied load the interaction on load carrying capacity of pile and soil is important to understand whether the ground below the structure can take the load safely without causing any structural damage. In this research the interaction of pile and soil for specific site in Addis Ababa city located in front of stadium project of Wogagen bank share company was selected to compare load carrying capacity of under-reamed and friction pile. Finite element simulation provides as a valuable resource as it saves time and money; thus, it can be used at least for preliminary design of foundation to understand load carrying capacity and settlement of foundation. For carrying out elastoplastic analysis in this research geotechnical software called plaxis 3D foundation is used and this software applies finite element analysis method for simulation of the models. From the simulation displacement of the under-reamed and friction pile is used as a comparing parameter. The displacement of under-reamed and friction pile decreases as the diameter of the piles increases, which shows decreasing displacement behaviour of the piles is good for foundation. Comparing the simulated displacement output of the under-reamed pile of 600mm, 900mm and 1200mm diameter it shows greater displacement by 83%, 75% and 67% respectively than of the frictional piles of diameter 600mm, 900mm and 1200mm.

Key Words: Under-reamed pile, Friction pile, Finite element methods, Plaxis 3D Foundation, Displacement of pile, Load carrying capacity

TABLE OF CONTENTS

LIST OF FIGURE

LIST OF TABLE

LIST OF ANNEX

LIST OF SYMBOLS AND ABRIVATIONS

BH	:	Bore Hole
C	:	Cohesion
CN	:	Adjustment for Overburden Pressure
E	:	Young's Modulus
fc	:	Compressive Strength of Concrete
FEM	:	Finite Element Methods
f_i	:	Yield Function
FP	:	Friction Pile
g_i	:	Plastic Potential Function
GWT	:	Ground Water Table
K_O	:	Initial Stress Coefficient
LL	:	Liquid Limit
N	:	Vertical Load
Ø	:	Internal Friction Angle
P	:	Isotropic Stress or Mean Stress
PI	:	Plastic Index
PL	:	Plastic Limit
q	:	Deviatoric Stress or Equivalent Shear Stress
SPT	:	Standard Penetration Test
URP	:	Under-Reamed Pile
U_Y	:	Vertical Displacement
γ	:	Unit Weight
ε	:	Strain
σ	:	Stress
τ	:	Shear Stress
υ	:	Poisson’s Ratio
ψ	:	Dilatancy Angle
SPI	:	Soil Pile Interaction
FEA		Finite Element Analysis
H	:	Height of Pile

CHAPTER 1. INTRODUCTION

1.1.Background

The capital city of Ethiopia the seat of African Union Addis Ababa is currently constructing houses, condominium, high rise buildings, transport and another infrastructure that is revolutionizing the city. Land prices are rising as the infrastructure of the city expands. Thus, land for development purpose is becoming shortage that leads to demolishing works on the heart of the capital city to rebuild infrastructures replacing existing with new ones. Following proposals of high rise buildings, railway infrastructures, real estate developments and commercial buildings; areas where soils are poor and incompetent are becoming an alternative used for infrastructural developments. The challenges in poor and incompetent soil sites in the aspects of geotechnical engineering is on getting authentic data and studies for designing of foundation. Geotechnical engineers are in great need to have knowledge about behaviours of soil corresponding to different pile foundation systems. Pile constitute a common foundation solution for tall buildings or special structures such as bridges, Wind turbine and liquid storage tanks resting on soil layers of low stiffness and strength. In this research, attempt was made to compare the load carrying capacity of under reamed pile and friction pile on selected area by collecting some data on engineering properties of the selected sites. This research answers questions related to application of finite element models to determine load carrying capacity of under reamed and friction pile with geotechnical behaviour of given soil parameters. The research also used plaxis 3d foundation, that bases finite element programming language to simulate load carrying capacity of under reamed and friction pile.

1.2. Statement of Problem

There are several characteristics of tall buildings that can have a significant influence on foundation design. The building weight, and thus the vertical load to be supported by the foundation, can be substantial. Moreover, the building weight increases non-linearly with height, and so both ultimate bearing capacity and settlement need to be considered carefully (Poulos, 2015).

Pile constitutes a common foundation solution for tall building structures and other infrastructures that is built on incompetent and poor soil ground thus it is used nowadays for foundation construction of different projects in Addis Ababa city. The Studies on interaction of soil considering different pile foundation systems and their comparative relationships is important to understand the performance of those piles that are constructed nowadays. This implies the type of piles such as under-reamed and friction pile which are one of the possibility; thus, studies are needed to the design of such foundation types in Addis Ababa.

According to Zeleke, (2015) in different projects, determination of load carrying capacities of piles usually performed using in-situ loading tests thus, the cost of running this tests and the time it takes is one of the difficulties. So, in this thesis the possibility of applying a finite element model that's widely accepted science to simulate pile load carrying capacities is applied.

1.3. Scope of The Study

To achieve the research objectives, required data were collected from a project in Addis Ababa. The data is collected from soil investigation and design reports of Wogagen S.C. project and some data are obtained using correlation techniques.

The load on piles is vertical and its used to simulate pile soil interaction using finite element model for under reamed and friction pile to compare load carrying capacity. The output and finding of this study is applicable for particular studied area projects and other similar soil conditions in the country.

1.4. Objective

1.4.1. General Objective

The main objective of this study is to analyse, determine and compare load carrying capacity of under-reamed and friction pile.

1.4.2. Specific Objective

- Analyze load carrying capacity of under reamed pile and friction pile using PLAXIS 3D FOUNATION which basis its analysis on FEM for different depth and diameter of piles based on soil parameters collected from selected site.
- Compare load carrying capacity of under reamed pile and friction pile for different depth and diameter.
- Show the possibility of application of finite element method to determine load carrying capacity of under reamed pile and friction pile.

1.5. Significance of the Study

Pile foundation is one of the common deep foundation techniques that are used in soft soil strata to support the super structural loads without any detrimental settlement and bearing capacity failures. To determine load carrying capacities of the under reamed and friction pile, loading tests are usually performed in different projects. However, the cost of running this tests and the time it takes is one of the difficulties that engineers faced in current geotechnical practices. So, in this study the possibility of applying a finite element model to simulate those pile load carrying capacities to compare to each other by use of this model and output; as one alternative for determining pile capacities, at least for preliminary design purposes is considered.

1.6. Application of this Study

Application of this study is for pile foundation structures; hence the use of pile foundation is increasing day to day for construction of multi-story buildings and other infrastructures in order to use the land in the city properly. Heavy multi story buildings, wind turbine towers, railway structures are being constructed and load from these structures cannot be directly transferred to the ground it needs a safe foundation system and one of this system is using foundation types like friction and under-reamed pile. So, the study in this part will be applicable for such structures and can be used as an instance to apply the FEM and compare the different pile foundation types for different projects in our country in order to choose safe type of foundation type.

1.7. Thesis Outline

1.7.1. What is on this thesis

The thesis is organized in to six chapters. Chapter one of the study includes background, objective and scope of the study in addition it shows the conceptual frame work to elaborate the work that is conducted in a flow chart form. The background describes general ideas about the need for this study and the pile foundation systems that is compared using FEM. The objective describes the general goals of the study and what to expect at the end of the study. The scope and limitation of the study describes the range of the study and applicability of the study.

The second chapter is focused on literature survey and findings by other authors on the relative study areas. It addresses the general overview about the geotechnical engineering and its findings on the friction pile and under-reamed pile. It also shows the finite element method is a leading science that's is used now a day to solve geotechnical problems by reducing time and money.

Chapter three describes the materials and methods in a logical order including procedures shown in a flow chart form.

The selected site and its geotechnical parameters are thoroughly discussed in chapter four. It includes the numerical presentation on the soil parameters depending on the soil investigation report. It also shows the correlation of parameters which are not found directly in the report.

The fifth chapter discuss on the formulation of fundamental stress, strain, and Mohr coulomb model. It also shows the modelling and analysis of the soil and pile in PLAXIS 3D foundation by applying basic finite elements methods.

Sixth chapter deals with the result and discussions. Comparative study on friction and under-reamed pile using the graphical representations.

The final and seventh chapter summarize the findings in concluding statement and recommendation.

1.7.2. Conceptual Frame Work

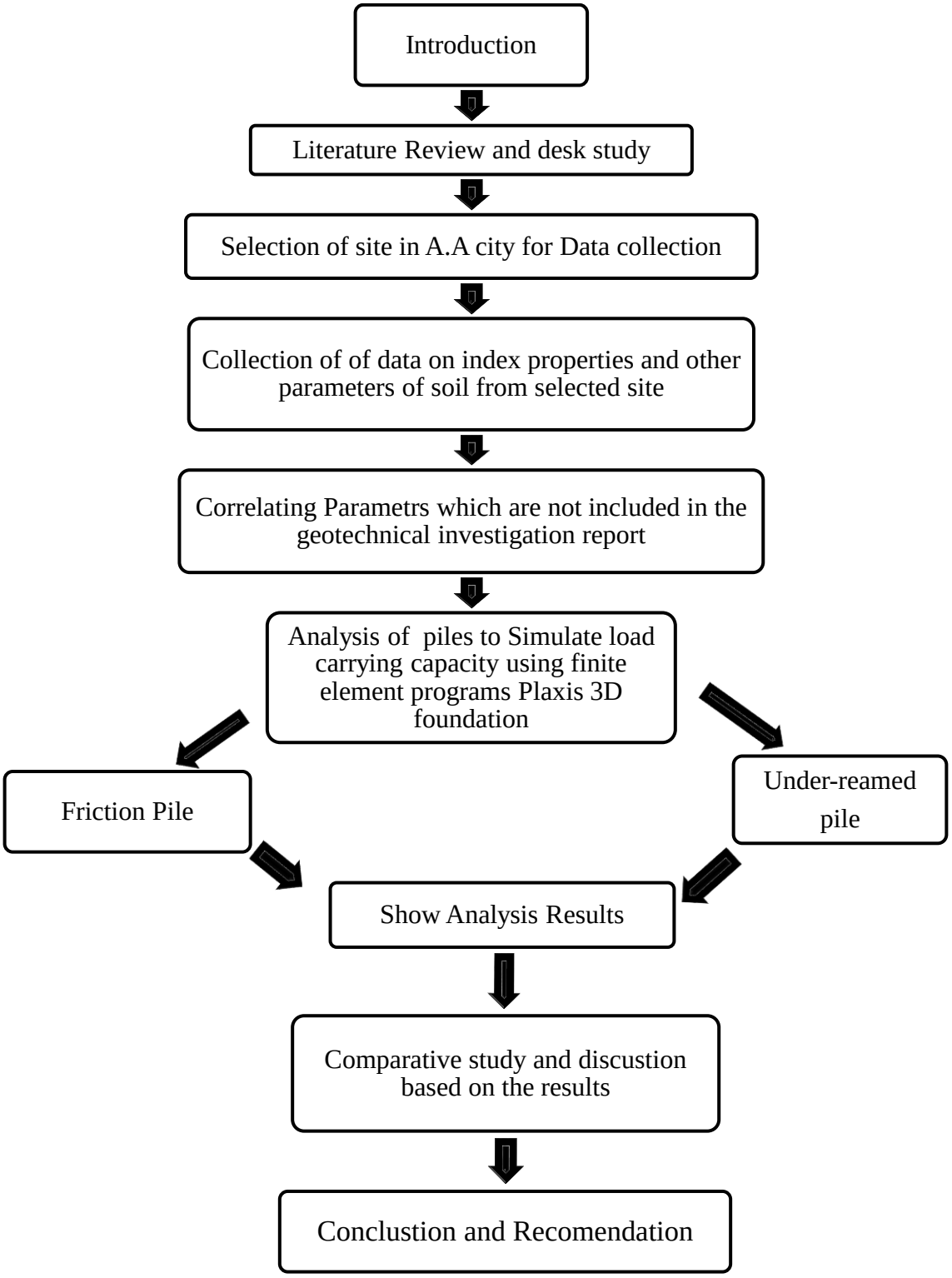

CHAPTER 2. LITERATURE REVIEW

2.1. General

Soil–pile interaction plays an important role in the analysis and design of foundations and structures. Geotechnical engineers have recognized this role, and many studies have focused on several aspects of the topic in the past four decades. As the third millennium begins, geotechnical engineers are challenged to provide more reliable and efficient foundation solutions to support larger, heavier, and more complicated structures. SPI must be thoroughly understood to properly address the issues that arise when designing foundations to meet these challenges (Hesham & Naggar, 2002).

Foundation is the lowest load-bearing part of engineering structures such as buildings and dams, typically below ground level.

Pile foundations are often used in weaker soil to transfer the loads of superstructures to underlying ground, aiming to increase the bearing capacity or lessen the settlement of infrastructures. However, the load transfer mechanism and failure mode of pile foundations are very complex and not fully understood yet (Johnson, 2006). There are two usual approaches to the calculation of ultimate load carrying capacities of pile: the “Static” approach, which uses the normal soil-mechanics method to calculate the load capacity from measured soil properties; and the “Dynamic” approach, which estimates the load capacity of driven piles from analysis of pile driving data (Poulos, 1980).

The bearing capacity of isolated piles may be determined from one of the following methods:

- Loading Test
- Prevailing building codes
- Sounding test
- Dynamic pile-driving formulas
- Analytical methods

Recently, with the rapid development of computational technology, numerical analysis involving finite element method (FEM) is widely used to understand the behaviour of pile soil interactions. The advantage of numerical analysis methods lies in their ability to address complex soil formations and the interaction between soil and structures (Zeleke, 2015).

2.2. Behaviour of Soil

The nature of soils is different from materials such as steel or concrete, where the mechanical behaviour can be considered linear if the deformations are not too large. The mechanical properties of soils are often strongly non-linear, with irreversible plastic deformations during loading and unloading. Additionally, soils usually show anisotropic behaviour, creep and dilatancy, where the latter is a volume change during shear, as stated in (Verruijt, 2012).

Because of the inhomogeneous structure of soils, the mechanical behaviour is hard to predict. Assuming a linear or piece-wise linear response can only give an approximate response and a constitutive model for the inelastic behaviour is generally needed (Desai & Zaman, 2013).

To further complicate the behaviour of soils, there may exist water in the pores, giving rise to a pore water pressure within the soil. A special property of soils is that the stiffness and strength of the soil increases when subjected to compressive stresses. This is due to the fact that when compressed, the forces between the individual soil particles increase, which in turn leads to an increased strength, (Helwany, 2007).

In shear, however, soils become softer. If the shear stresses reach a certain level, failure will occur and soils generally fail in shear, as stated in (Craig, 2004). For example, a sand pile cannot have a slope larger than about 35^0 and at greater slopes the particles would slide over each other, and failure occurs. This is a typical failure mechanism that has occurred all over the world, as mentioned in (Verruijt, 2012). A steep slope is possible for fine soils, such as clay, for a limited period of time. When a soil is subjected to shear, a volume change usually occurs, called dilatancy. For example, very loose sand has a tendency to contract during shear whereas dense sand undergoes a volume expansion. This is due to the fact that the particles shear over each other. Fine soils with small grain sizes such as clay, show little or none dilatancy (Craig, 2004).

Creep is another phenomenon of interest when studying soils, which means that the deformations are dependent upon time. Clay is a soil type which is particularly influenced by creep and this must be taken into account when, for example, predicting the settlement of a building over a period of time. If the settlement is not uniform, the building may be damaged.

In analyses of soil stresses, a common approach is to divide the stress into an effective stress and a pore pressure, meaning that the total stress is the sum of the two quantities. However, this applies only to the normal stresses, as the pores are not able to transfer shear stresses, as stated in (Verruijt, 2012). It cannot be stressed enough that soil is a natural material created by various geological processes. Therefore the mechanical properties can be hard to predict via desk studies as the complete geological history is often unknown. For an accurate prediction of the mechanical behaviour of a certain soil, the engineer should resort to laboratory or field testing (Craig, 2004).

A great deal of residential and office buildings are located in the eastern and southern part of Addis Ababa, where expansive soils are predominant. These soils are either black or grey in colour with thickness ranging from few centimetres to several meters. It is a common occurrence that structures which foundations are not adequately designed to withstand the stresses and strains caused by alternate heaving and shrinkage of the foundation soil crack. Cracks do not only affect the structural safety and aesthetics of the buildings but also bring about additional financial burden to owners for repair, if the structure is to be salvaged at all (Alemayehu & Solomon, 1986). Expansive soils are found in fine-grained cohesive soils such as clay and shale. Clays come in several different groups that are categorized by their mineral makeup. Expansive soils are associated with the clay group smectite. The smectite particles are thin sheets with a very high specific surface (surface area per unit mass) and a negative charge. The combination of the high specific surfaces and negative charges lead to significant interaction between the clay particles and ions in water, causing great volumetric change when water is added or removed (Millot, 1979)and (Michell, 2001).

2.2.1. Material Parameters

Because of the complex behaviour of soils under loading, the applicability range of a certain parameter is restricted to a limited set of problems. To find a soil's properties, nothing can beat experimental results, either in situ or in the laboratory, as mentioned in (Craig, 2004). Subsequently, in engineering practice the determination of soil parameters are of vital importance for accurate soil modelling.

Some geotechnical parameters to be used in this study are reviewed below.

- **Atterberg Limit**

The Swedish soil scientist A. Atterberg (1911) developed a method for describing quantitatively the effect of varying water content on the consistency of fine-grained soils like clays and silts (Lymon, et al., 2006). When a clayey soil is mixed with an excessive amount of water, it may flow like a semi liquid. If the soil is gradually dried it will behave like a plastic, semisolid, or solid material, depending on its moisture content, in percent at which the soil changes from a liquid limit to a plastic state is defined as the liquid limit (LL). Similarly, the moisture content, in percent at which the soil changes from a semisolid state to a solid state are defined as the plastic limit (PL) this limits are referred to as Atterberg Limit (Braja, 2007).

- **Ground Water Table**

The water table is the elevation in the soil profile at which water will exist in an open excavation or borehole, given sufficient time for steady-state conditions to be reached. The presence of the water table is of interest to the foundation designer for two principal reasons. Firstly, the position of the water table is needed to establish the profile of effective stress in the soil versus depth. Secondly, the depth of the water table determines the depths below which special procedures must be used to control the groundwater during construction (Lymon, *et al*., 2006).

- **Shear strength parameters (C and Ø)**

The shear strength of soil or rocks is the most important soil and rock property used by the foundation designer. The foundation designer will often base the selection of the foundation type on the shear strength and use the values for shear strength in computations of axial and lateral capacity of the foundation. Typically, the shear strength of cohesive and cohesionless soils is expressed using the Mohr Coulomb shearing parameters. Any implementation of the Mohr-Coulomb shearing parameters or any of the advanced models for shearing parameters will utilize the value of effective stress. Thus, the position of the water table must be known for their application (Lymon, *et al*., 2006).

- **Poisson’s ratio(ν)**

Poisson's ratio is a measure of the Poisson effect, the phenomenon in which a material tends to expand in directions perpendicular to the direction of compression. Conversely, if the material is stretched rather than compressed, it usually tends to contract in the directions transverse to the direction of stretching. The Poisson's ratio of a stable, isotropic, linear elastic material will be greater than −1.0 or less than 0.5 because of the requirement for

Young's modulus, the Shear modulus and Bulk modulus to have positive values (Gercek & H., 2007).

- **Young's modulus (Es)**

Hooke's generalized stress-strain law is commonly used in solving geotechnical problems of stress and settlement. The use of a practical and reasonable stiffness values representing the in-situ conditions is of great importance in finite element analysis for better simulation of the actual condition of the soil. Several methods are available for estimating the stiffness modulus of a soil as described by (Bowles, 1997). Unconfined compression tests, tri-axial compression tests and in situ tests are among the test methods. While unconfined compression tests tend to give conservative values, tri-axial tests tend to produce more usable values of E_s since any confining stress "stiffens" the soil so that a larger initial tangent modulus is obtained.

2.3. Under-Reamed Pile

According to Indian code of standards Under-reamed piles are of bored cast in situ and bored compaction concrete types having one or more bulbs formed by suitably enlarging the borehole for the pile stem. With the provision of bulb(s), substantial bearing or anchorage is available. These piles find application in widely varying situations in different types of soils where foundations are required to be taken down to a certain depth in view of considerations like the need

- to avoid the undesirable effect of seasonal moisture changes as in expansive soils
- to reach firm strata;
- to obtain adequate capacity for downward, upward and lateral loads and moments;
- to take the foundations below scour level (Anon., 1981).

(Gupta & Sundaram, 1986) states in a study on clayey and silty soils found when soil moisture around the bulb is near the liquid limit, the force causing failure in the pile is enough lower than calculated quantities and it's because of soil resistance reduction around the bulb and thus tension disordering in this zone. (Zahra, *et al.*, 2013), states numerically studies on tensile bearing capacity of under-reamed pile using finite element method and results was shown that under-reamed piles have a greater bearing capacity comparing to normal piles with uniform stem with the same volume and length.

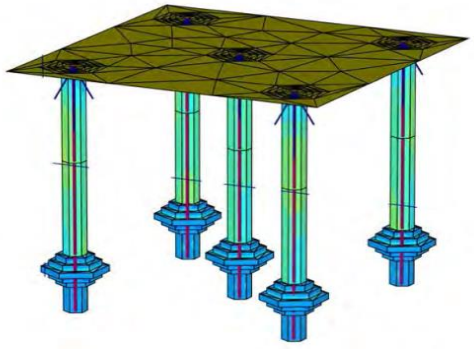

Figure 2.1 Shading views of stress values for Square and Triangle arrangements, generated by PLAXIS 3D Foundation software (Hamid, *et al.*, 2014)

Plaxis 3d Foundation has no option to model an under-reamed pile, so it should be considered in different layers to model under reamed pile which has bulb as per (Hamid, *et al.*, 2014).

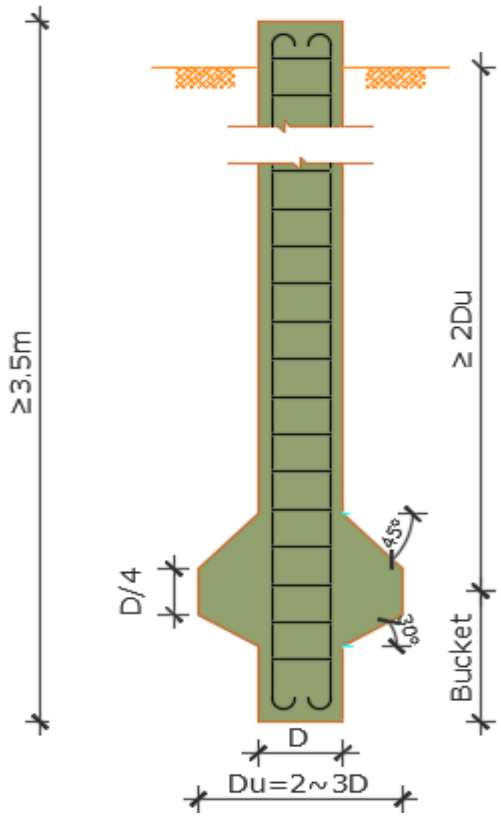

D(cm)	Bucket
20	40 ± 5
25	40 ± 5
30	45 ± 5
37.5	50 ± 5
40	55 ± 5
45	65 ± 5
50	70 ± 5

Figure 2.2 Schematic section of single under-reamed pile (Meymand , 1998)

(Bale & Hari, 2015) have studied under reamed piles load carrying capacity using numerical investigation. In the research the load carrying of different diameter piles were studied. Comparing the results, load carrying of 0.5m diameter under reamed pile is 76% greater than 0.3m diameter under reamed pile in state of compression. It shows that when the diameter

of the under reamed pile increases the load carrying capacity increases but the volume of the concrete used is increased.

2.4.Friction Pile

According to Braja, (2007) when no layer of rock or rocklike material is present at a reasonable depth at a site, point bearing piles become very long and uneconomical. In this type of subsoil, piles are driven through the softer material to specified depths. These piles are called friction piles, because most of their resistance is derived from skin friction. In clayey soils, the resistance to applied load is also caused by adhesion.

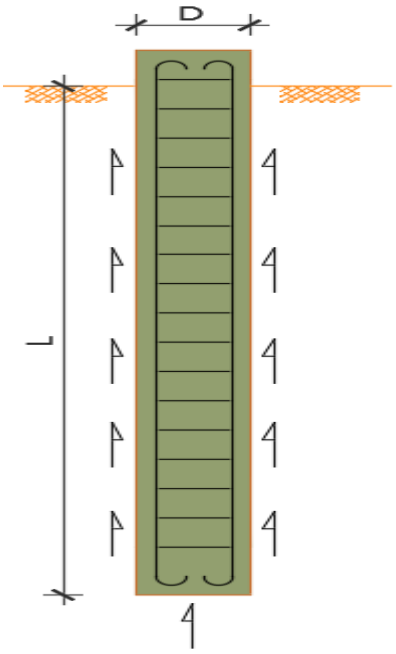

Figure 2.3 Schematic section of considerations for single Friction pile

The study using finite element investigation of the interaction between a pile and a soft soil by (Pablo, *et al*., 2016) shows in Figure 2.4 analytical and field results that represents measured settlement at 315 days after loading and a Plaxis output. It shows that the Plaxis result is near to that of the field results and the settlement decreases with respect to depth.

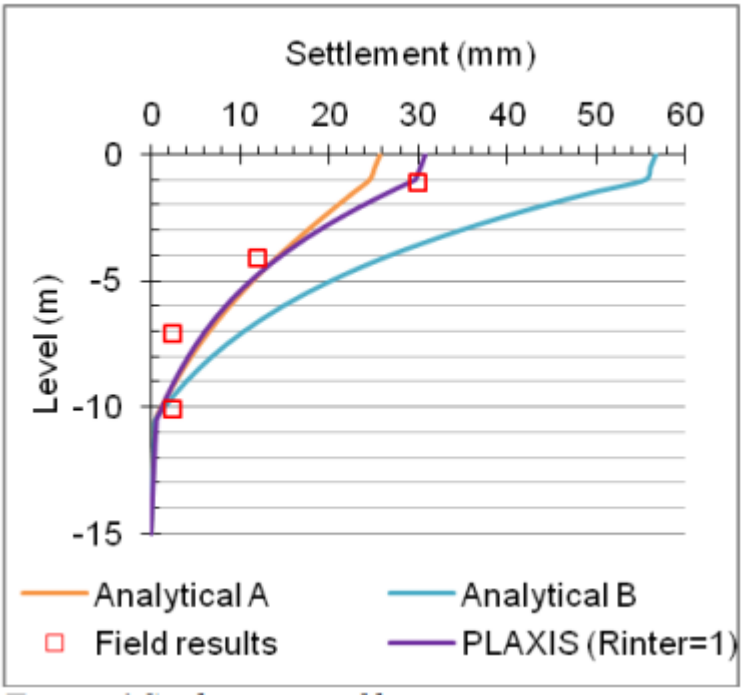

Figure 2.4 Settlement profile (Pablo, *et al.*, 2016)

2.5. Pile Capacity

Several methods for determining pile capacity have been summarized. Static testing, if performed until failure, is an ideal way to assess a pile's ultimate static bearing capacity. It is, however, very expensive, time consuming, and in certain instances, physically impossible to perform. These conditions limit the number of test piles to just a few (Meymand , 1998). Axial load capacities of piles vary from one method of calculation to another. Per (Ergys, *et al.*, 2014) study using SPT based calculation of the Japanese design law the result of load carrying capacity vary from 500 to 4010 KN. From this data, the axial load to be applied on piles can be chosen referring to the graph below.

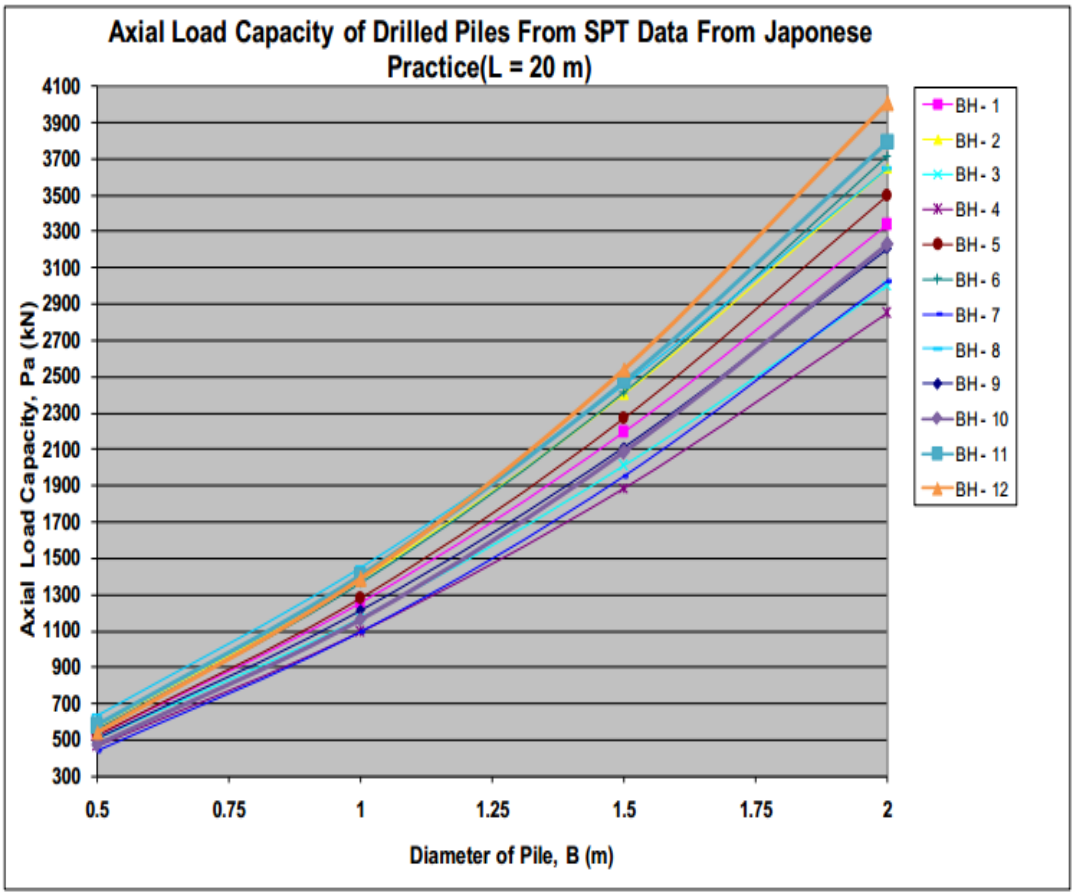

Figure 2.5 Axial load capacity of cast in place piles by SPT and based calculation methods (Ergys, *et al*., 2014).

2.6.Soil Pile Interaction Using FEM

In the case of piles, given the strong stress coupling of the foundation with the surrounding soil and the associated high-energy dissipation, the effect of soil compliance may lead to substantially different structural designs as compared to the case of rigid supports. For this reason, several numerical and analytical methods have been proposed for the analysis of soil-pile-structure systems based on simplified interaction models such as the Beam on Dynamic Winkler Foundation approach, as well as more rigorous FEM formulations (Rovithis, 2008). Finite element is used to model the soil and foundation. The soil and the piles are represented by first-order solid finite-elements of hexahedron (brick) and triangular prism (wedge) shape. The plaxis software is a one of the software used now a day and as per (Simeneh , 2009) plaxis gives different outputs per the requirements of the user. Among the major outputs, deformations, stresses, strains, forces, etc. can be included. In relation to this work, deformations are the main concern. The plaxis 3d foundation software output can be in contour plot and used to show output results.

The load carrying capacity of a pile foundation system is usually performed using loading test but due to recent development of finite element analysis, researchers are studying the behaviour of piles by using those methods. The researches done shows studies for one type of pile foundation system on a selected area soil stratum. Therefore, the goals of this research are to compare load carrying capacity of two types of pile foundation system namely under-reamed and friction pile on selected site area in Addis Ababa city by using the finite element analysis methods

CHAPTER 3. MATERIALS AND METHODS

Accomplishment of the research required the review of applicable practices, research findings and data on soil parameters of selected site in Addis Ababa that is used for analysis of pile soil interaction and compare the load carrying capacity of under reamed pile and friction pile using FEM based software.

3.1.Study Area

From geotechnical investigation firm, data is collected on soil parameter of a purposely selected site in Addis Ababa city. In this research the data of soil parameter is collected from a site located in front of stadium and the name of the site project is Wogagen Bank Share Company. Some of the soil the parameters which are not included in the soil investigation report are correlated using different practices and used in the model.

3.2.Finite Element Methods (FEM)

The finite element method is a numerical method for solving problems in engineering and mathematical physics. The formulation of the problem results in a system of algebraic equations. The method yields approximate values of unknowns at discrete number of points over the domain. To solve the problem, it subdivides a large problem into smaller, simpler parts that are called finite elements. The simple equations that model this finite element are then assembled into large system equation that models the entire problem then uses variation methods from calculus to approximate a solution by minimizing error function. This makes it possible to be applied in engineering analysis. Finite element simulations provide a valuable resource as they remove multiple expensive creation and testing of geotechnical problems in-situ (Daryl , 2011) and (Reddy, 2006).

For carrying out elastoplastic analysis in this research, geotechnical software PLAXIS 3D Foundation is used which applies Finite Element Analysis (FEA) for simulation of model.

3.3.PLAXIS 3D Foundation

Plaxis 3d foundation is a three-dimensional finite element program, developed for the analysis of foundation constructions including pile foundations. Foundations form the interaction between an upper structure and the soil. Settlements depend on local soil conditions and on the construction method, especially for pile foundations there is an important interplay between the pile and the soil to support the forces from the upper structure.

In this interaction deformations are a key factor thus, such a situation can only be analysed effectively by means of three-dimensional finite element calculations in which proper models are incorporated to simulate soil behaviour and soil-structure interaction (Brinkgreve & Broere, 2006).

- **Method used for Simulation and Analysis of Piles in PLAXIS 3D Foundation**

The procedure for simulating models in PLAXIS 3D foundation is explained in a flow chart shown below.

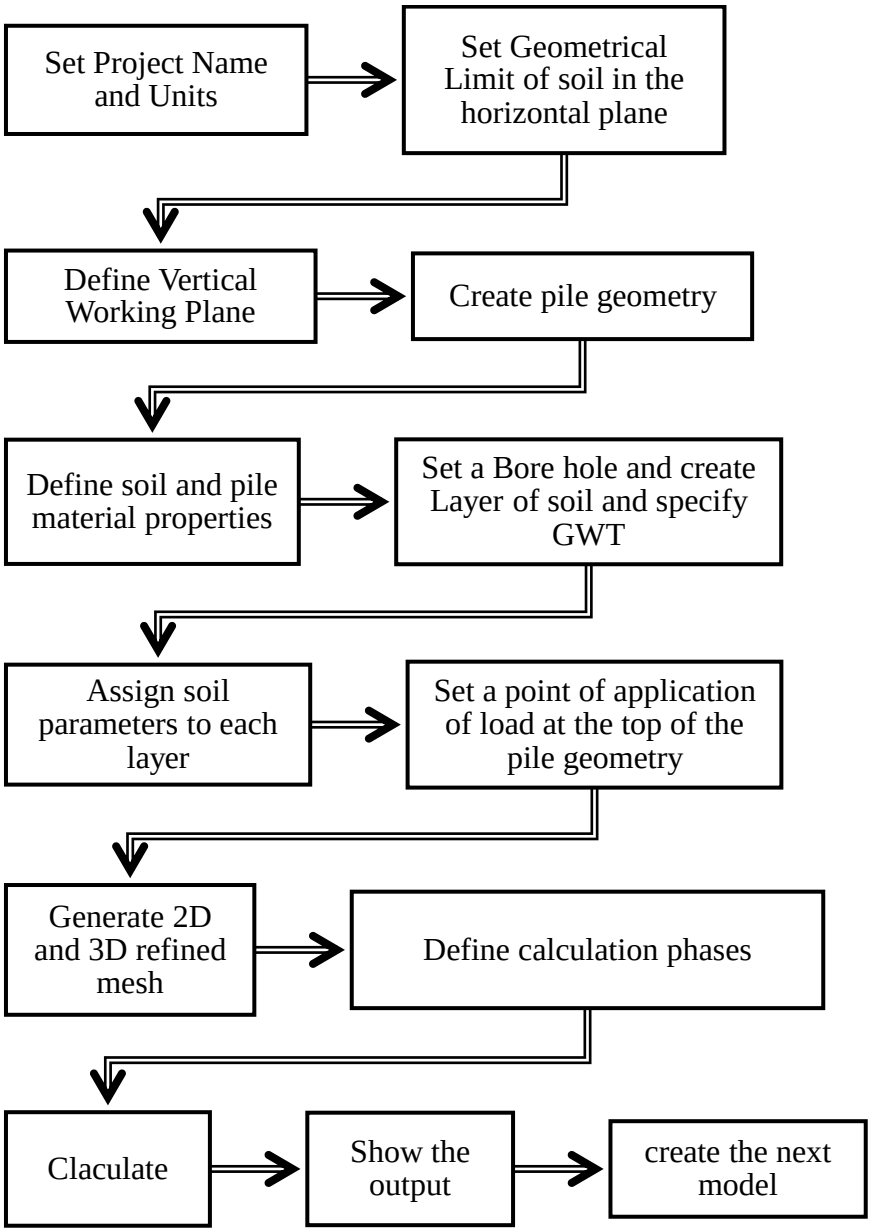

3.4. Validation Examples from Literatures

To validate the program used in this thesis and check the results of Plaxis 3D foundation are consistent or not examples are shown below from literatures.

The first example is taken from a study on by (Reul & Randolph, 2003). The second examples were taken from a study by (Engin, *et al*., 2009) on modelled foundation by means of embedded pile.

(Reul & Randolph, 2003) have given analysis and measurement results for three buildings in Germany. These buildings have piled raft foundation along with many other in Frankfurt, Germany. In the research Westend 1, the Messeturm and Torhaus were studied using three-dimensional elasto-plastic finite-element analyses. For the validation Westend 1 results were used to verify the output of finite element analysis according to verification example shown by (Simeneh,2005).

(Engin, *et al*., 2009)have considered a number of cases to demonstrate the 3D modelling and numerical capability of the developed embedded pile models to compare the results with actual tested pile displacement measurements. The cases selected to show validation of plaxis 3D foundation software are South Surra pile load test and Umr Gudayr pile load test.

3.4.1. WESTEND 1.

A raft 47m x 62m is used with thickness of 3 to 4.65m. Forty bored piles with a length of 30m and diameter of 1.3m supports the raft with an arrangement shown Table 3.1.

- **Structural Model**

Finite element is used to model the soil and foundation. The soil and the piles are represented by first-order solid finite-elements of hexahedron (brick) and triangular prism (wedge) shape. The raft is modelled using first order shell elements of square and rectangular shape. The drained (long-term) shear parameters of soil were used. The non-linear material behaviour of the soil (grains) has been modelled with a cap model that consists of three yield surface segment.

The contact zone between soil and raft, and soil and the large diameter bored piles, was modelled with thin solid continuum elements instead of special interface elements. A perfectly rough structure-soil contact was assumed. The raft and piles are considered to behave linear-elastically.

- **Subsoil stratum**

The subsoil condition is characterized by clay at the top and underlain by Frankfurt limestone. The distribution of the young's modulus of the Frankfurt clay with depth is assumed as nonlinear. In modelling using PLAXIS, only the Frankfurt clay is used in addition, a linear variation of young's modulus is used.

The step-by-step analysis of the construction process employed is outlined below on tabular from.

Table 3.1. Westend 1 step by step analysis of the construction process in finite element analysis

Step	Applied load P_{eff} (MN)	Mean vertical effective stress at the foundation level (Kpa)
1. In-situ stress state	-	192
2. Excavation to a depth of 7m below ground level	-	66
3. Installation of the piles	-	66
4. Excavation to a depth of 14.5m below ground level	-	0
5. Application of weight of raft minus uplift due to pore pressures as uniform load on subsoil	61.9	21.9
6. Installation of the Raft	61.9	21.9
7. Loading on the raft	956.9	338

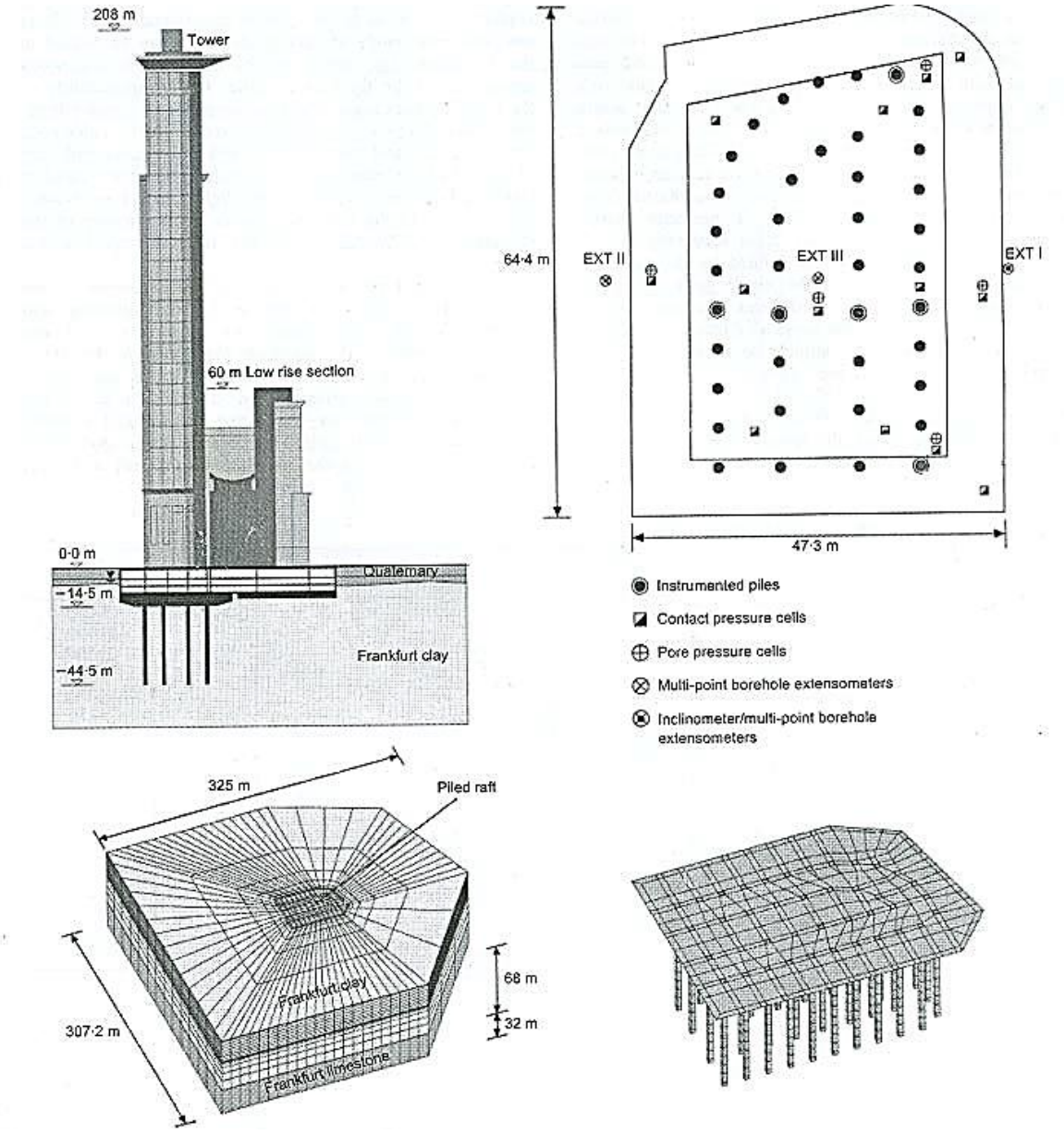

Figure 3.1. Westend 1 building with its raft layout and finite element models (Reul & Randolph, 2003).

A similar modeling has been done using PLAXIS as a verification example. A rectangular raft is used instead of the shown above. A similar construction stages have been used to simulate all the ideas in the above table (Simeneh , 2009). The three-dimensional model used is shown in Figure 3.2.

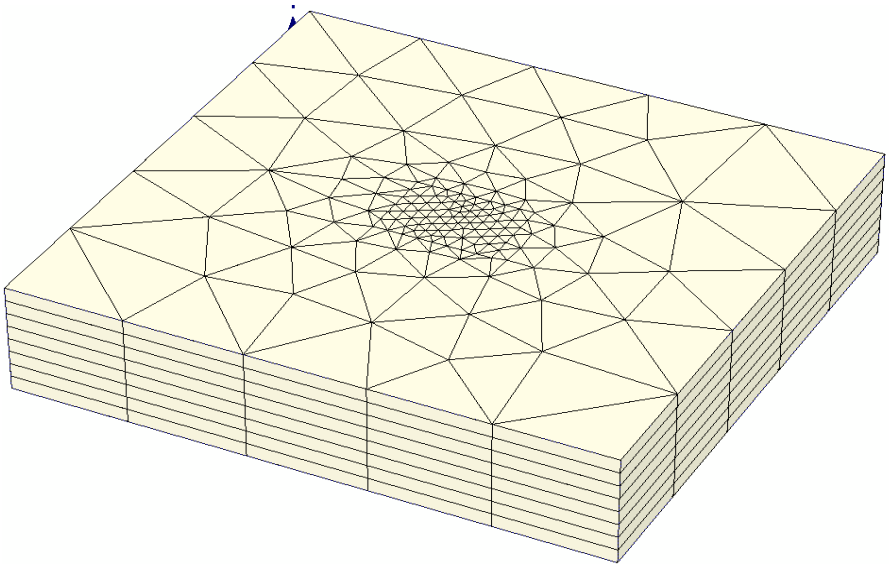

Figure 3.2. Three-dimensional model of Westend 1 in PLAXIS 3D Foundation Software (Simeneh , 2009).

The PLAXIS software gives different outputs according to the requirements of the user. Among the major outputs, deformations, stresses, strains, forces, etc. can be included. In relation to this work, deformations are the main concern; but for this verification example pile forces are also considered (Simeneh , 2009). The PLAXIS software output in contour plot is shown on Figure 3.3 for deformation of Westend 1 raft.

Figure 3.3. Three-dimensional model of Westend 1 in PLAXIS 3D Foundation Software (Simeneh , 2009).

The piled raft coefficient (αpr) can be defined as the ratio of the load taken by the piles to the total load applied. The load sharing between the piles and the raft can be described using this coefficient. The coefficient can be given as;

$$\alpha_{pr} = \frac{P_{piles}}{P_{tot}} \quad \textbf{(3.1)}$$

Where Ppiles = Total load taken by the piles

P_{tot} = Total load applied on the piled raft foundation

From Table 3.1, the total force carried by the piles is 655.37 MN while the total applied load is 956.9 MN. Thus, the ratio results in 68.5%.

A bar chart comparison is made for center settlement, the maximum pile load and plied raft coefficient from the different methods listed below. The PLAXIS result is included here also for comparison purpose as shown in

1) Simplified hand calculation method, (Poulos & Davis, 1980)
2) Strip on springs, (Poulos, 1991)
3) Plate on springs, (Poulos, 1994)
4) Combined finite element and boundary element method, (Ta & Small, 1996)
5) Combined finite element and boundary element method, Sinha (1996)
6) Combined finite element and boundary element method, Franke et al (1996)
7) Flexibility matrix method, (Randolph, 1983)
8) Load transfer approach for individual piles combined with elastic interaction between piles and raft, (Clancy & Randolph, 1993)

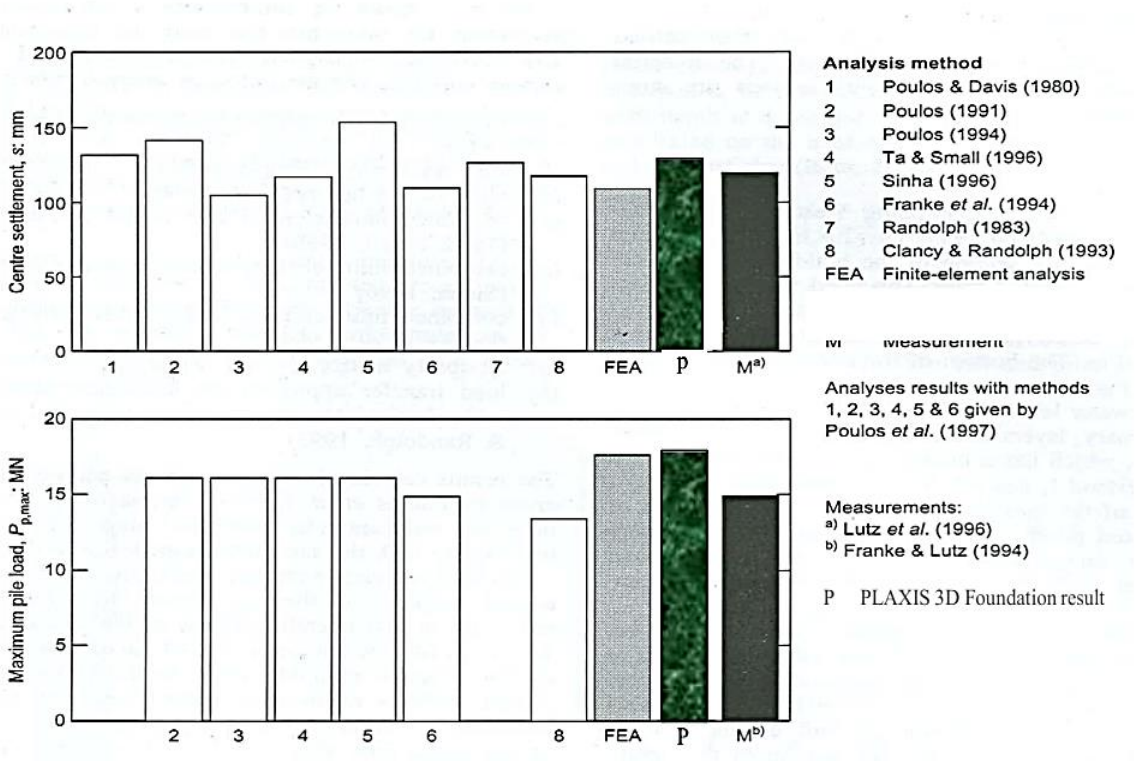

Figure 3.4. Comparisons of different methods and measurements (Reul & Randolph, 2003) and (Simeneh , 2009).

The measured center settlement amounts to 120 mm, a maximum pile load of 14.9 MN and a minimum load of 9.2 MN. The PLAXIS output shows a center settlement of 130 mm, a maximum pile load of 17.5 MN and a minimum pile load of 14.48 MN. A piled raft coefficient (ratio of load taken by the piles to total load applied) is found to be 68.5%. The results from Plaxis agree well with both the measured as well as the numerical methods and finite element analysis outputs (Simeneh , 2009).

3.4.2. South Surra pile load test.

The site is located in Kuwait and has profile of medium dense and very dense weekly cemented calcareous sand. The soil parameters are shown in Table 3.2. Two short bored piles, which were 0.3m diameter and having depth of 3.3m and 5.3m were tested in axial tension to failure. The embedded pile elements were modelled using Plaxis 3D foundation software and the results of the field tests are used to validate the outputs.

Table 3.2. Model parameters used in the analysis (South Surra)

Property	Unit	L1**	L2**
Unit weights γ_{sat} / γ_{dry}	KN/m^3	18/19.5	18.5/20
Secant stiffness, E_{50}	KN/m^2	$1.5*10^4$	$3.5*10\wedge4$
Oedometer stiffness, E_{oed}	KN/m^2	$1.5*10^4$	$3.5*10\wedge4$
Unloading-reloading stiffness, E_{ur} ref	KN/m^2	$3.5*10^4$	$1.0*10\wedge4$
Stress dependency power, m	-	0.5	0.5
Poisson's ratio, υ	-	0.2	0.2
Cohesion, C'	KN/m^2	20	0.001
Internal friction angle	º	35	40
Dilation angle, ψ	º	5	8
At rest lat. Press. Coeff. For NC, K_o^{NC}	-	0.426	0.4
Over-consolidation ratio, OCR	-	1	1
Past overburden press. POP	KN/m^2	0	0
Interface stiffness ratio, R_{int}	-	1	1
Material Model	-	Hs*	HS*

*HS; Hardening soil. **L1, L2; Soil layers (L1: medium dense cemented silty sand, L2: medium to very dense silty sand)

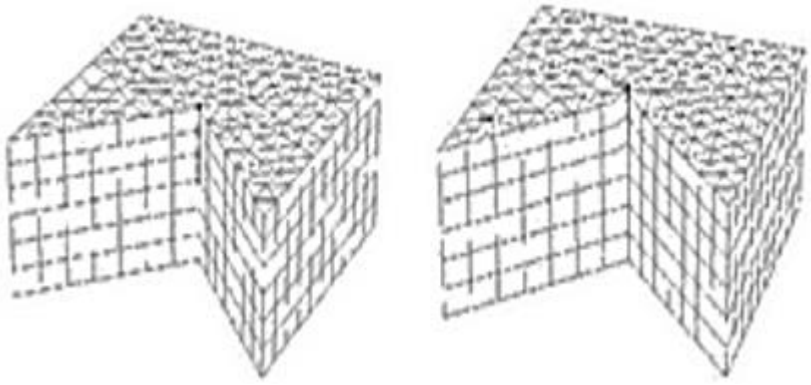

Figure 3.5. Finite element model of South Surra test piles (Engin, *et al.*, 2009).

Finite element model analysis output and test of pile results are shown in Figure 3.6 in graphical presentation.

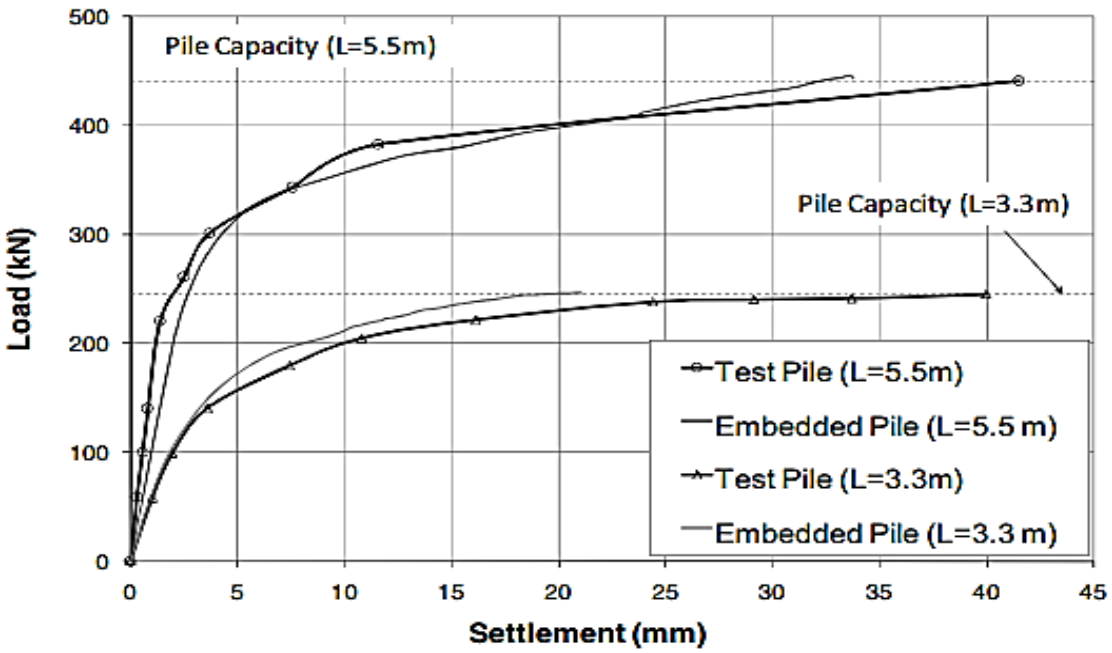

Figure 3.6. Load-displacement behavior of South Surra test piles and Plaxis 3D Foundation embedded pile models (Engin, et al., 2009).

It can be seen from the load displacement curve that the results obtained for the embedded pile model is quite in good agreement with the pile load test results.

3.4.3. Umr Gudayr pile load test.

In this site, a tension test about the design and construction of a transmission line was carried out on uncemented cohesionless sand deposit. This site has soil conditions and penetration resistance similar to the soil depositions of South Surra except that no cementation exists. The soil parameters used in the finite element analysis are given in Table 3.3.

Table 3.3. Model parameters used in the analysis (Umr Gudayr)

Property	Unit	L1**	L2**
Unit weights γ_{sat} / γ_{dry}	KN/m^3	17	18.5
Secant stiffness, E_{50}	KN/m^2	$0.5*10^4$	$1.5*10\wedge4$
Oedometer stiffness, E_{oed}	KN/m^2	$0.5*10^4$	$1.5*10\wedge4$
Unloading-reloading stiffness, E_{ur} ref	KN/m^2	$1.5*10^4$	$3.5*10\wedge5$
Stress dependency power, m	-	0.7	0.5
Poisson's ratio, υ	-	0.2	0.2
Cohesion, C'	KN/m^2	0.001	0.001
Internal friction angle	^{o}	27	35
Dilation angle, ψ	^{o}	0	0
At rest lat. Press. Coeff. For NC, K_o^{NC}	-	0.546	0.426
Over-consolidation ratio, OCR	-	1	1
Past overburden press. POP	KN/m^2	0	0
Interface stiffness ratio, R_{int}	-	1	1
Material Model	-	Hs*	HS*

*HS; Hardening soil. **L1, L2; Soil layers (L1: medium dense cemented silty sand, L2: medium to very dense silty sand)

The load displacement behavior of embedded pile model is presented with Umr Gudayr test pile Figure 3.7.

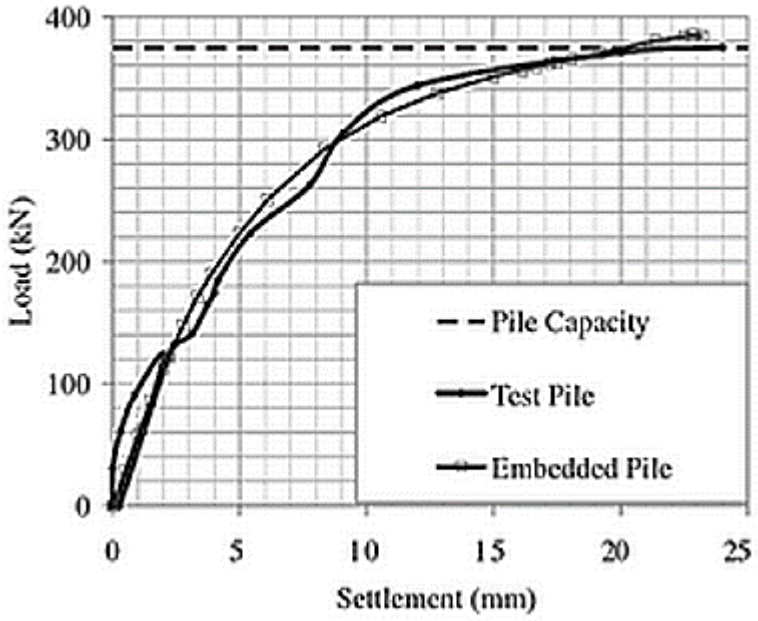

Figure 3.7. Load-displacement behavior of Umr Gudayr test piles and Plaxis 3D Foundation embedded pile models. (Engin, *et al*., 2009).

It can be seen from the load displacement curve that the results obtained for the embedded pile model for the test pile 5m long with 4.7m embedded length is quite in good agreement with the pile load results (Engin, *et al*., 2009).

CHAPTER 4. GEOLOGY AND SOIL PARAMETERS OF THE SELECTED SITE

4.1. Introduction

This Thesis output is mainly governed by availability of basic soil data and investigation reports that is used as input in FEM analysis. Basic inputs for FEM analysis is gathered from a detailed geotechnical investigation that is collected from consulting and geotechnical investigation firms. Thus, the required geotechnical data have been adapted from investigation reports and some parameters are correlated and shown if the investigation report does not include it.

Soil investigation data of Wogagen bank 3B+G+24 office building located in Addis Ababa in front of the national stadium was used to compare the load carrying capacity of friction and under-reamed piles.

Site Name - Wogagen Bank S.C. project (3B+G+24 Shop and Office Building)

The selected site geology and soil parameters are presented as follows.

4.2. Wogagen Bank S.C. (3b+G+24 Shop and Office Building)

The project site is in Addis Ababa city adjacent to Lalibela Restaurant in front of Addis Ababa Stadium.

Figure 4.1 Wogagen Bank S.C 3B+G+24 Building site on Google Earth

The project site is generally characterized by flat topography. geotechnical investigation was carried out by ETG Designers and consultant Plc.

Three bore holes were drilled in the investigation. The co-ordinates and elevation of the bore holes measured using hand held GPS are shown in Table 4.1:

Table 4.1 Co-ordinates and elevations of bore holes.

Borehole ID	Easting	Northing	Elevation(m)
BH-1	0473084	0995956	2352
BH-2	0473088	0995935	2352
BH-3	0473094	0995924	2352

For this thesis borehole number one (BH-1) was selected and its soil parameters are thoroughly discussed and studied, thus it is used as a soil stratum property for simulation of the interaction between friction and under-reamed piles.

- **Site Geology**

Backfill materials characterize the top most part of project site with maximum depth of 1.45m below existing ground level. Underlying the backfill layer, dark to reddish brown, high plastic clayey Silt was encountered having maximum depth of 2.55m. Reddish brown to yellowish grey, stiff to very stiff, high plastic clayey silt was encountered underlying the above soil layer with maximum thickness of 13m. Below the high plastic clayey soil layer, yellowish grey to reddish brown, very stiff, low plastic clayey silt was encountered having maximum depth 9.70m. Yellowish grey to brown, very stiff to hard, high plastic clayey silt was encountered underlying the above low plastic clayey silt layer having a maximum thickness of 10.45m. The detailed strata is presented in the borehole logs attached in the Appendix 3.

4.1.1. Soil Parameters of Strata under Wogagen Bank S.C Site.

In this thesis soil parameters are collected from geotechnical reports of actual project of Wogagen Bank S.C projects site located in area of Addis Ababa city adjacent to Lalibela in front of Stadium. Some geotechnical parameters to be used in this study are correlated and shown below.

- **Atterberg Limits**

Atterberg limit tests performed for layers of soil at Wogagen bank S.C project site is revised and the results are shown in

Table 4.2.

$$PI = LL - PL \quad (4.1)$$

Table 4.2 Description of soil layer and Atterberg limit obtained from soil investigation report done by ETG Designers and consultants.

Atterberg Limit For BH-1									
Soil Layer				Station (BH)	Description	Depth (m)	Atterberig Limit		
Layer No.	Colour	Description	Depth(m)				Liquid Limit (LL) %	Plastic Limit (PL) %	Plastic index (PI) %
1		Reddish Brown to yellowish red, stiff to very stiff, high plastic Clayey Silt	3.5-13.85	BH-1	Low Plastic sandy silty CLAY	5.00-6.00	39	22	17
				BH-1	Highly Plastic CLAYEY SILT	6.8-7.75	66	39	27
				BH-1	Highly Plastic CLAYEY SILT	8.8-9.75	64	42	22
				BH-1	Highly Plastic CLAYEY SILT	12-12.75	64	36	28
2		Yellowish gray to gray, very stiff, high plastic Clayey Silt with sand and gravel	13.85-17.2	BH-1	Highly Plastic CLAYEY SILT with few gravel and sand	15-15.95	55	37	18
3		Yellowish gray to reddish brown, very stiff to hard, high plastic Clayey Silt with sand	17.2-27.6	BH-1	Highly Plastic CLAYEY SILT	18.3-19.35	65	34	31
				BH-1	Highly Plastic CLAYEY SILT with sand	21.60-22.60	65	42	23
				BH-1	Highly Plastic CLAYEY SILT	24.50-25.50	69	43	26

- **Initial Stress Coefficient (K_O)**

The ratio of the horizontal principal effective stress to the vertical principal effective stress is called the lateral earth pressure coefficient at rest (Ko), that is,

$$\boldsymbol{K_o = \frac{\sigma_3'}{\sigma_1'}} \qquad \textbf{(4.2)}$$

The at-rest condition implies that no deformation occurs and Ko applies only to effective principal, not total principal, stresses. For a soil that was never subjected to effective stresses higher than its current effective stress (normally consolidated soil), $K_o = K_o^{nc}$ is reasonably predicted by an equation suggested by Jacky (1944) and Holtz and Kovacs (1981) empirical correlation formulas have been taken respectively as follows:

$$\boldsymbol{K_o = 1 - sin(\emptyset)} \qquad \textbf{(4.3)}$$

$$\boldsymbol{K_o = 0.44 + 0.0042\ x\ I_p} \qquad \textbf{(4.4)}$$

Where:

K_O = Coefficient of earth pressure at rest

I_P = Plasticity index

Ø = angle of internal friction

Using the two-equation lateral earth pressure coefficient at rest (Ko) values for soil in the study site is summarized in Table 4.3.

Table 4.3 Initial stress Coefficient K_O of soil in the study site.

Soil Layer				Station (BH)	Description	Depth (m)	Plastic index (PI) %	$K_o = 0.44 + 0.0042\ x\ I_p$	Avg. Ko
Layer No.	Colour	Description	Depth (m)						
1		Reddish Brown to yellowish red, stiff to very stiff, high plastic Clayey Silt	3.5-13.85	BH-1	Low Plastic sandy silty CLAY	5.00-6.00	17	0.51	0.54
				BH-1	Highly Plastic CLAYEY SILT	6.8-7.75	27	0.55	
				BH-1	Highly Plastic CLAYEY SILT	8.8-9.75	22	0.53	
				BH-1	Highly Plastic CLAYEY SILT	12-12.75	28	0.56	
2		Yellowish grey to grey, very stiff, high plastic Clayey Silt with sand and gravel	13.85-17.2	BH-1	Highly Plastic CLAYEY SILT with few gravel and sand	15-15.95	18	0.52	0.5
3		Yellowish grey to reddish brown, very stiff to hard, high plastic Clayey Silt with sand	17.2-27.6	BH-1	Highly Plastic CLAYEY SILT	18.3-19.35	31	0.57	0.55
				BH-1	Highly Plastic CLAYEY SILT with sand	21.60-22.60	23	0.54	
				BH-1	Highly Plastic CLAYEY SILT	24.50-25.50	26	0.55	

- **Shear strength parameters (C and Ø)**

Shear strength parameters of the study sites were obtained empirically as shown in Table 4.4. Cohesive soils are clay type soils. Cohesion is the force that holds together molecules or like particles within a soil. Cohesion, C, is usually determined in the laboratory from the Direct Shear Test. Unconfined Compressive Strength, S_{UC}, can be determined in the laboratory using the Triaxial Test or the Unconfined Compressive Strength Test. There are also correlations for S_{UC} with shear strength as estimated from the field using Vane Shear Tests.

$$C = \frac{S_{uc}}{2} \qquad \textbf{(4.5)}$$

Table 4.4 Empirical Values for Consistency of Cohesive Soil, (from Foundation Analysis, Bowels)

SPT Penetration (blows/ 0.3m)	Estimated Consistency	S_{UC} (KN/m^2)
0 - 2	Very Soft	0 – 24
2 - 4	Soft	24 – 48
4 - 8	Medium	48 – 96
8 - 16	Stiff	96 – 192
16 - 32	Very Stiff	192 - 383
>32	Hard	>383

Some typical values of soil frictional angle are taken from USCS soil classification systems and C values are calculated using the Empirical Values for Consistency of Cohesive Soil using

Table 4.4 and equation (4.5) respectively for soil at study site.

Table 4.5 Summary of shear strength parameters of Wogagen Bank S.C. project site.

Soil Layer				Station (BH)	N_{55} value	S_{UC} (KN/m^2)	$C = \frac{S_{uc}}{2}$ (KN/m^2)	Soil Clasfi.	Ø (°) Per USCS
Layer No.	Colour	Description	Depth(m)						
1		Reddish Brown to yellowish red, stiff to very stiff, high plastic Clayey Silt	3.5-13.85	BH-1	10	120	60	MH	23
2		Yellowish gray to gray, very stiff, high plastic Clayey Silt with sand and gravel	13.85-17.2	BH-1	12	144	72	MH	30
3		Yellowish gray to reddish brown, very stiff to hard, high plastic Clayey Silt with sand	17.2-27.6	BH-1	12	144	72	MH	30

N.B: from the investigation report C values were taken from previous soil investigation by SABA Engineering plc. And the value of C= 70 KPA.

- **Poisson's ratio(v)**

Bowles (1996) gives range of values of Poisson's ratio between 0.2 to 0.4 for cohesionless medium dense to medium loose soil types and 0.4 to 0.5 for most clay soil. Considering this studies by Bowles the Poisson's ratio for Wogagen bank S.C project site is shown below in Table 4.6.

Table 4.6 Poisson's ratio for Wogagen Bank S.C. project site.

Soil Layer				Station (BH)	ν
Layer No.	Colour	Description	Depth(m)		
1		Reddish Brown to yellowish red, stiff to very stiff, high plastic Clayey Silt	3.5-13.85	BH-1	0.35
2		Yellowish gray to gray, very stiff, high plastic Clayey Silt with sand and gravel	13.85-17.2	BH-1	0.30
3		Yellowish gray to reddish brown, very stiff to hard, high plastic Clayey Silt with sand	17.2-27.6	BH-1	0.30

- **SPT N values**

SPT test provides assessments of soils properties and foundation design parameters. It measures the soil resistance to penetration through computation of the number of blows required to drive the sampler 300 mm into the ground, after it has been advances 150 mm. In recent years, the N-value measured by SPT has been subjected to various corrections and is standardized to a reference value of 60% of the potential energy of SPT hammer (Schnaid, 2009).

$$N'_{70} = CNxNxn1xn2xn3xn4 \quad \textbf{(4.6)}$$

$$CN = \left(\frac{P''_o}{P'_o}\right)^{\frac{1}{2}} = \left(\frac{95.76}{\gamma xD}\right)^{\frac{1}{2}} \quad \textbf{(4.7)}$$

Where;

N70= Standard Penetration N seventy value

CN = adjustment for overburden pressure

P'_o = overburden pressure

P''_o = reference overburden pressure (95.76 kPa or 1.0 kg/cm2)

$n1$ = Er/Erb (where Er is average energy ratio that depends on the drill system and Erb is the standard energy ratio). Er is taken as 50 and Erb as 70.

$n2$ = Rod length correction

Rod length > 10 m = 1,

Rod length 6-10 m = 0.95,

Rod length 4-6 m = 0.85,

Rod length 0-4 m = 0.75

$\boldsymbol{n3}$ = sampler correction (1.00 in this case)

$\boldsymbol{n4}$ = borehole diameter correction (1.00 in this case)

Table 4.7 SPT N'$_{70}$ values for Wogagen Bank S.C. project site.

SPT N'$_{70}$ VALUES For BH-1														
Soil Layer				N'=CN x N x n1 x n2 x n3 x n4					AVG SPT N_{70}	C_N	N value	unit wt.KN /m3	depth (m)	n2
Layer No.	Colour	Description	Depth(m)											
1		Reddish Brown to yellowish red, stiff to very stiff, high plastic Clayey Silt	3.5-13.85	5	=	5.12	≈	5	8	1.06	9	17	5.00	0.75
				7	=	8.65	≈	9		0.90	18	17	7.00	0.75
				8.8	=	8.26	≈	8		0.80	17	17	8.80	0.85
				12	=	9.79	≈	10		0.69	20	17	12.00	1.00
2		Yellowish gray to gray, very stiff, high plastic Clayey Silt with sand and gravel	13.85-17.2	15	=	9.63	≈	10	10	0.61	22	17	15.00	1.00
3		Yellowish gray to reddish brown, very stiff to hard, high plastic Clayey Silt with sand	17.2-27.6	18.3	=	8.32	≈	8	9	0.55	21	17	18.30	1.00
				21.6	=	9.12	≈	9		0.51	25	17	21.60	1.00
				24.5	=	10.62	≈	11		0.48	31	17	24.50	1.00

The values of N'55 is used to calculate young's modulus (E) so the values of SPT N'70 is changed to SPT N55 using Eqn. (4.8)

$$N'_{55} = \frac{70}{55.}\ x\ N'_{70} \qquad \textbf{(4.8)}$$

Table 4.8 SPT N'$_{55}$ values for Wogagen Bank S.C. project site.

Soil Layer				N'70	$N'_{55} = \frac{70}{55}\, x\, N'_{70}$
Layer No.	Colour	Description	Depth(m)		
1		Reddish Brown to yellowish red, stiff to very stiff, high plastic Clayey Silt	3.5-13.85	8	10
2		Yellowish gray to gray, very stiff, high plastic Clayey Silt with sand and gravel	13.85-17.2	10	13
3		Yellowish gray to reddish brown, very stiff to hard, high plastic Clayey Silt with sand	17.2-27.6	9	12

- **Young's modulus (Es)**

The use of a practical and reasonable stiffness values representing the in-situ conditions is of great importance in finite element analysis for better simulation of the actual condition of the soil.

The in-situ test of SPT tends to use empirical correlation to obtain stress-strain modulus E_S shown in Table 4.10 . Because the laboratory values of E_S are expensive to obtain and are generally not very good anyways owning to sample disturbance, the standard penetration test (SPT) have been widely used to obtain the stress-strain modulus E_S resulting from empirical correlation (Bowles, 1997).

Table 4.9 Equations for stress-strain modulus ES from SPT values (Bowles, 1997).

1	Sand (Normally Consolidated)	$E_S = 500(N + 15)$ $E_S = 7000\sqrt{N}$ $E_S = 6000N$	**(4.9)**
2	Sand (saturated)	$E_S = 250(N + 15)$	**(4.10)**
3	Gravely Sand	$E_S = 1200(N + 6)$ $E_S = 600(N + 6) \quad N \leq 15$ $E_S = 600(N + 6) + 2000 \quad N > 15$	**(4.11)**
4	Clayey Sand	$E_S = 320(N + 15)$	**(4.12)**
5	Silt, Sandy silty or clayey silt	$E_S = 300(N + 6)$	**(4.13)**

NB: Stress-strain modulus ES is in KPA and for SPT the N values should be estimated as N_{55} and not N_{70}.

Table 4.10 Stress-strain modulus E_S of Wogagen bank S.C project site.

Layer No.	Colour	Description	Depth(m)	N_{55}	E_S Eqn. from Table 4.9	E_S (Kpa)
1		Reddish Brown to yellowish red, stiff to very stiff, high plastic Clayey Silt	3.5-13.85	10	$E_S = 300(N + 6)$	4800
2		Yellowish gray to gray, very stiff, high plastic Clayey Silt with sand and gravel	13.85-17.2	13	$E_S = 600(N + 6)$	11,400
3		Yellowish gray to reddish brown, very stiff to hard, high plastic Clayey Silt with sand	17.2-27.6	12	$E_S = 320(N + 15)$	8640

- **Ground Water Table**

Ground water level for Wogagen Bank S.C projects was monitored by drilling operation and ground water was encountered at depth of ***5m*** in borehole BH-1.

- **Static Modulus of Elasticity of Pile Material (E_{SP})**

The elasticity of pile material (E_{SP}) is an important material parameter for interpretation of both static and dynamic loading tests and analysis on piles. Concrete is the material most of the time used for construction of piles and it's not a linearly elastic material thus its young's modulus (stiffness) is not constant. Static modulus of concrete pile (E_{SP}) is obtained from static loads on cube or cylinder specimens. The values of (E_{SP}) can be also inferred from the compressive strength (f_c) by using the following empirical relationship.

$$\boldsymbol{E_{SP} = 8.48(f_c)^{\frac{1}{3}}} \qquad \textbf{(4.14)}$$

Where E_{SP} is given in GPA and fc is in MPA using Eqn.(4.14), the fc data shown in Figure 4.2a have been converted to the static modulus values and the results are shown in Figure 4.2b it can be seen the values of E_{SP} at a depth 70m is about 20% higher than that close to the top (Joram M, et al., n.d.).

a) Compressive strength f_c (MPA) b) Static Young's modulus E_{SP} (MPA)

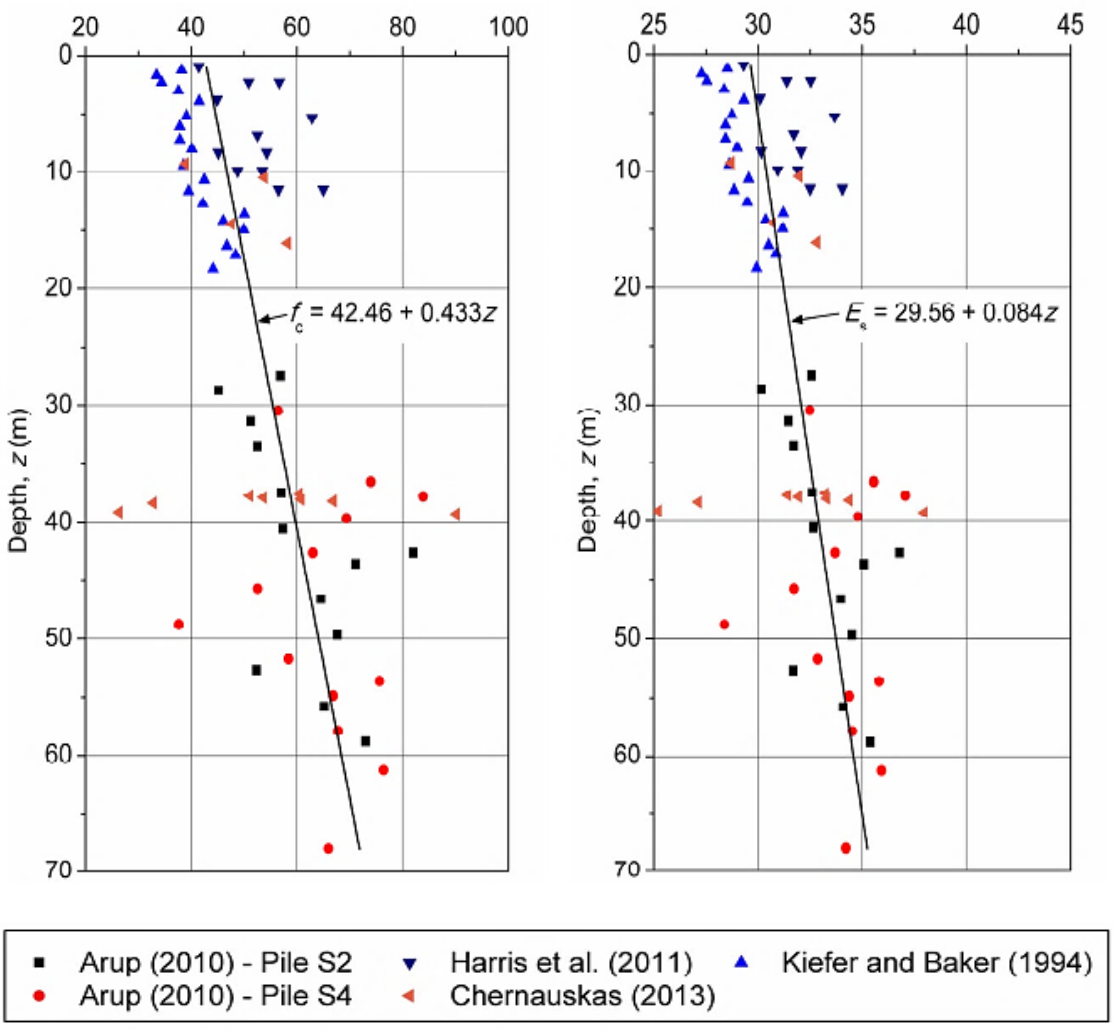

Figure 4.2 Compressive strength (left) and modulus (right) versus depth for four different studies (data after Kiefer and Bakar 1994; Arup 2010; Harris et al. 2011; Chernauskas2013) (Joram M, *et al.*, n.d.)

In this study the maximum depth of pile is 18m considering this; the value of modulus of elasticity of pile is shown in Table 4.11.

Table 4.11 Stress-strain modulus of pile (E_{SP}) with respect to depth using eqn. 4.14 and fig.4.2

Modulus of Elasticity of pile E_{SP}		
depth	fc (MPA)	E_{SP} (GPA)
1	42.89	29.68
2	43.33	29.78
3	43.76	29.88
4	44.19	29.98
5	44.63	30.08
6	45.06	30.18
7	45.49	30.27
8	45.92	30.37
9	46.36	30.46
10	46.79	30.56
11	47.22	30.65
12	47.66	30.74
13	48.09	30.84
14	48.52	30.93
15	48.96	31.02
16	49.39	31.11
17	49.82	31.20
18	50.25	31.29

4.1.2. Summary of Soil Parameters for Wogagen Bank S.C Building Site.

Basic soil parameters which is discussed and correlated above are summarized in a table below, this values are used in the modelling of the soil formation in PLAXIS 3D foundation.

Table 4.12 Summary of soil parameters for Wogagen Bank S.C. project site.

No	Parameters	Name	Layer-1	Layer-2	Layer-3	Unit	
1	Initial Stress Coefficient	K_O	0.54	0.5	0.55	-	
2	Cohesion	C	60	72	72	*Kpa*	
3	Internal Friction Angle	$\emptyset$	23	30	30	^{o}	
4	Poisson's Ratio	υ	0.35	0.3	0.3	-	
5	Young's Modulus	E_S	4800	11400	8640	*Kpa*	
6	Dilatancy Angle	ψ	0	0	0	^{o}	

CHAPTER 5. FEM MODELING AND PILE SOIL INTERACTION

5.1.Preliminaries on Material Modelling

A material model is described by a set of mathematical equations that give a relationship between stress and strain. Material models are often expressed in a form in which infinitesimal increments of stress (or 'stress rates') are related to infinitesimal increments of strain (or 'strain rates'). All material models implemented in plaxis are based on a relationship between the effective stress rates,σ' and the strain rates, ε'.

The analysis conducted for this study considers the linear elastic and Mohr-coulomb model. Thus, a brief description of this material models is given below by referring plaxis 3D foundation manual version 1.5. In the following section, it is described how stresses and strains are defined in plaxis.

5.1.1. General Definition of Stress

Stress is a tensor which can be represented by a matrix in Cartesian coordinates:

$$\boldsymbol{\sigma} = \begin{bmatrix} \boldsymbol{\sigma_{xx}} & \boldsymbol{\sigma_{xy}} & \boldsymbol{\sigma_{xz}} \\ \boldsymbol{\sigma_{yx}} & \boldsymbol{\sigma_{yy}} & \boldsymbol{\sigma_{yz}} \\ \boldsymbol{\sigma_{zx}} & \boldsymbol{\sigma_{zy}} & \boldsymbol{\sigma_{zz}} \end{bmatrix} \quad \textbf{(5.1)}$$

In the standard deformation theory, the stress tensor is symmetric such that $\sigma_{xy} = \sigma_{yx}$, $\sigma_{yz} = \sigma_{zy}$ and $\sigma_{zx} = \sigma_{zx}$. In this situation, stresses are often written in vector notation, which involve only six different components:

$$\boldsymbol{\sigma} = \left[\boldsymbol{\sigma_{xx}}\, \boldsymbol{\sigma_{yy}}\, \boldsymbol{\sigma_{zz}}\, \boldsymbol{\sigma_{xy}}\, \boldsymbol{\sigma_{yz}}\, \boldsymbol{\sigma_{zx}}\right]^{\boldsymbol{T}} \quad \textbf{(5.2)}$$

Per Terzaghi's principle, stresses in the soil are sum of effective stresses, $\boldsymbol{\sigma'}$, and pore pressures, $\boldsymbol{\sigma_w}$:

$$\boldsymbol{\sigma} = \boldsymbol{\sigma'} + \boldsymbol{\sigma_w} \quad \textbf{(5.3)}$$

Pore pressures are generally provided by water in the pores. Water is considered not to sustain any shear stresses. Thus, effective shear stresses are equal to total shear stresses. Positive normal stress components are considered to represent tension, whereas negative normal stress components indicate pressure (or compression). Moreover, water is considered to be fully isotropic, so all pore pressure components are equal.

Material models for soil and rock are generally expressed as a relationship between infinitesimal increments of effective stress and infinitesimal increments of strain. In such a relationship, infinitesimal increments of effective stress are represented by stress rates (with a dot above the stress symbol):

$$\dot{\boldsymbol{\sigma}}' = \left[\dot{\sigma}'_{xx}\ \dot{\sigma}'_{yy}\ \dot{\sigma}'_{zz}\ \dot{\sigma}_{xy}\ \dot{\sigma}_{yz}\ \dot{\sigma}_{zx}\ \right]^{T} \qquad \textbf{(5.4)}$$

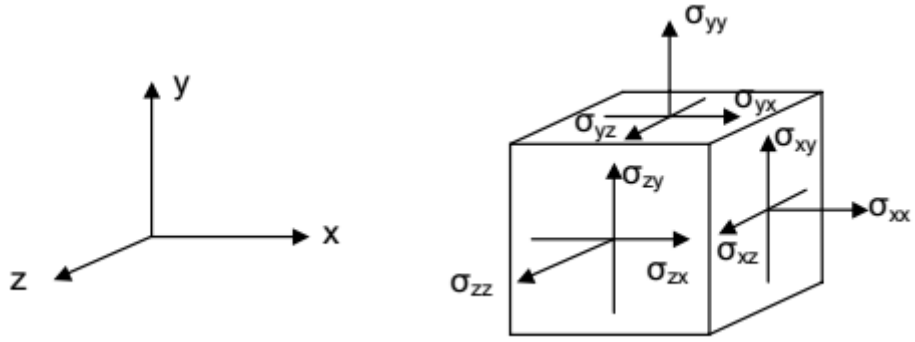

Figure 5.1 General three-dimensional coordinate system and sign convention for stress

It is often useful to apply principal stresses rather than Cartesian stress components when formulating material models. Principal stresses are the stresses in such a coordinate system direction that all shear stress components are zero. Principal stresses are, in fact, the eigenvalues of the stress tensor. Principal effective stresses can be determined in the following way:

$$\boldsymbol{\sigma} = \boldsymbol{\sigma}' + \boldsymbol{\sigma}_{\boldsymbol{w}} \qquad \textbf{(5.5)}$$

where I is the identity matrix, this equation gives three solutions for $\boldsymbol{\sigma}'$, i.e. the principal effective stresses $(\sigma'_1, \sigma'_2, \sigma'_3)$. In PLAXIS the principal effective stresses are arranged in algebraic order of $(\sigma'_1 \leq \sigma'_2 \leq \sigma'_3)$ and models are often presented with reference to the principal stress space, as indicated in Figure 2.2.

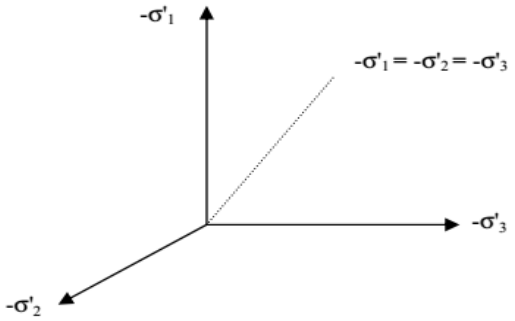

Figure 5.2 principal stress space

In addition to principal stresses it is also useful to define invariants of stress, which are stress measures that are independent of the orientation of the coordinate system. Two useful stress invariants are:

$$\boldsymbol{p' = \frac{1}{3}(\sigma'_{xx} + \sigma'_{yy} + \sigma'_{zz})} \quad \textbf{(5.6)}$$

$$\boldsymbol{q = \sqrt{\frac{1}{2}(\sigma'_{xx} - \sigma'_{yy})^2 + (\sigma'_{yy} - \sigma'_{zz})^2 + (\sigma'_{zz} - \sigma'_{xx})^2 + 6(\sigma^2_{xy} + \sigma^2_{yz} + \sigma^2_{zx})}} \quad \textbf{(5.7)}$$

where p' is the isotropic effective stress, or mean effective stress, and q is the equivalent shear stress. The equivalent shear stress, q, has the important property that it reduces to $q = |\sigma'_1 - \sigma'_3|$ for triaxial stress states with $\sigma'_2 = \sigma'_3$.

5.1.2. General Definition of Strain

Strain is a tensor which can be represented by a matrix with Cartesian coordinates as:

$$\boldsymbol{\varepsilon = \begin{bmatrix} \varepsilon_{xx} & \varepsilon_{xy} & \varepsilon_{xz} \\ \varepsilon_{yx} & \varepsilon_{yy} & \varepsilon_{yz} \\ \varepsilon_{zx} & \varepsilon_{zy} & \varepsilon_{zz} \end{bmatrix}} \quad \textbf{(5.8)}$$

Strains are the derivatives of the displacement components, i.e. $\varepsilon_{ij} = \partial u_i / \partial_i$, where i is either x, y or z. According to the small deformation theory, only the sum of complementing Cartesian shear strain components ε_{ij} and ε_{ji} result in shear stress. This sum is denoted as the shear strain γ. Hence, instead of ε_{xy}, ε_{yx}, ε_{yz}, ε_{zy}, ε_{zx} and ε_{xz} the shear strain components γ_{xy}, γ_{yz} and γ_{zx} are used respectively. Under the above conditions, strains are often written in vector notation, which involve only six different components:

$$\boldsymbol{\varepsilon = \left[\varepsilon_{xx}\ \varepsilon_{yy}\ \varepsilon_{zz}\ \gamma_{xy}\ \ \gamma_{yz}\ \gamma_{zx}\ \right]^T} \quad \textbf{(5.9)}$$

$$\boldsymbol{\varepsilon_{xx} = \frac{\partial U_x}{\partial_x} \quad ; \quad \varepsilon_{xx} = \frac{\partial U_x}{\partial_x} \quad ; \quad \varepsilon_{xx} = \frac{\partial U_x}{\partial_x}} \quad \textbf{(5.10)}$$

$$\boldsymbol{\gamma_{xy} = \varepsilon_{xy} + \varepsilon_{yx} = \frac{\partial U_x}{\partial_y} + \frac{\partial U_y}{\partial_x}} \quad \textbf{(5.11)}$$

$$\gamma_{yz} = \varepsilon_{yz} + \varepsilon_{zy} = \frac{\partial U_y}{\partial_z} + \frac{\partial U_z}{\partial_y} \quad (5.12)$$

$$\gamma_{zx} = \varepsilon_{zx} + \varepsilon_{xz} = \frac{\partial U_z}{\partial_x} + \frac{\partial U_x}{\partial_z} \quad (5.13)$$

Similarly, as for stresses, positive normal strain components refer to extension, whereas negative normal strain components indicate compression. In the formulation of material models, where infinitesimal increments of strain are considered, these increments are represented by strain rates (with a dot above the strain symbol).

$$\dot{\varepsilon} = \left[\dot{\varepsilon}_{xx}\ \dot{\varepsilon}_{yy}\ \dot{\varepsilon}_{zz}\ \dot{\gamma}_{xy}\ \ \dot{\gamma}_{yz}\ \ \dot{\gamma}_{zx}\ \right]^T \quad (5.14)$$

In analogy to the invariants of stress, it is also useful to define invariants of strain. A strain invariant that is often used is the volumetric strain, ε_v, which is defined as the sum of all normal strain components:

$$\varepsilon_v = \varepsilon_{xx} + \varepsilon_{yy} + \varepsilon_{zz} = \varepsilon_1 + \varepsilon_2 + \varepsilon_3 \quad (5.15)$$

The volumetric strain is defined as negative for compaction and as positive for dilatancy. For elastoplastic models, as used in PLAXIS, strains are decomposed into elastic and plastic components: in superscript e is used to denote elastic strains and the superscript p is used to denote plastic strains.

$$\varepsilon = \varepsilon^e + \varepsilon^p \quad (5.16)$$

The superscript e is used to denote elastic strains and the superscript p is used to denote plastic strains.

The simplest material model in PLAXIS is based on Hooke's law for isotropic linear elastic behaviour. This model is available under the name Linear Elastic model, but it is also the basis of other models. Hooke's law can be given by the equation:

$$\begin{bmatrix} \dot{\sigma}'_{xx} \\ \dot{\sigma}'_{yy} \\ \dot{\sigma}'_{zz} \\ \dot{\sigma}'_{xy} \\ \dot{\sigma}'_{yz} \\ \dot{\sigma}'_{zx} \end{bmatrix} = \frac{E'}{(1-2\nu')(1+\nu')} \begin{bmatrix} 1-\nu' & \nu' & \nu' & 0 & 0 & 0 \\ \nu' & 1-\nu' & \nu' & 0 & 0 & 0 \\ \nu' & \nu' & 1-\nu' & 0 & 0 & 0 \\ 0 & 0 & 0 & \frac{1}{2}-\nu' & 0 & 0 \\ 0 & 0 & 0 & 0 & \frac{1}{2}-\nu' & 0 \\ 0 & 0 & 0 & 0 & 0 & \frac{1}{2}-\nu' \end{bmatrix} \begin{bmatrix} \dot{\varepsilon}_{xx} \\ \dot{\varepsilon}_{yy} \\ \dot{\varepsilon}_{zz} \\ \dot{\gamma}_{xy} \\ \dot{\gamma}_{yz} \\ \dot{\gamma}_{zx} \end{bmatrix} \quad \textbf{(5.17)}$$

5.2. The Mohr-Coulomb Model (Perfect-Plasticity)

The Mohr-Coulomb failure or strength criterion has been widely used for geotechnical applications. Indeed, many of the routine design calculations in the geotechnical area are still performed using the Mohr- Coulomb criterion. To evaluate if plasticity occurs in a calculation, a yield function, *f*, is introduced as a function of stress and strain. Plastic yielding is related with the condition $f = 0$. This condition can often be presented as a surface in principal stress space. A perfectly plastic model is a constitutive model with a fixed yield surface, i.e. a yield surface that is fully defined by model parameters and not affected by (plastic) straining (Brinkgreve & Broere, 2006).

In this study a Mohr-Coulomb model perfect plasticity is used in geotechnical engineering application and simulation of pile loading test applying finite element methods.

5.2.1. Elastic Perfectly-Plastic Behaviour

Per the classical theory of plasticity (Hill, 1998), plastic strain rates are proportional to the derivative of the yield function with respect to the stresses. This means that the plastic strain rates can be represented as vectors perpendicular to the yield surface. This classical form of the theory is referred to as associated plasticity.

When an elastic material is subjected to load, it sustains elastic strains. Elastic strains are reversible in the sense that the elastic material will spring back to its un-deformed condition if the load is removed. On the other hand, if a plastic material is subjected to a load, it sustains elastic and plastic strains. If the load is removed, the material will sustain permanent plastic (irreversible) strains, whereas the elastic strains are recovered. Hooke's law, which is based

on elasticity theory, is sufficient (in most cases) to estimate the elastic strains. To estimate the plastic strains, one needs to use plasticity theory.

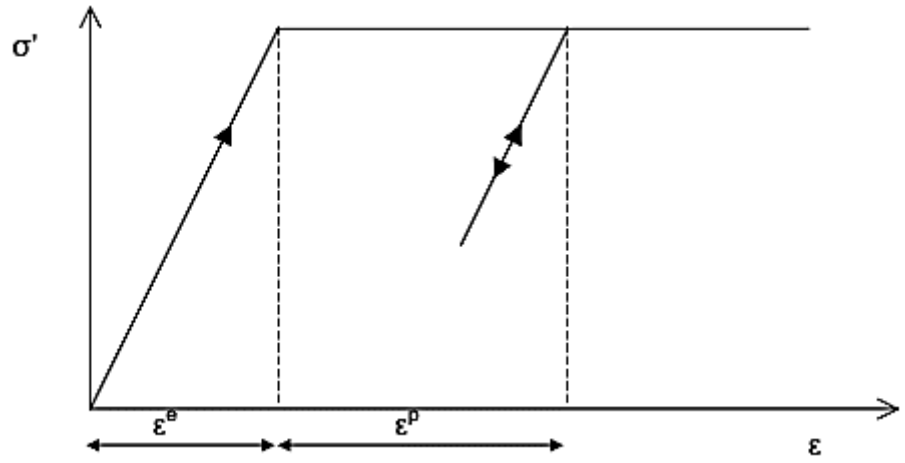

Figure 5.3 Basic Idea Of an elastic Perfectly Plastic Model (Brinkgreve & Broere, 2006)

Simulation of Pile Load Test Using Finite Element Method Plasticity theory was originally developed to predict the behaviour of metals subjected to loads exceeding their elastic limits. Similar models were developed later to calculate the irreversible strains in concrete, soils, and polymers (Helwanys, 2007).

5.2.2. Formulation of The Mohr-Coulomb Model

The Mohr-Coulomb yield condition is an extension of Coulomb's friction law to general states of stress. In fact, this condition ensures that Coulomb's friction law is obeyed in any plane within a material element, Thus the Mohr-Coulomb criterion can be written as:

$$\boldsymbol{\tau = C - \sigma \tan \emptyset} \qquad \textbf{(5.18)}$$

Where $\boldsymbol{\tau}$ is the shear stress, $\boldsymbol{\sigma}$ is the normal stress (negative in compression), $\boldsymbol{C}$ is the cohesion of the material, and $\boldsymbol{\emptyset}$ is the material angle of friction.

$$\boldsymbol{\tau = S \cos \emptyset} \qquad \textbf{(5.19)}$$

$$\boldsymbol{\sigma = \sigma_m + S \sin \emptyset} \qquad \textbf{(5.20)}$$

Substituting for $\boldsymbol{\tau}$ and $\boldsymbol{\sigma}$, the Mohr-Coulomb criterion can be rewritten as

$$\boldsymbol{S + \sigma_m \sin \emptyset - C \cos \emptyset = 0} \qquad \textbf{(5.21)}$$

Where;

$$S = \frac{1}{2}(\sigma_1 - \sigma_3) \tag{5.22}$$

$$\sigma_m = \frac{1}{2}(\sigma_1 + \sigma_3) \tag{5.23}$$

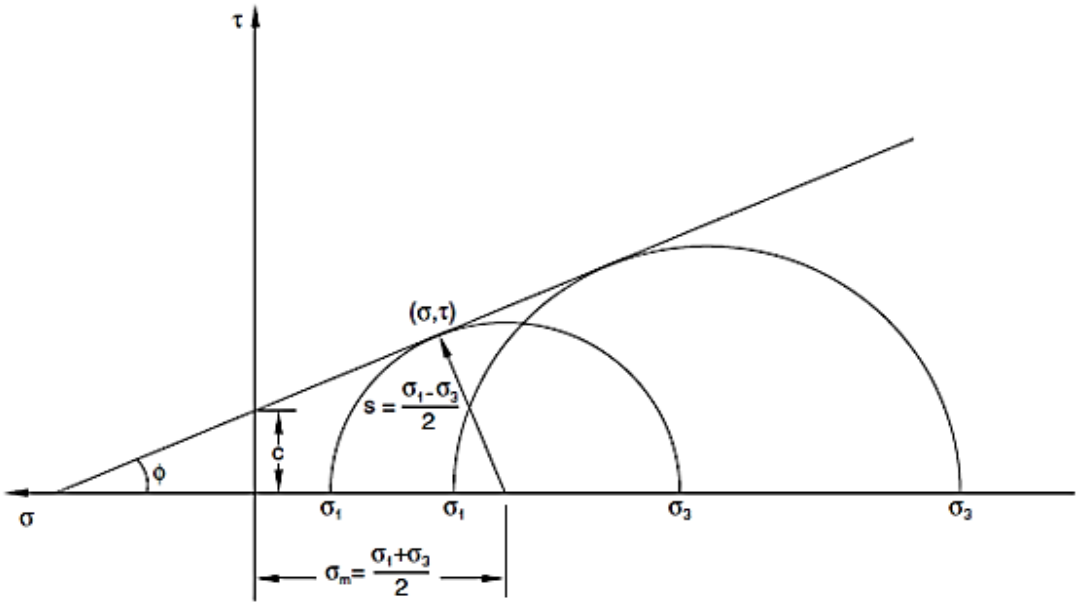

Figure 5.4 Mohr-Coulomb Failure Criteria

The full Mohr-Coulomb yield condition in PLAXIS 3D consists of six yield functions when formulated in terms of principal stresses:

$$f_{1a} = \frac{1}{2}(\sigma'_2 - \sigma'_3) + \frac{1}{2}(\sigma'_2 + \sigma'_3)\sin\emptyset - C\cos\emptyset \leq 0 \tag{5.24}$$

$$f_{1b} = \frac{1}{2}(\sigma'_3 - \sigma'_2) + \frac{1}{2}(\sigma'_3 + \sigma'_2)\sin\emptyset - C\cos\emptyset \leq 0 \tag{5.25}$$

$$f_{2a} = \frac{1}{2}(\sigma'_3 - \sigma'_1) + \frac{1}{2}(\sigma'_3 + \sigma'_1)\sin\emptyset - C\cos\emptyset \leq 0 \tag{5.26}$$

$$f_{2b} = \frac{1}{2}(\sigma'_1 - \sigma'_3) + \frac{1}{2}(\sigma'_1 + \sigma'_3)\sin\emptyset - C\cos\emptyset \leq 0 \tag{5.27}$$

$$f_{3a} = \frac{1}{2}(\sigma'_1 - \sigma'_2) + \frac{1}{2}(\sigma'_1 + \sigma'_2)\sin\emptyset - C\cos\emptyset \leq 0 \tag{5.28}$$

$$f_{3b} = \frac{1}{2}(\sigma'_2 - \sigma'_1) + \frac{1}{2}(\sigma'_2 + \sigma'_1)\sin\emptyset - C\cos\emptyset \leq 0 \tag{5.29}$$

The two plastic model parameters appearing in the yield functions are the well-known friction angle $\emptyset$ and the cohesion C. The condition $f_i = 0$ for all yield functions together

(where f_i is used to denote each individual yield function) represent a hexagonal cone in principal stress space as shown in Figure 3.2.

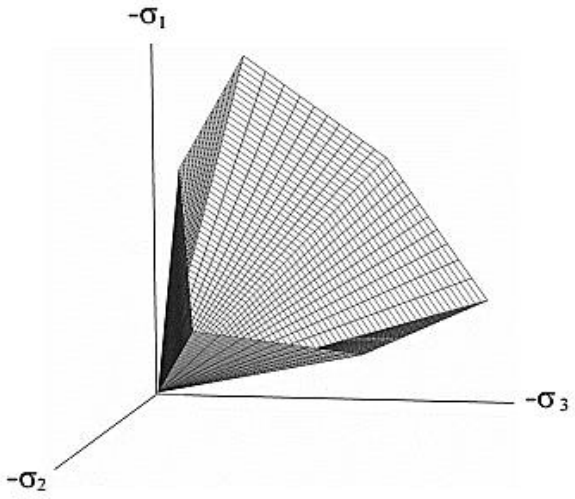

Figure 5.5 The Mohr-Coulomb yield surface in principal stress space (c = 0) (Brinkgreve & Broere, 2006)

In addition to the yield functions, six plastic potential functions are defined for the Mohr-Coulomb model:

$$g_{1a} = \frac{1}{2}(\sigma'_2 - \sigma'_3) + \frac{1}{2}(\sigma'_2 + \sigma'_3)\sin\psi \quad (5.30)$$

$$g_{1b} = \frac{1}{2}(\sigma'_3 - \sigma'_2) + \frac{1}{2}(\sigma'_3 + \sigma'_2)\sin\psi \quad (5.31)$$

$$g_{2a} = \frac{1}{2}(\sigma'_3 - \sigma'_1) + \frac{1}{2}(\sigma'_3 + \sigma'_1)\sin\psi \quad (5.32)$$

$$g_{2b} = \frac{1}{2}(\sigma'_1 - \sigma'_3) + \frac{1}{2}(\sigma'_1 + \sigma'_3)\sin\psi \quad (5.33)$$

$$g_{3a} = \frac{1}{2}(\sigma'_1 - \sigma'_2) + \frac{1}{2}(\sigma'_1 + \sigma'_2)\sin\psi \quad (5.34)$$

$$g_{3b} = \frac{1}{2}(\sigma'_2 - \sigma'_1) + \frac{1}{2}(\sigma'_2 + \sigma'_1)\sin\psi \quad (5.35)$$

The plastic potential functions contain a third plasticity parameter, the dilatancy angle ψ. This parameter is required to model positive plastic volumetric strain increments (dilatancy) as actually observed for dense soils.

5.2.3. Basic Parameters of The Mohr-Coulomb Model

The Mohr-Coulomb model requires a total of five parameters, which are generally familiar to most geotechnical engineers and which can be obtained from basic tests on soil samples. These parameters with their standard units are listed below:

E	$Young's\ Modulus$	**(KN/m^3)**
υ	$Poisson's\ Ratio$	**(-)**
$Ø$	$Friction\ Angle$	**(^{o})**
C	$Cohesion$	**(KN/m^2)**
ψ	$Diletancy\ Angle$	**(^{o})**

5.3.FEM Modelling and Analysis of Piles and Soil

The model consists of a single pile with cylindrical (circular) geometry and an under-reamed pile with single bubble of diameter 600mm, 900mm and 1200mm respectively for both types of piles that will be compared to each other on their load carrying capacity on the next chapter. In the model four different material are used the piles which have a material properties of a reinforced concrete and three layers of soil stratum with different soil parameters.

The geometrical representation of the piles is shown below in a two-dimensional schematic drawing thus, used as a very helpful demonstration for modelling of the piles and the soil layers in plaxis 3D foundation. All measurements shown in the geometrical presentation are in meter.

- **Geometrical representation of Friction Pile and Soil Layer**

The pile used have 18-meter length of depth with diameter of 600mm, 900mm and 1200 mm and it's a massive circular type of pile. The geometrical representation is shown below.

a) Diameter 600mm

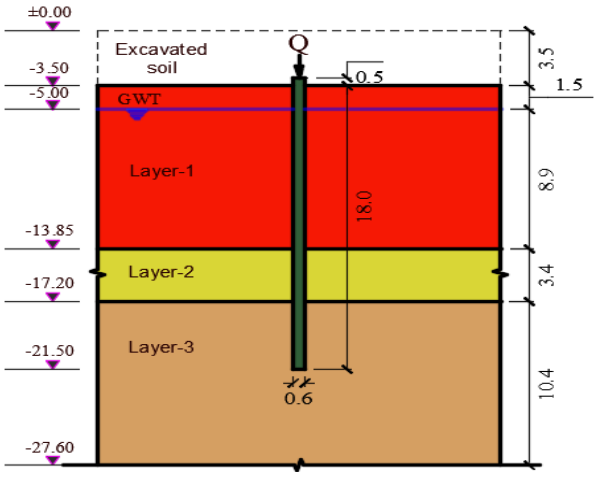

b) Diameter 900mm

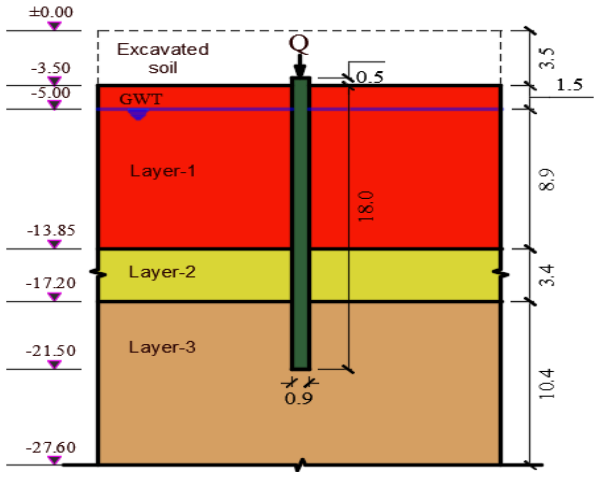

c) Diameter 1200mm

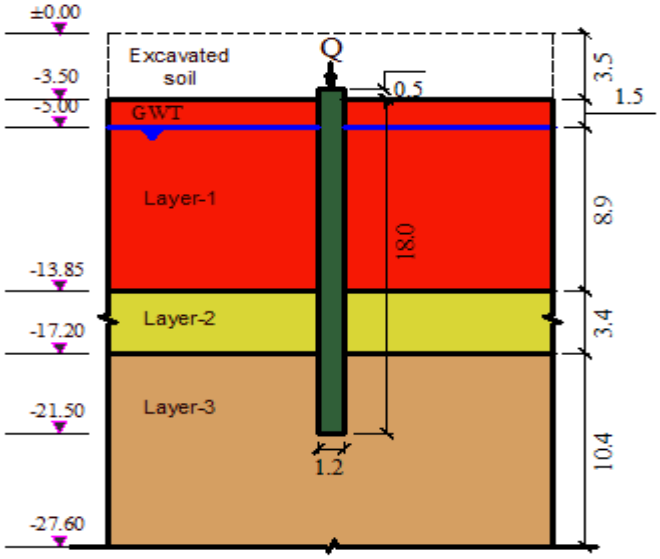

Figure 5.6 Geometrical representation Friction Pile and Soil Layer

- **Geometrical representation of Under-Reamed Pile and Soil Layer**

The pile Length and geometrical dimensions are calculated as per Indian code and (Meymand , 1998). The geometrical provisions are described in Literature review and refer to Figure 2.2. using the diagram and the table besides the diagram the geometrical representation of the under reamed pile for diameter 600mm, 900mm and 1200mm is shown below.

a) Diameter 600mm

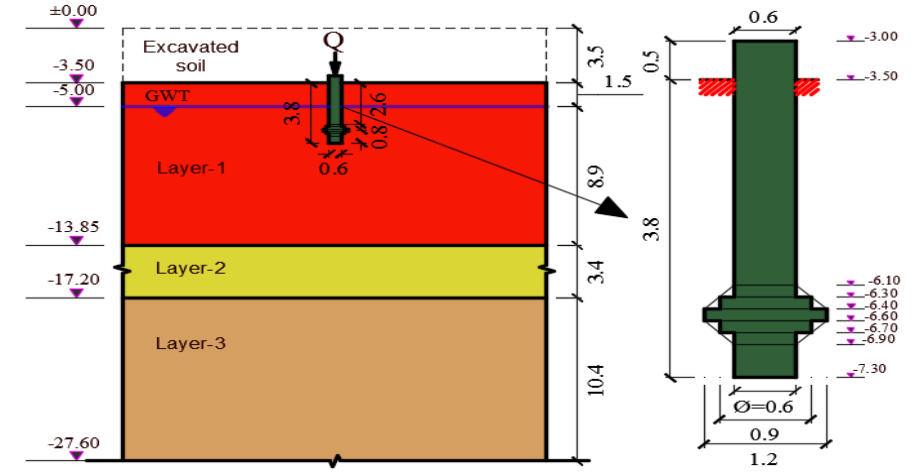

b) Diameter 900mm

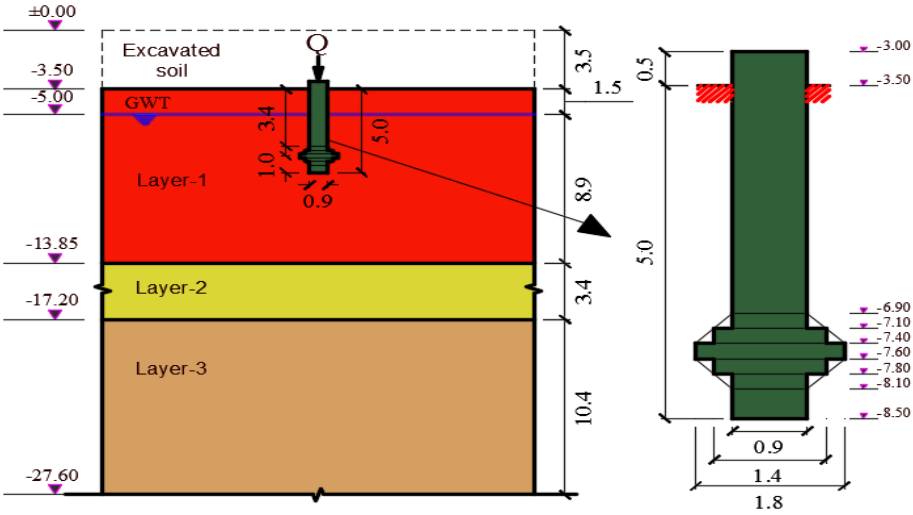

c) Diameter 1200mm

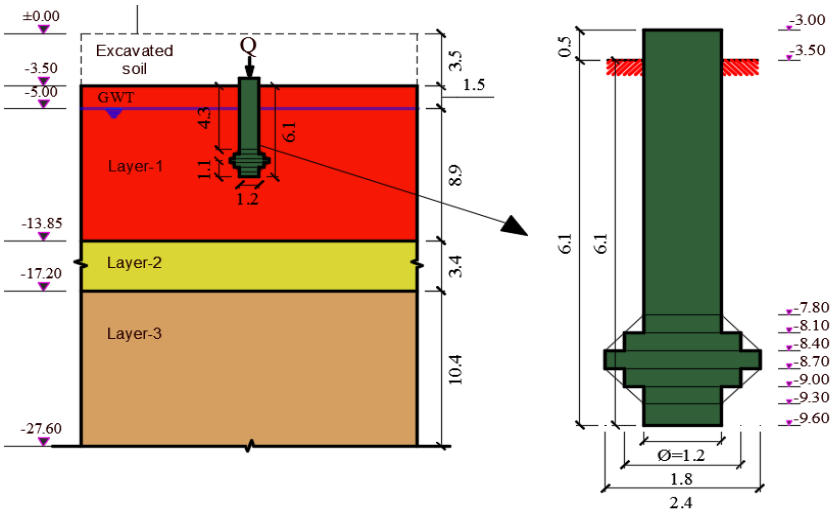

Figure 5.7 Geometrical representation of Under-Reamed Pile and Soil Layer

5.3.1. Geotechnical and Material Parameter for Input

The soil parameter used in this study is collected from Wogagen Bank S.C. Project as discussed in chapter three and there are three geometrically different frictional and under-reamed piles analysed using this parameter; which are used as input in plaxis 3d foundation. The material Properties introduced in the plaxis 3d foundation are tabulated below. The tabulated values are the same exact parameters and properties of material applied for the entire analysis except the young's modulus value of under-reamed piles which is referred from Table 4.11 because of different pile length for under reamed pile analysis; hence, depth will have influence on the elasticity modulus. The soil Pile interface (R_{inter}=1) i.e. there is no slip or gap between the soil and the pile when the load is applied.

Table 5.1 Geotechnical and material Parameters for Input in PLAXIS 3D Foundation

Parameter	Name	Layer-1	Layer-2	Layer-3	Friction Pile	Under-reamed pile			Units
						Ø600	Ø900	Ø1200	
General									
Material Model	Model	Mohr-coulomb	Mohr-coulomb	Mohr-coulomb	Linear-Elastic	Linear-Elastic	Linear-Elastic	Linear-Elastic	-
Drainage Type	Type	Undrained	Undrained	Undrained	Non-porous	Non-porous	Non-porous	Non-porous	-
Dry unit weight	γ_{unsat}	7.19	7.19	7.19	25	25	25	25	KN/m^3
Saturated unit weight	γ_{sat}	17	17	17	-	-	-	-	KN/m^3
Parameters									
Young's Modulus	E	4800	11400	8640	3.129E+07	3.00E+07	3.01E+07	3.02E+07	KN/m^2
Cohesion	C	60	72	72	-	-	-	-	KN/m^2
Internal Friction Angle	Ø	30	23	23	-	-	-	-	^{o}
Diletancy Angle	ψ	0	0	0	0	0	0	0	^{o}
Poisson's Ratio	υ	0.35	0.3	0.3	0.2	0.2	0.2	0.2	-
Interfaces									
Interface strength	-	Rigid	Rigid	Rigid	Rigid	Rigid	Rigid	Rigid	-
Interface Reduction Factor	R_{inter}	1	1	1	1	1	1	1	-
Initial									
K_O determination	-	manual	manual	manual	-	-	-	-	-
earth pressure at rest	K_{OX}, K_{OY}	0.54	0.5	0.55	-	-	-	-	-
Depth									
Height	H	13.85	3.35	10.4	18	3.8	5	6.1	m
Loading									
P=2000KN Negative Y direction									

5.3.2. Modelling Soil and Pile in PLAXIS 3D Foundation

To start with modelling of pile and soil stratum first describe the project name and dimensions of units with geometrical limit of soil in the X-Z axis (horizontal plane) in general setting menu. The next step is to define the work planes that will help in defining the depth of the pile and depth of excavation for top soil layer.

- **Pile Geometry**

The next step is to create the pile geometry by using pile tool then the pile designer will appear by selecting the Massive circular option with diameter as Per the different Geometrical presentations shown in Figure 5.6 and Figure 5.7. Be reminded that for each option of piles individual analysis is performed.

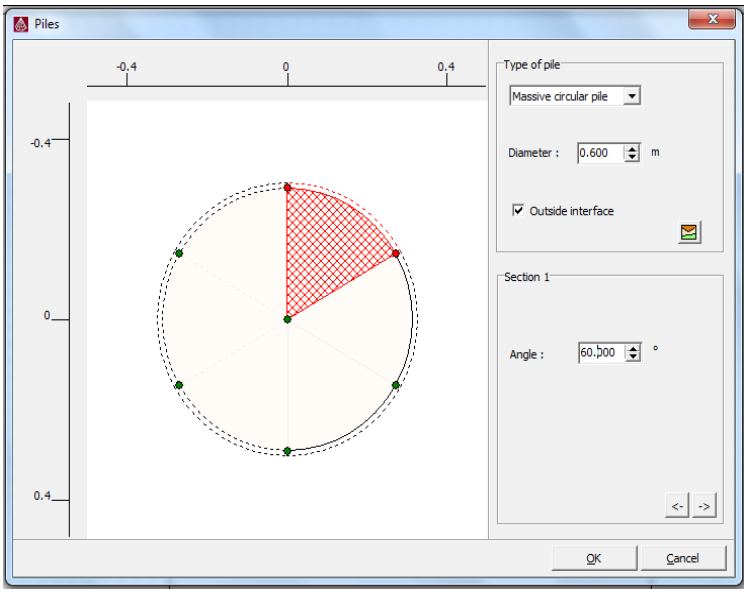

Figure 5.8 Pile Geometry Setup window

- **Setting Borehole and material properties**

Soil layers must be defined to do this a borehole needs to be added and material properties must be assigned therefore selected the borehole tool button and added a borehole at z- x plane (5,5) point. In this part the ground water table (GWT) was defined and coefficient of earth pressure at rest (K_O) is interred as an input.

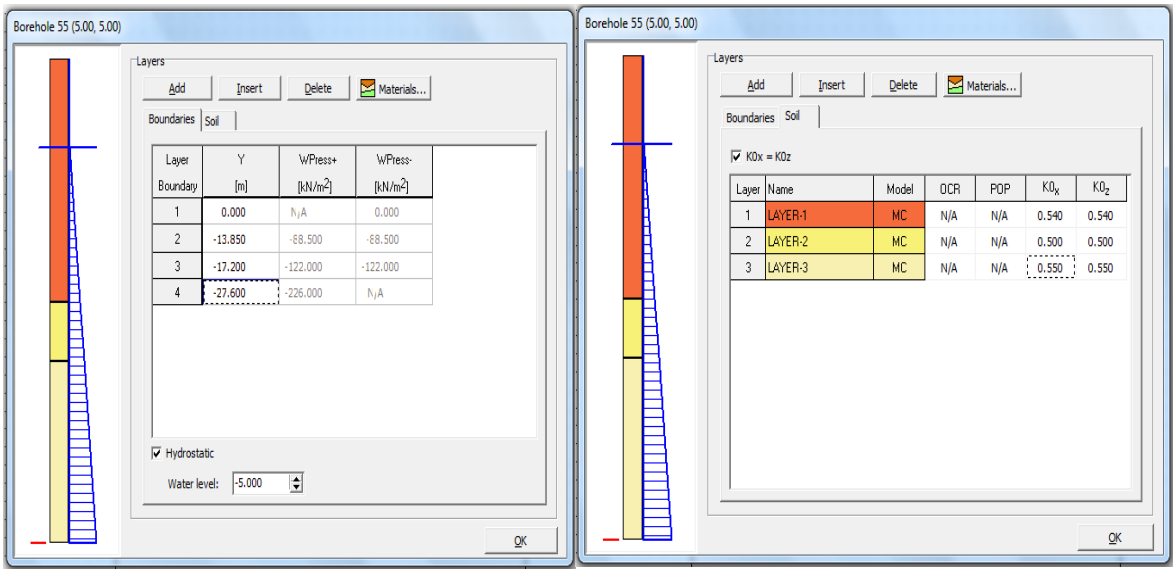

Figure 5.9 Bore-Hole and Material assigning windows

- **Setting Pile Loading Point**

To simulate the load test, a point load is added at the top of the pile. The loading is axially to negative Y direction and the same type and amount of loading is applied for all simulations in this study. Applied load is 2000KN for individual pile simulation. Point A in figure below is the point at which the load is applied at coordinate of (15,15, -3) of the three-dimensional work space.

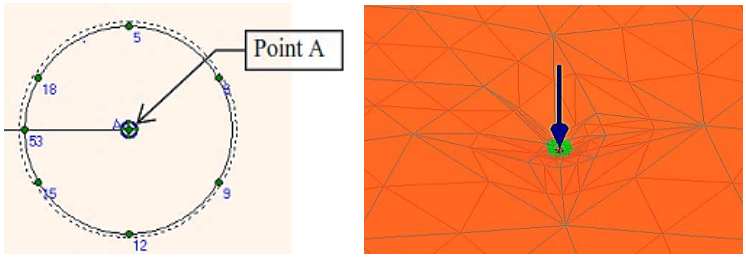

Figure 5.10 Loading Point in X-Z axis and 3D view

- **Mesh generation**

To perform finite element calculation, the model must be divided in to elements. The composition of finite element is called finite element mesh. First 2D mesh of work planes is generated to be fully satisfactory refinement is applied to global and local refinements. After 2D mesh refinement the 3D finite element mesh is generated that have 15 node wedge elements which are generated from 6 node triangular elements as shown in Figure 5.11.

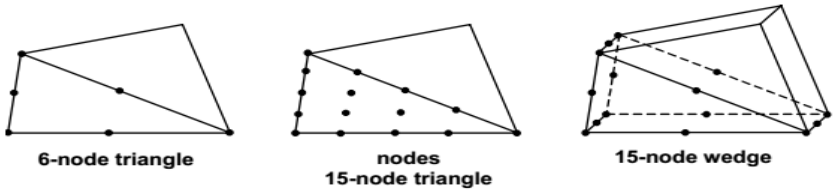

Figure 5.11 2D and 3D Elements in PLAXIS 3D foundation (Brinkgreve & Broere, 2006)

With the 3D mesh generation, the geometry, soil layer parameter and material parameter sets are all completed.

a) 2D mesh b) refined 2D mesh c) 3D refined mesh

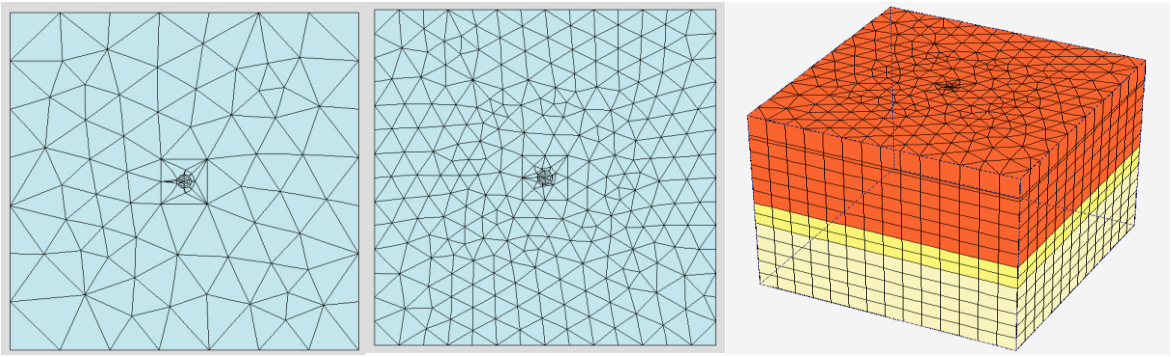

Figure 5.12 Mesh of the Model in PLAXIS 3D foundation

- **Defined Calculation stages**

The calculation stage is the next step that is done in the analysis by selecting calculation button above the geometry toolbar in the input program of Plaxis 3D foundation. Finite element calculation of the soil pile interaction is done by dividing the works in to several successive calculation phases. The phases used for the simulation of the piles soil interaction are shown in Table 5.2.

A plastic calculation is used to carry out an elastic-plastic deformation analysis according to small deformation theory. The stiffness matrix in a plastic calculation is based on the original undeformed geometry. This type of calculation is appropriate in most practical geotechnical applications. In general, a plastic calculation does not take time effects into account

Table 5.2 Sequential Calculation Phases

PLAXIS - Finite Element Code for Soil and Rock Analyses

Project description : FP Dia. 600mm — Plaxis 3D Foundation Version 1.6.0.193

User name : Construction Design S. Co.

Output : Calculations list

Identification	Phase No.	Start	Calculation type	Loading input	Time
Initial phase	0	N/A	K0 procedure	Staged construction	0.00 day
Construction of Pile	1	0	Plastic	Staged construction	0.00 day
Excavation of Soil	2	1	Plastic	Staged construction	0.00 day
Pile Loading	3	2	Plastic	Staged construction	0.00 day

CHAPTER 6. RESULTS AND DISCUSSION

In the model, there are three different friction pile and three different under-reamed pile which were simulated and analysed for getting the results. The result in terms of load carrying capacity with depth and displacement is shown separately for both types of piles thus, it is compared and discussed with help of graphical representation.

6.1.Result for Friction Pile

For frictional piles the model have three different options which is different in diameter and are the same in length, Young's modulus and soil stratum properties. Detailed model in graphics form is shown in Appendix 6.

As discussed in chapter five the modelling process have gone through the successive calculation phases and the out puts for the displacement of the piles with respect to depth of pile is shown below.

- **Diameter 600mm Friction Pile**

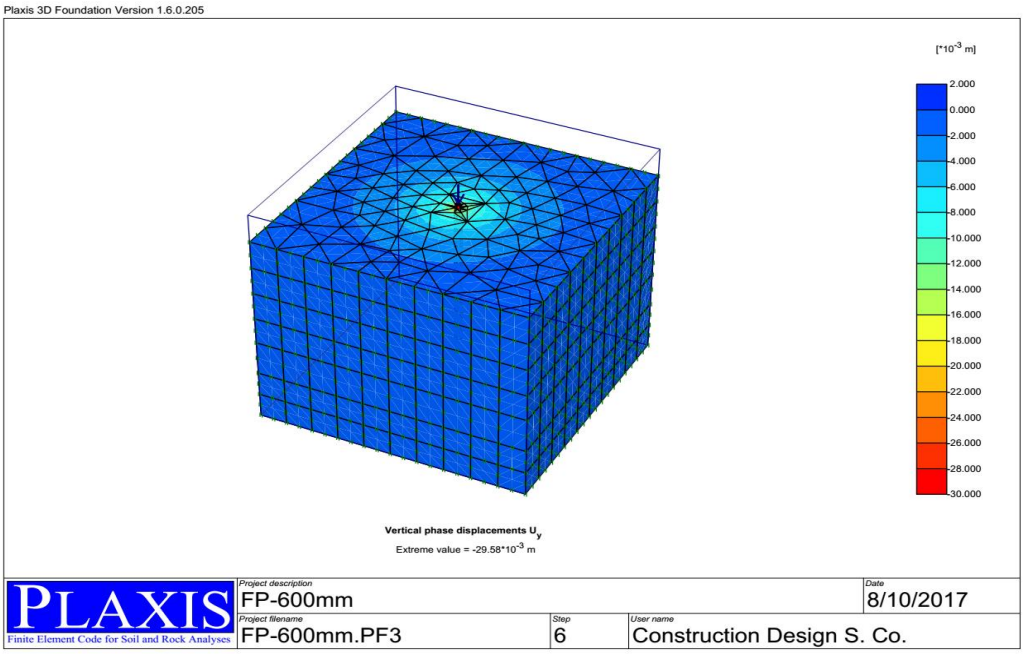

Figure 6.1 Vertical Phase Displacement U_Y for friction pile 600mm diameter 3D output

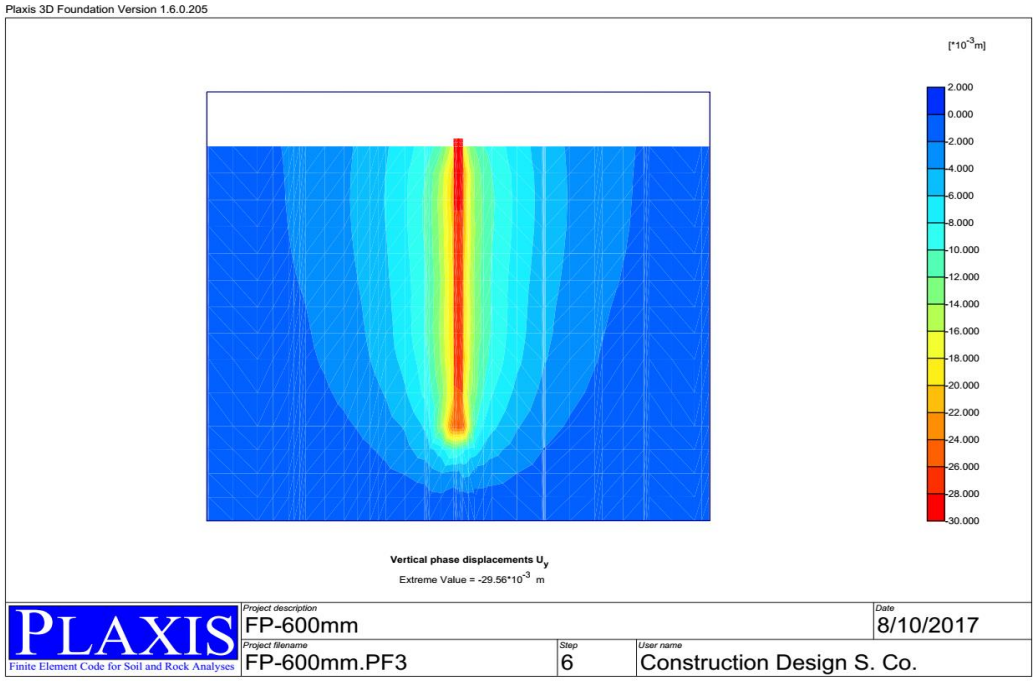

Figure 6.2 Vertical Phase Displacement U_Y for friction pile 600mm diameter sectional output view

- **Diameter 900mm Friction Pile**

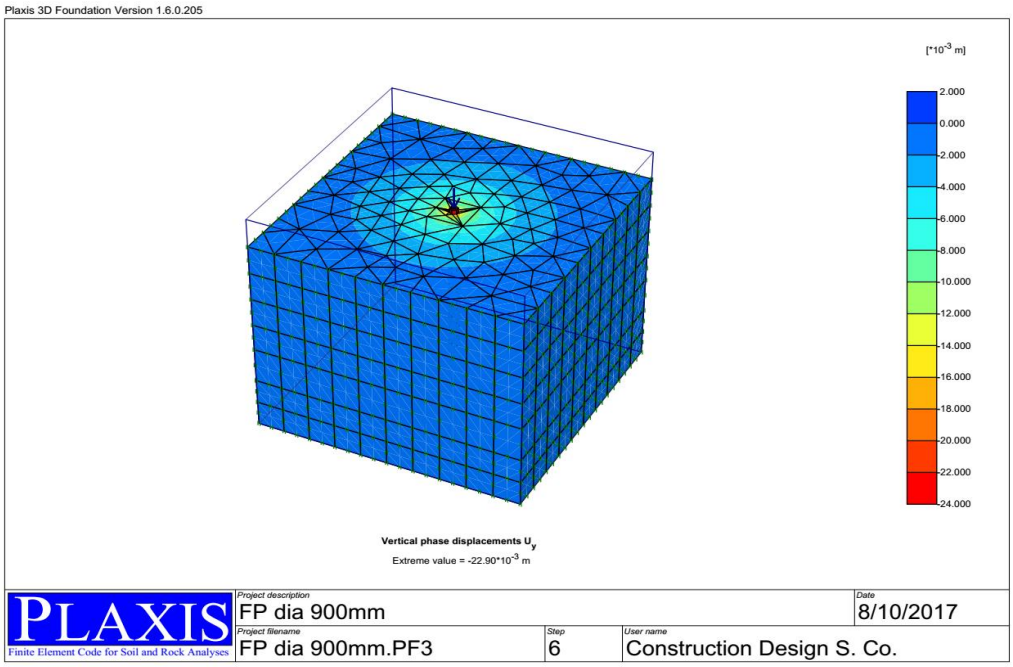

Figure 6.3 Vertical Phase Displacement U_Y for friction pile 900mm diameter 3D output

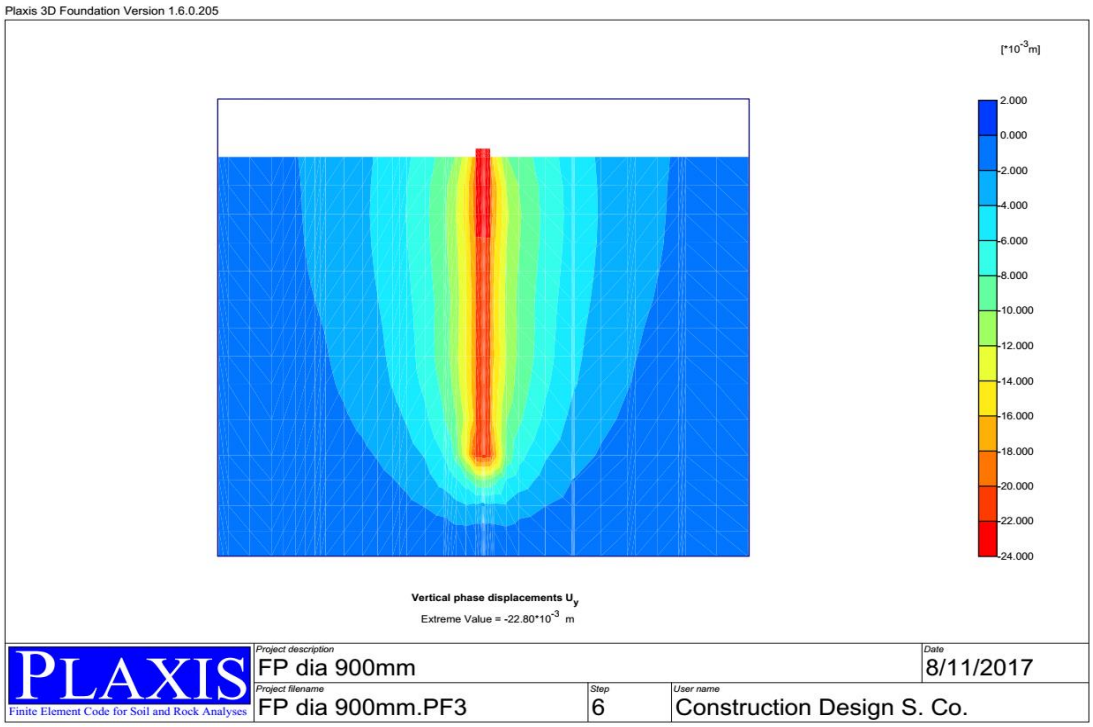

Figure 6.4 Vertical Phase Displacement U_Y for friction pile 900mm diameter sectional output view

- **Diameter 1200mm Friction Pile**

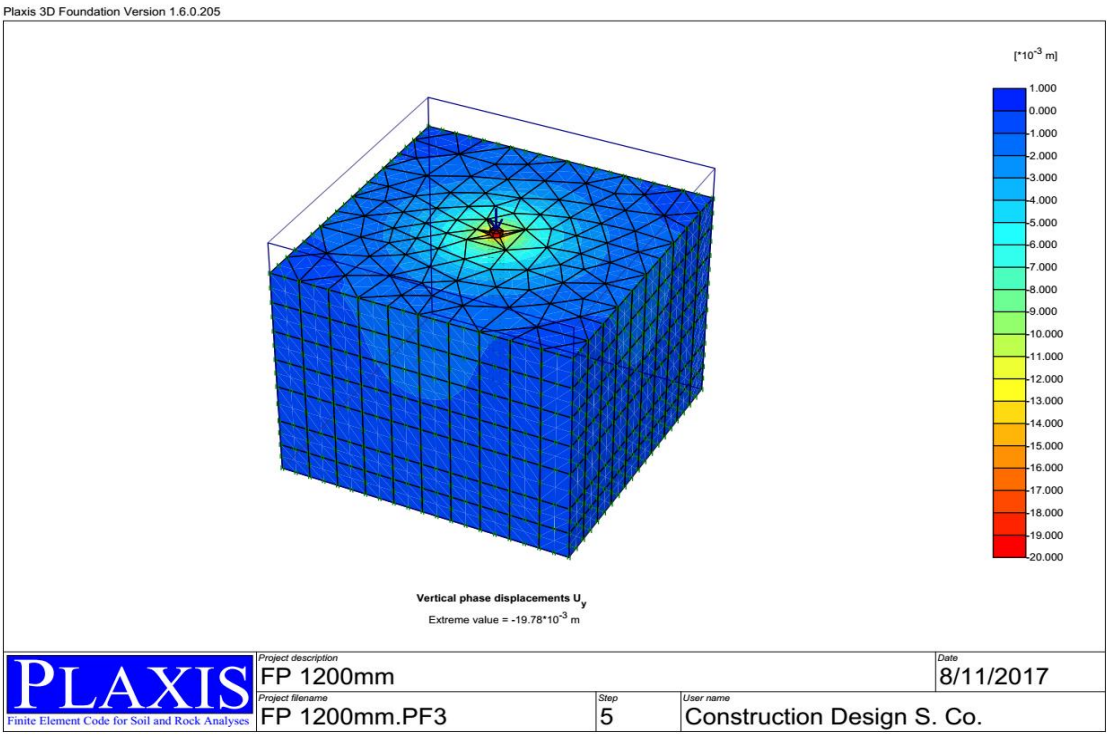

Figure 6.5 Vertical Phase Displacement U_Y for friction pile 1200mm diameter sectional output view

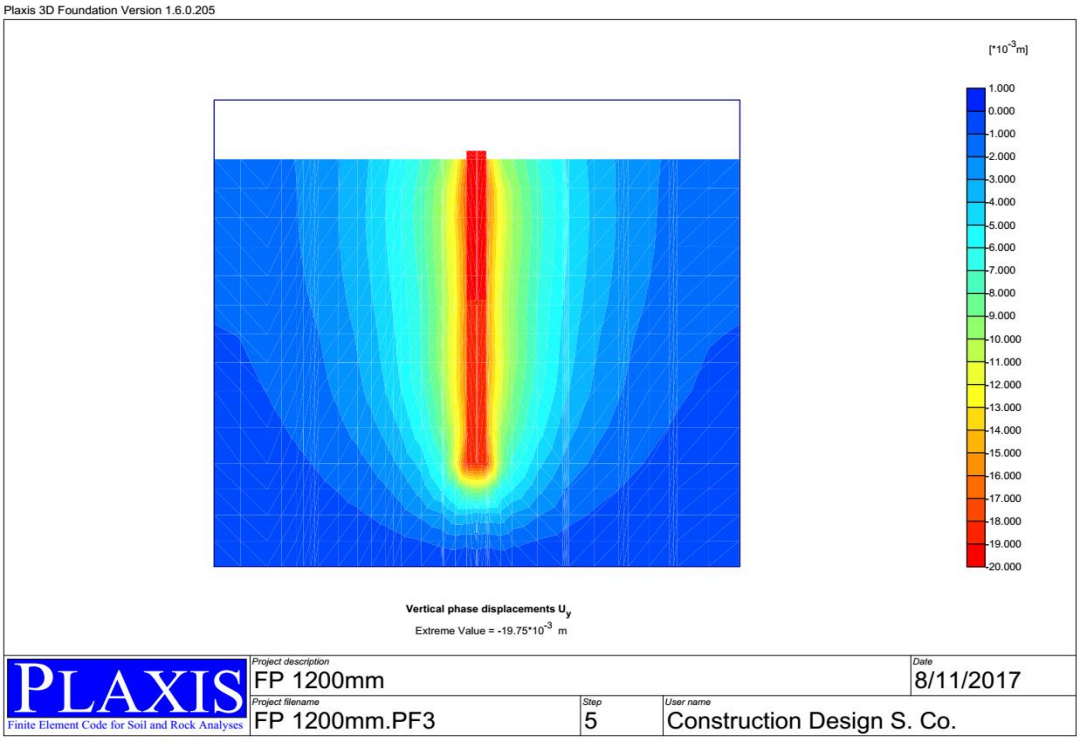

Figure 6.6 Vertical Phase Displacement U_Y for friction pile 1200mm diameter sectional output view

6.1.1. Variation of Vertical Phase Displacement of Friction Pile

For clear understanding of the outcome in PLAXIS the out puts for the displacement of the friction piles with respect to loading and depth is summarized in Table 6.1.

Table 6.1 PLAXIS output of vertical phase displacement for friction pile

Depth Y [m]	Friction Pile Diameter 600mm			Friction Pile Diameter 900mm			Friction Pile Diameter 1200mm		
	Node No.	N [kN]	Uy [mm]	Node No.	N [kN]	Uy [mm]	Node No.	N [kN]	Uy [mm]
-3.000	6103	-2000	-29.56	5907	-2000	-22.88	5858	-2000	-19.76
-3.250	6104	-2001	-29.19	5908	-2003	-22.66	5859	-2006	-19.61
-3.500	6105	-2003	-29.05	5909	-2007	-22.54	5860	-2012	-19.51
-5.225	6089	-1764	-28.59	5893	-1722	-22.33	5844	-1709	-19.37
-6.950	6091	-1554	-28.18	5895	-1495	-22.16	5846	-1475	-19.28
-8.675	6092	-1369	-27.76	5896	-1297	-21.97	5847	-1275	-19.17
-10.400	6094	-1179	-27.38	5898	-1098	-21.80	5849	-1076	-19.08
-12.125	6095	-1038	-27.02	5899	-961	-21.64	5850	-947	-18.98
-13.850	6097	-894	-26.69	5901	-821	-21.50	5852	-814	-18.91
-15.525	6098	-671	-26.41	5902	-618	-21.36	5853	-626	-18.83
-17.200	6100	-435	-26.19	5904	-399	-21.27	5855	-424	-18.78
-19.350	6101	-300	-25.98	5905	-302	-21.16	5856	-358	-18.71
-21.500	6102	-165	-25.84	5906	-206	-21.12	5857	-292	-18.69

Figure 6.7 Shows the load displacement curves of friction piles for diameter 600mm,900mm and 1200mm. The simulation was done using maximum load 2000KN applied at top of piles. Due to the load applied displacement of piles increases with the increase of load on piles taking depth of the pile.

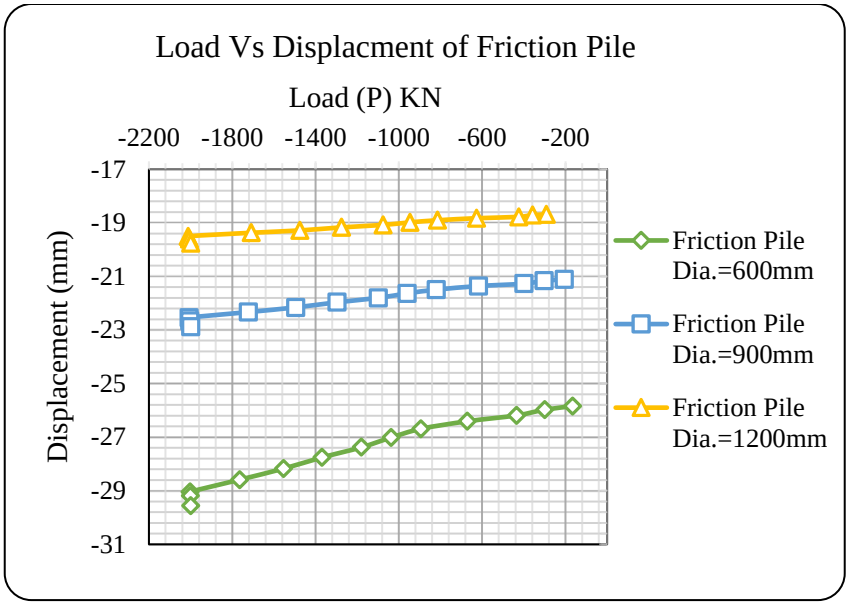

Figure 6.7 Load-Displacement relationship of friction piles

Figure 6.8 shows the relationship between the displacement of the piles with respect to the depth of piles. when the depth of piles increases the displacement of piles decreases.

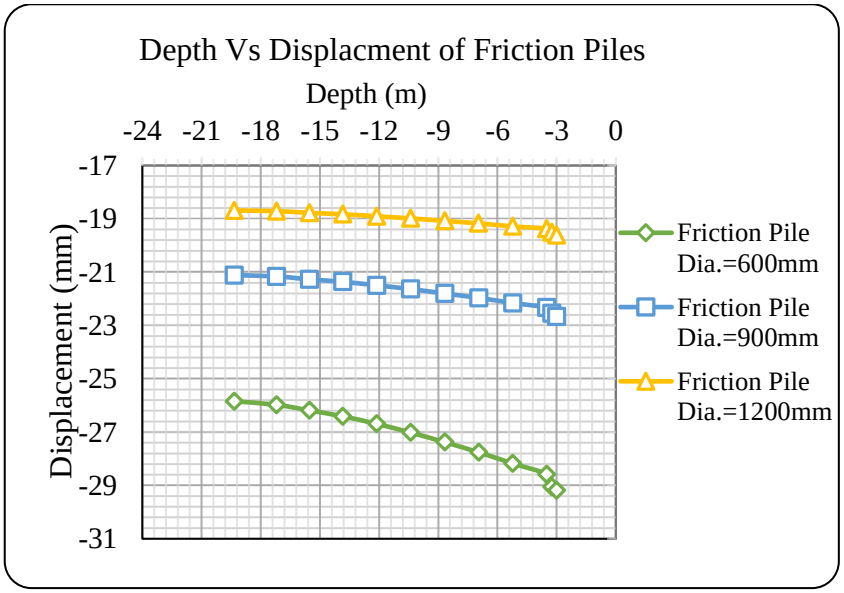

Figure 6.8 Depth-Displacement relationship of friction piles

6.2.Result for Under-Reamed Pile

For under-reamed piles the model have three different options which is different in diameter, length and Young's modulus parameters. Detailed model in graphics form is shown in Appendix 6.

The modelling process have gone through the successive calculation phases as discussed in chapter four using the geometrical demonstration in Figure 5.7 and the out puts for the deformation of the piles in terms of variation of phase vertical displacement over a depth of pile is shown below.

- **Diameter 600mm Under-reamed pile**

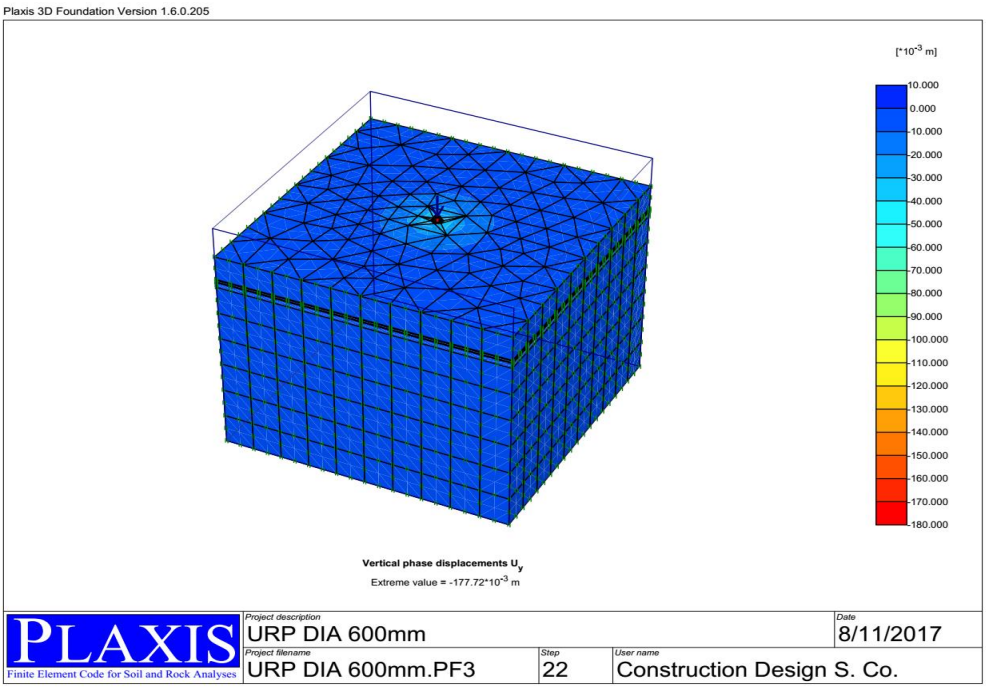

Figure 6.9 Vertical Phase Displacement U_Y for under-reamed pile 600mm diameter 3D output

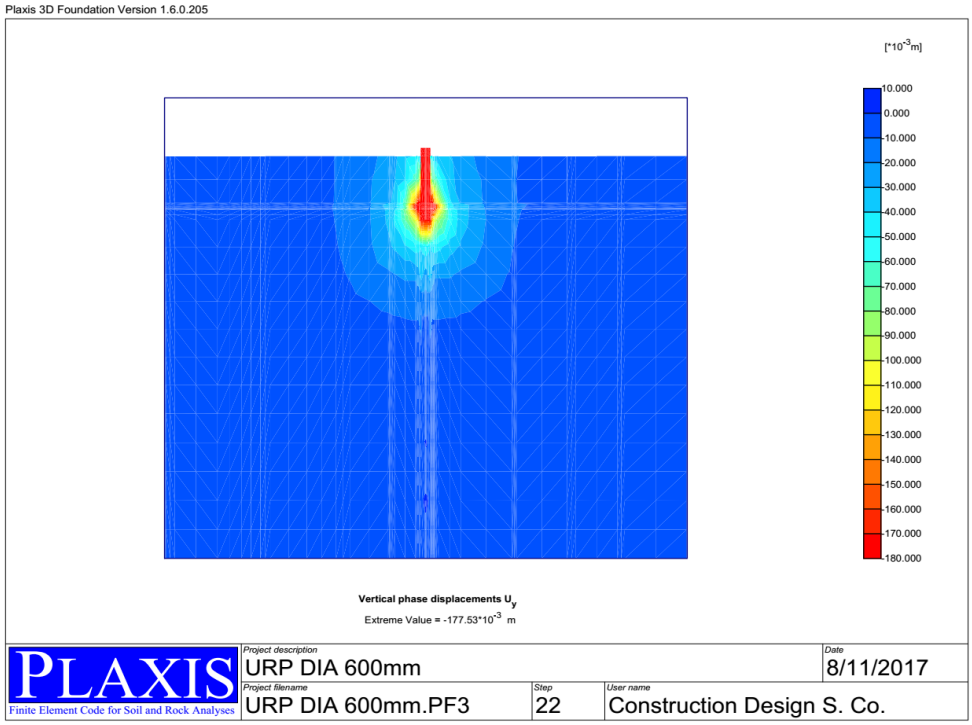

Figure 6.10 Vertical Phase Displacement U_Y for under-reamed pile 600mm diameter sectional output view

- **Diameter 900mm Under-reamed pile**

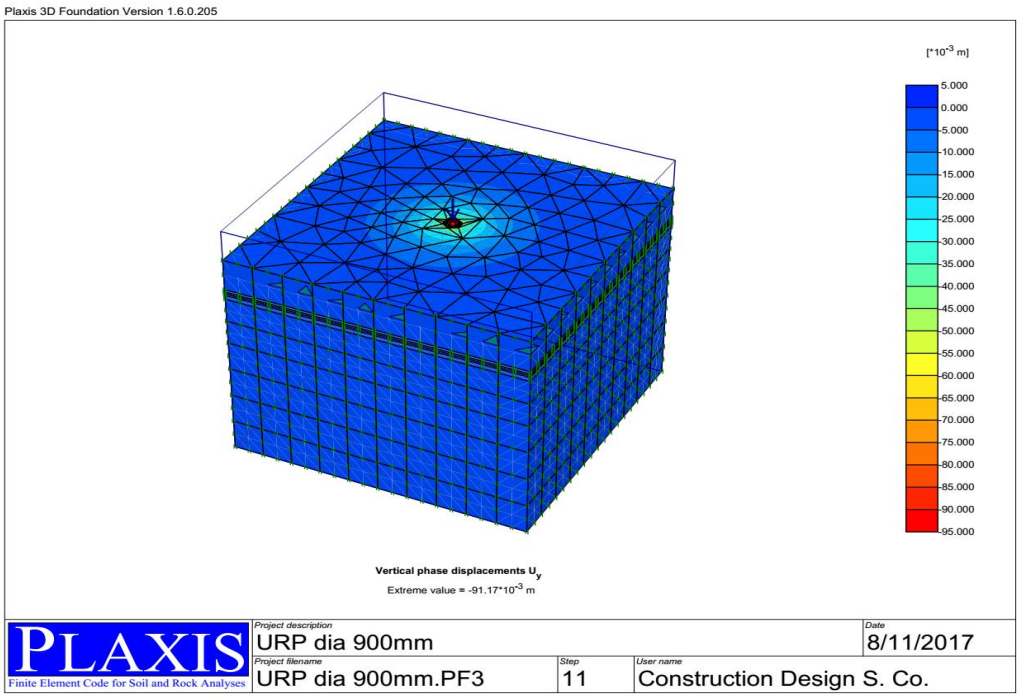

Figure 6.11 Vertical Phase Displacement U_Y for under-reamed pile 900mm diameter 3D output

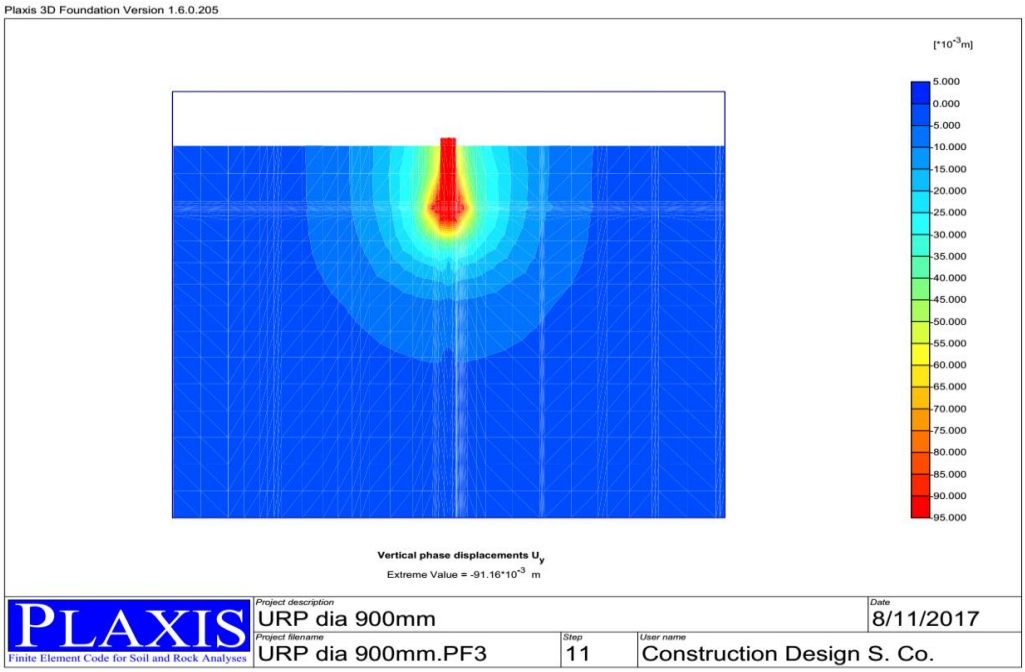

Figure 6.12 Vertical Phase Displacement U_Y for under-reamed pile 900mm diameter sectional output view

- **Diameter 1200mm Under-reamed pile**

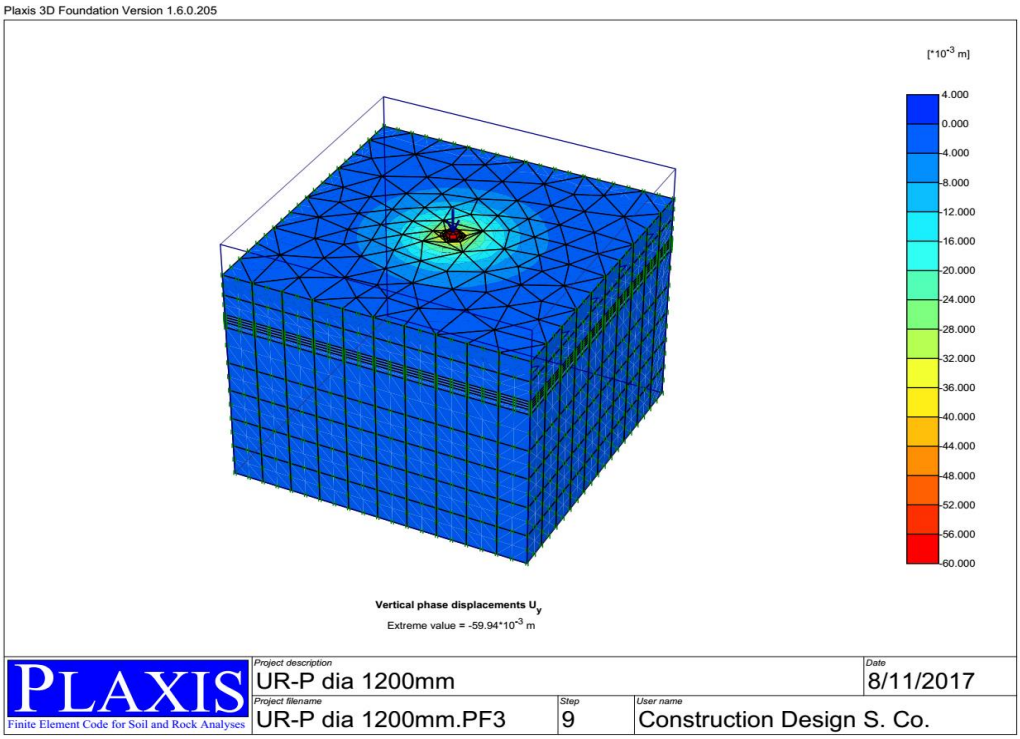

Figure 6.13 Vertical Phase Displacement U_Y for under-reamed pile 1200mm diameter 3D output

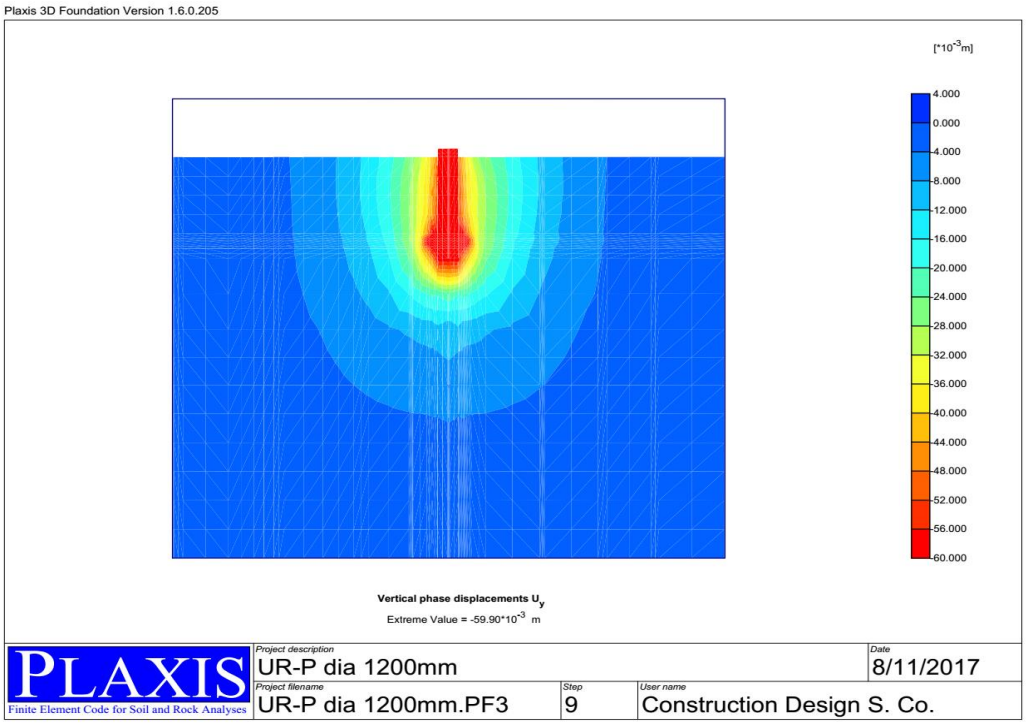

Figure 6.14 Vertical Phase Displacement U_Y for under-reamed pile 1200mm diameter sectional output view

6.2.1. Variation of Vertical Phase Displacement of Under-Reamed Pile

For clear understanding of the outcome in PLAXIS the out puts for the displacement of the under-reamed piles with respect to loading and depth is summarized in Table 6.2.

Table 6.2 PLAXIS output of vertical phase displacement for Under-reamed pile

Depth Y [m]	Under-reamed Pile Diameter 600mm			Depth Y [m]	Under-reamed Pile Diameter 900mm			Depth Y [m]	Under-reamed Diameter 1200mm		
	Node No.	N [kN]	Uy [mm]		Node No.	N [kN]	Uy [mm]		Node No.	N [kN]	Uy [mm]
-3	9076	-2000	-176.58	-3	9076	-2000	-91.15	-3	9114	-2000	-59.92
-3.25	9077	-2001	-176.18	-3.25	9077	-2003	-90.92	-3.25	9115	-2006	-59.76
-3.5	9078	-2003	-176.05	-3.5	9078	-2007	-90.80	-3.5	9108	-1973	-59.66
-4.9	9074	-1749	-175.66	-5.3	9074	-1605	-90.58	-4.65	9109	-1769	-59.56
-6.3	9075	-1496	-175.38	-7.1	9075	-1255	-90.45	-5.8	9111	-1540	-59.51
-6.35	9071	-1483	-175.36	-7.25	9071	-1251	-90.43	-6.95	9112	-1423	-59.44
-6.4	9072	-1485	-175.35	-7.4	9072	-1252	-90.42	-8.1	9113	-1306	-59.39
-6.5	9068	-1168	-175.34	-7.5	9068	-1031	-90.41	-8.25	9106	-1325	-59.39
-6.6	9069	-1169	-175.32	-7.6	9069	-1036	-90.41	-8.4	9107	-1332	-59.38
-6.65	9065	-537	-175.33	-7.7	9065	-570	-90.41	-8.55	9103	-1175	-59.37
-6.7	9066	-538	-175.32	-7.8	9066	-572	-90.41	-8.7	9104	-1187	-59.37
-7	9062	-339	-175.29	-8.05	9062	-316	-90.40	-8.85	9100	-628	-59.37
-7.3	9063	-317	-175.30	-8.3	9063	-312	-90.40	-9	9101	-635	-59.37
								-9.3	9097	-345	-59.36
								-9.6	9098	-346	-59.36

Figure 6.15 Shows the load displacement curves of under-reamed piles for diameter 600mm,900mm and 1200mm. The simulation was done using maximum load 2000KN applied at top of piles. Due to the load applied displacement of piles increases a slight with the increase of load on piles taking depth of the pile.

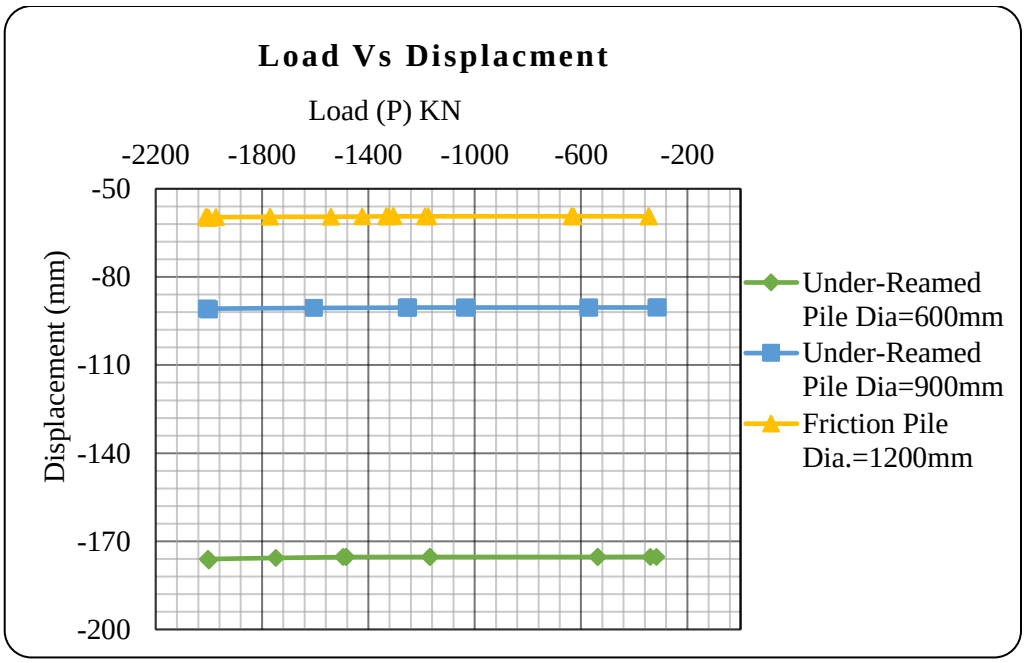

Figure 6.15 Load-Displacement relationship of Under-reamed piles

Figure 6.16 shows the relationship between the displacement of the piles with respect to the depth of piles. when the depth of piles increases the displacement of piles decreases slightly.

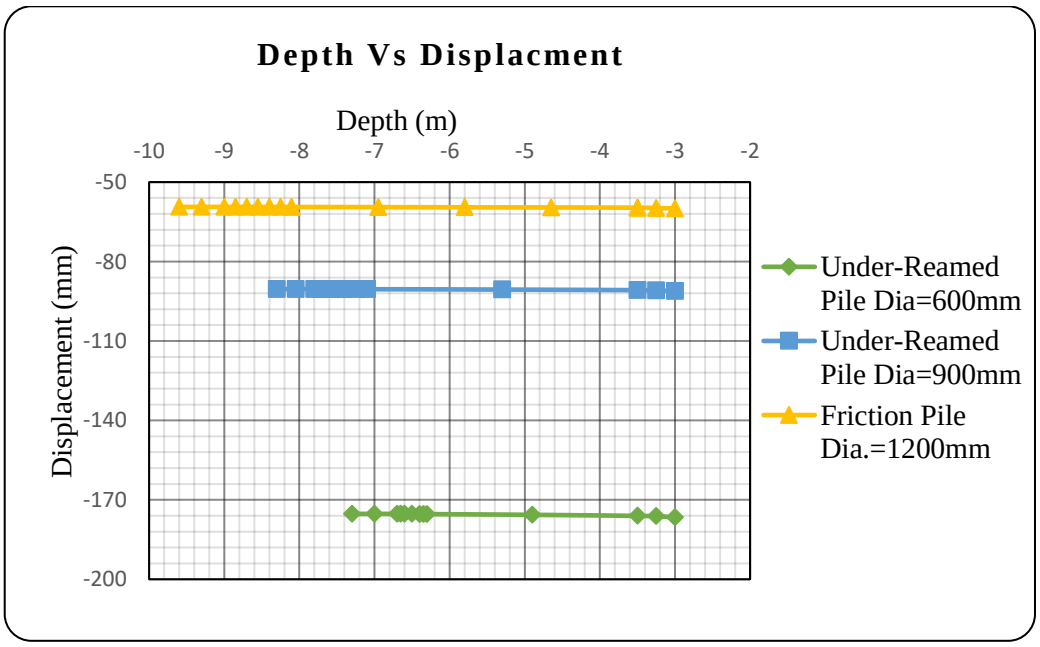

Figure 6.16 Depth-Displacement relationship of under-reamed piles

6.3. Comparative Study on Load Carrying Capacities of Piles

The displacement of the pile decreases as the diameter of the piles increases. The decrease in displacement of the piles indicates that the foundation load carrying capacity is good in return if the displacement of the piles increases then the piles load carrying capacity is less and the foundation must improve. Comparing the displacement relationships of friction pile and under-reamed pile referring Figure 6.17 percentile decrease in displacement of the piles is discussed below.

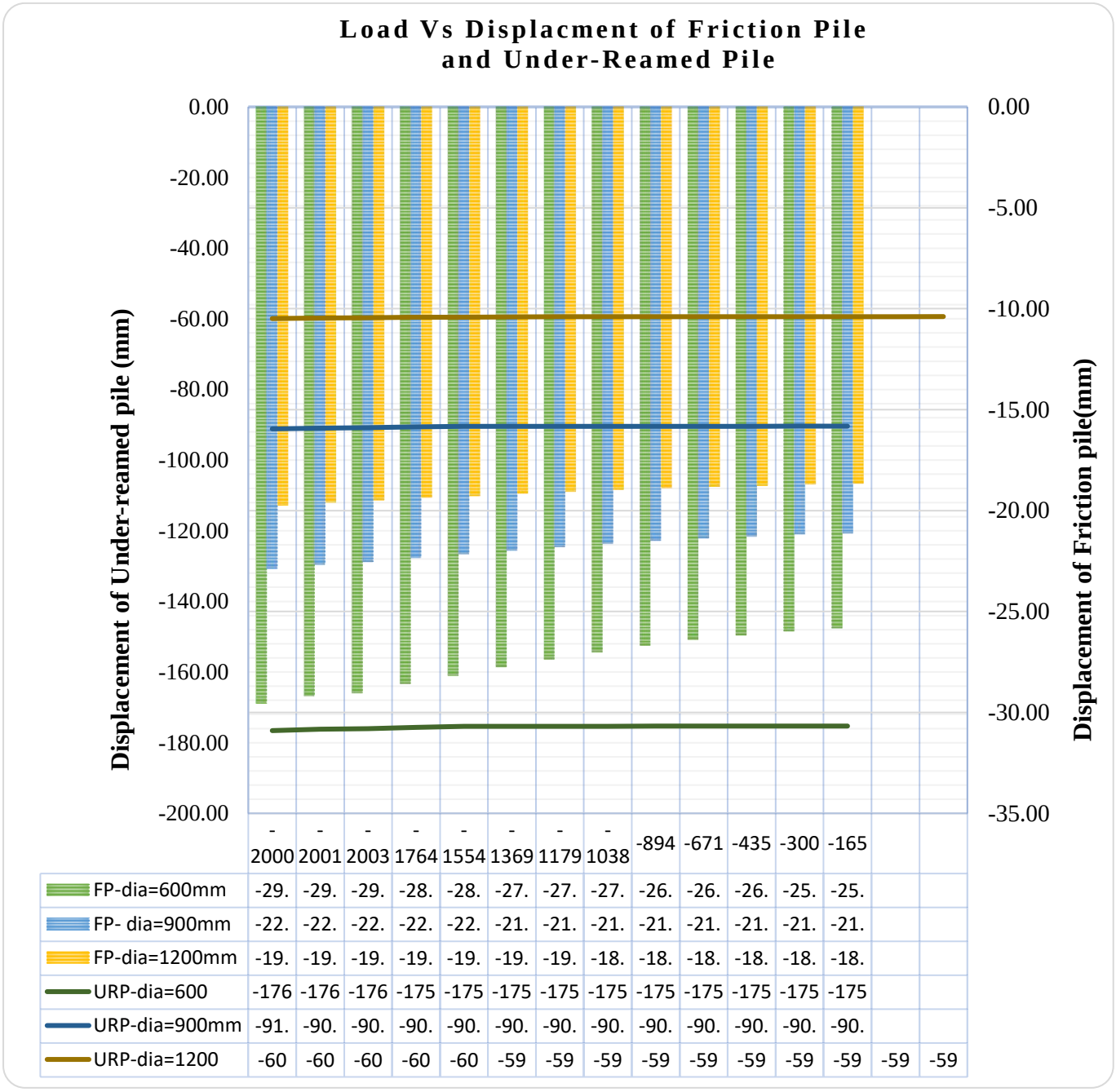

	-2000	-2001	-2003	-1764	-1554	-1369	-1179	-1038	-894	-671	-435	-300	-165		
FP-dia=600mm	-29.	-29.	-29.	-28.	-28.	-27.	-27.	-27.	-26.	-26.	-26.	-25.	-25.		
FP- dia=900mm	-22.	-22.	-22.	-22.	-22.	-21.	-21.	-21.	-21.	-21.	-21.	-21.	-21.		
FP-dia=1200mm	-19.	-19.	-19.	-19.	-19.	-19.	-19.	-18.	-18.	-18.	-18.	-18.	-18.		
URP-dia=600	-176	-176	-176	-175	-175	-175	-175	-175	-175	-175	-175	-175	-175		
URP-dia=900mm	-91.	-90.	-90.	-90.	-90.	-90.	-90.	-90.	-90.	-90.	-90.	-90.	-90.		
URP-dia=1200	-60	-60	-60	-60	-60	-59	-59	-59	-59	-59	-59	-59	-59	-59	-59

Figure 6.17 Load-Displacement relationship of Under-reamed pile and friction pile

For frictional pile diameter 600mm the displacement of the pile decrease by 83 % from the under-reamed pile of diameter 600mm. The displacement of friction pile 900mm diameter decreases by 75% from under-reamed pile of diameter 900mm, and the displacement of friction pile diameter of 1200mm decreases by 67% from under-reamed pile of 1200mm diameter.

The results obtained for under reamed pile shows that load carrying capacity of 1200mm diameter under-reamed pile is 66% greater than a 600 mm diameter under-reamed pile this implies the result obtained in this study have directly proportional relationship to the study by (Bale & Hari, 2015). Per (Bale & Hari, 2015) on under reamed piles it showed that increased diameter of under-reamed pile decreases the displacement of the under-reamed pile.

Considering the height of piles; the displacement of the piles decreases as the height of the pile increases.

CHAPTER 7. CONCLUSIONS AND RECOMMENDATIONS

7.1. Conclusion

The purpose of this thesis was to compare load carrying capacity of friction and under-reamed pile under an axial load and determine the load settlement relations. Numerical analysis method such as finite element method, is widely used to predict the bearing capacity and settlement of pile foundations. In this study PLAXIS 3D foundation a soil and rock analysis finite element software package is used as its preferred in many geotechnical problems due to its powerful capabilities in non-linear analysis. The conclusion from these numerical studies are drawn as follows.

- Mohr coulomb soil model and linear elastic model of pile can model the pile soil interaction mechanism for simulating the load carrying capacities of friction and under-reamed piles.
- Modeling of the interface behavior between the pile and the soil is important in the analysis of pile under vertical loading. In the numerical analysis done, Rinter = 1 interface constant was used and the pile is assumed in perfect contact with adjacent soils. From the result obtained so far, it can be deduced that the ideal contact interface used in this study can model the pile soil interaction mechanism.
- The observation in the case of frictional pile, shows that the displacement of pile decreases with the increase of diameter without changing the height of pile. This result shows the improvement in displacement of the friction pile by 33% because of the increase in diameter of piles from 600mm to 1200mm.
- The observation in the case of under-reamed pile, shows that the displacement of pile decreases with the increase of diameter, height and elasticity modulus of the pile. This result shows the improvement in displacement of the pile by 66% because of the increase in diameter and height of the pile.
- From the comparative study on the load carrying capacity of the piles the change in the improved displacement is much greater for under-reamed pile than friction piles. The improvement shows its two times greater for under- reamed pile than of friction pile.
- the displacement of the piles with respect to increasing depth of the pile have a decreasing relationship.
- Finally, with the rapid growing numerical analysis using a finite element method, practicing engineers currently are making use of finite element analysis to solve

different geotechnical problems. Thus, by combining more real soil data and parameters representing the actual soil features, and by choosing a suitable constitutive model and theories, simulation results of pile load carrying capacity can be engaged as one alternative to estimate the ultimate capacity of a vertically loaded pile without performing the static load test.

7.2. Recommendation

In following ways, this work can be extended and studied for the future in the geotechnical engineering discipline

- In this thesis, the soil was modelled using the well-known Mohr coulomb model. If more detailed comparisons are intended; thus, realistic behavior of the soil pile interaction can be done using hardening soil model with help of elaborated soil data.
- Soil parameters used for numerical analysis for this study are obtained from geotechnical investigation reports which need some parameters to be correlated by different standards. Limited parameters are directly taken from test result. This can be raised as one significant drawback in this study. A better FEM simulation result could have been obtained, if most soil parameters have been directly determined from laboratory and field test results specifically needed for this study.
- The analysis was carried out considering a vertical point load only but for further studies it could be possible to show the effect of using different loading like lateral load and dynamic load to show the simulations of finite element analysis.
- In this study a single friction pile and under-reamed pile with different diameter are analysed in finite element method to compare their load carrying capacity. Further study could be conducted on the group of piles for friction and under-reamed piles and study their comparative load carrying capacity.

References

Alemayehu, T. & Solomon, Y., 1986. Investigation on the Expanxive soil of Addis Ababa. *EAEA*, Volume 7, p. 1.

Anon., 1981. Code of Practice for Design and Construction of Pile Foundation. In: New Delhi: Bureau of indian standard.

Bale & Hari, 2015. *Numerical Investigation of Under Reamed Piles.* Chennai, India, the sixth international geotechnical symposium.

Bowles, J. E., 1997. *Foundation Analysis and Design.* Peoria Illinois: The McGraw-Hill Companies,Inc..

Braja, M. D., 2007. *Principles of foundation engineering.* 6th ed. united states: Chris Carson.

Braja, M. D., 2007. *PRINCIPLES OF FOUNDATION ENGINEERING.* 6th ed. united states: Chris Carson.

Brinkgreve, R. & Broere, W., 2006. Plaxis 3D Foundation Version 1.5 manual. In: Netherlands: Delf university of technolgy and plaxis.

Craig, R., 2004. *Craig's Soil Mechanics.* New York, USA: CRC Press.

Daryl , L., 2011. *A first course in the finite element method.* s.l.:Cengage Learning.

Desai, C. & Zaman, M., 2013. Advanced Geotechnical Engineering: Soil-Structure Interaction using Computer and Material Models. *Boca Raton, Florida, USA : CRC Press.*

Devendra, S., Jain, M. & Chandra, P., 1978. *Handbook on Under-reamed and Bored compactoin pile foundation.* Roorkee: Central Building Research Institute.

Engin, Brinkgreve , Septanika & Bonnier, 2009. Modelling piled foundation by means of embeded piles. pp. 132-136.

Ergys, A., Neritan, S. & Luisa, D., 2014. Axial Load Capacity of Cast in Place Piles from SPT and CPTU Data. *World Journal of Engineering and Technology.*

Gercek & H., 2007. Poisson's ratio values for rocks. *International Journal of Rock Mechanics and Mining Sciences.*

Gupta, S. & Sundaram, R., 1986. For which soil conditions are Under-reamed pile foundations superior to other foundations system. Volume II, pp. 131-133.

Hamid, A., Zahra, M. & Safa, D., 2014. Influence of Under-reamed Pile Groups Arrangement on Tensile Bearing Capacity using FE Method. *EJGE*, Volume 19.

Helwany, S., 2007. Applied Soil Mechanics with Abaqus Applications. *Hoboken, New Jersey, USA: John Wiley and Sons.*

Helwanys, S., 2007. In: *Applied soil mechanics with abacus application.* New Jersey: John wileys and sons.

Hesham, M. & Naggar, E., 2002. *The role of soil–pile interaction in foundation engineering.* Canada, NRC Research Press.

Hill, R., 1998. *The mathematical theory of plasticity.* s.l.:oxford university press.

Johnson, L. P. ,. K. a. S., 2006. Modelling the Load-deformation Response of Deep Foundations under Oblique loading.. *Environmental Modelling and Software,* pp. 1375-1380.

Joram M, A., Carlos , L. & Erez I, A., n.d. Modulus of elasticity in deep bored piles.

Lymon, C., William , M. & Shin-Tower, W., 2006. *Analysis and Design of shallow and deep foundation.* Canada: John Wiley & Sons, INC.

Meymand , 1998. Shaking Table Scale Model Tests Of Non linear Soil-Pile Superstructure Interaction In Soft Clay..

Michell, J., 2001. Reexamination of Swelling Phenomena in Earth Materials. Soil Behavior and Soft Ground. *Cambridge: ASCE.,* pp. 1-24.

Millot, G., 1979. Clay. *Scientific America,* pp. 109-118.

Muravha, S. E., 2012. Foundation on expansive. *UNIVERSITY OF PRETORIA, Department of Geology,* p. 1.

Pablo, B., Kenny , K. & Rune, C., 2016. *Finite element investigation of the interaction between a pile and a soft soil focussing on negative skin friction.* Denmark, NGM 2016 Proceedings.

Poulos, 1980. *Pile foundation analysis and design.* The university of Sydney: Rainbow-Bridge book co..

Poulos, H. G., 2015. *Soil-structure interaction in tall Buildings foundation design.* Australia, The HKIE Geotechnical division annual seminar.

Reddy, J., 2006. *An introduction to the finite element method.* third ed. Texas: McGraw-Hill, New York.

Reul & Randolph, 2003. Piled rafts in over consolidated clay: comparison of in-situ measurement and numerical analysis. Volume 53, pp. 301-315.

Rovithis, P. M., 2008. Seismic analysis of coupled soil-pile-structure systems leading to the definition of a pseudo-natural SSI frequency.

Schnaid, F., 2009. In Situ Testing in Geomechanics. In: 1st ed. London, New york: Taylor and Francis.

Simeneh , A., 2009. Analysis and Parametric Study of Piled Raft Foundation Using Finite Element Based Software. *M.Sc. Thesis, School of Graduate Studies of Addis Ababa University, AAiT/AAU Addis Ababa Ethiopia.*

Verruijt, A., 2012. Offshore Soil Mechanics. *Delft University of Technology.*

Verruijt, A., 2012. Soil Mechanics. In: Delft, the Netherlands: Delft University of Technology.

Xiao, H.-b., Chun-shun Zhang, S., Wang, Y.-h. & Fan, a. Z.-h., 2011. Pile-Soil Interaction in Expansive Soil Foundation:. *American Society of Civil Engineers.*

Zahra, M., Hamid, A. & Mortazari, S., 2013. *Numerical Evaluation of tensile bearing capacity of Under-reamed pile group in granular soil using finite element method.* Tabriz, Iran, Islamic Azad University of Tabriz.

Zeleke, B., 2015. Simulation of Pile Load Test Using Finite Element Methods. *M.Sc. Thesis, School of Graduate Studies of Addis Ababa University, AAiT/AAU Addis Ababa Ethiopia,* p. 1.

Annex

Appendix 1-Geological cross-section and Location Map

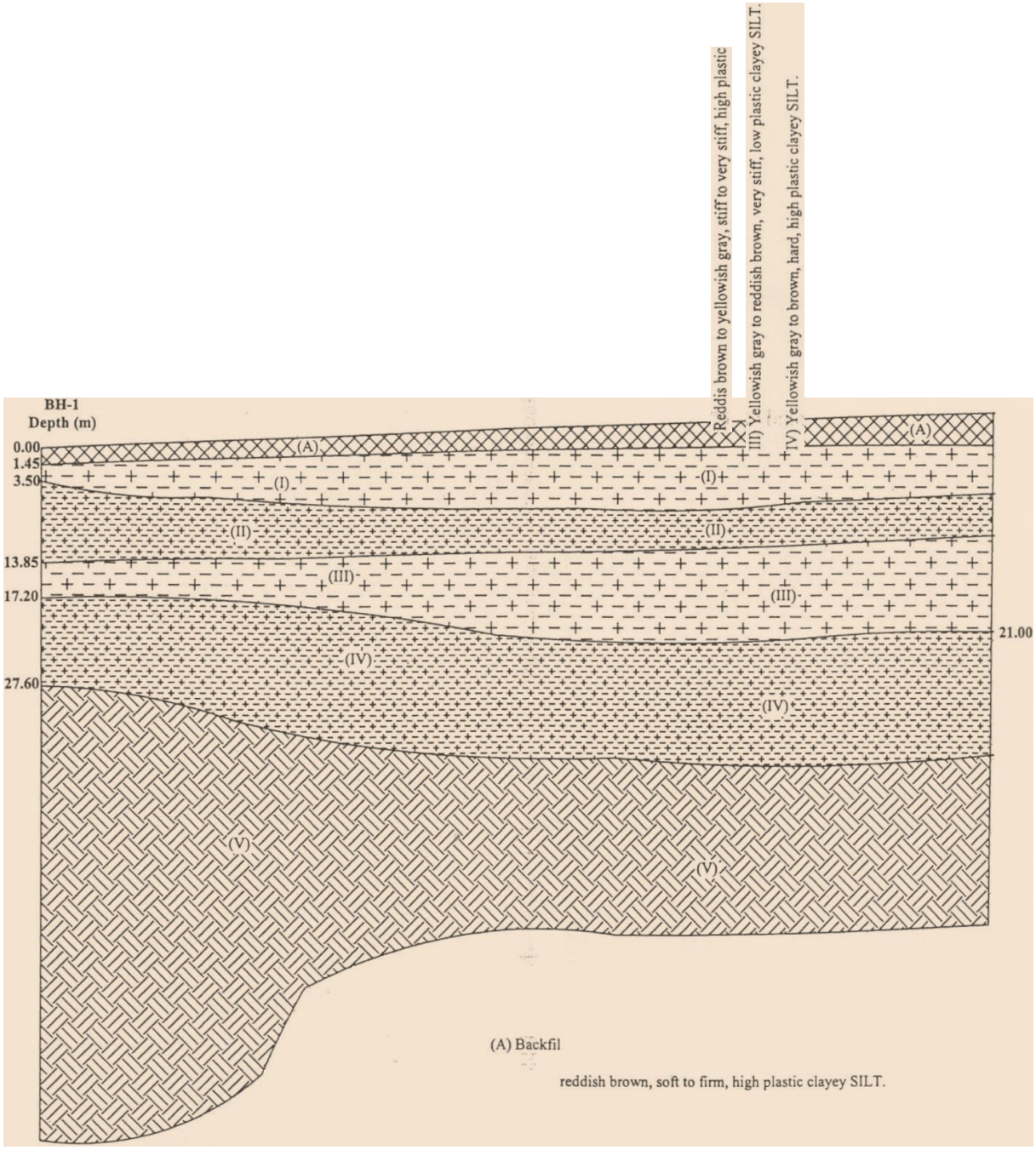

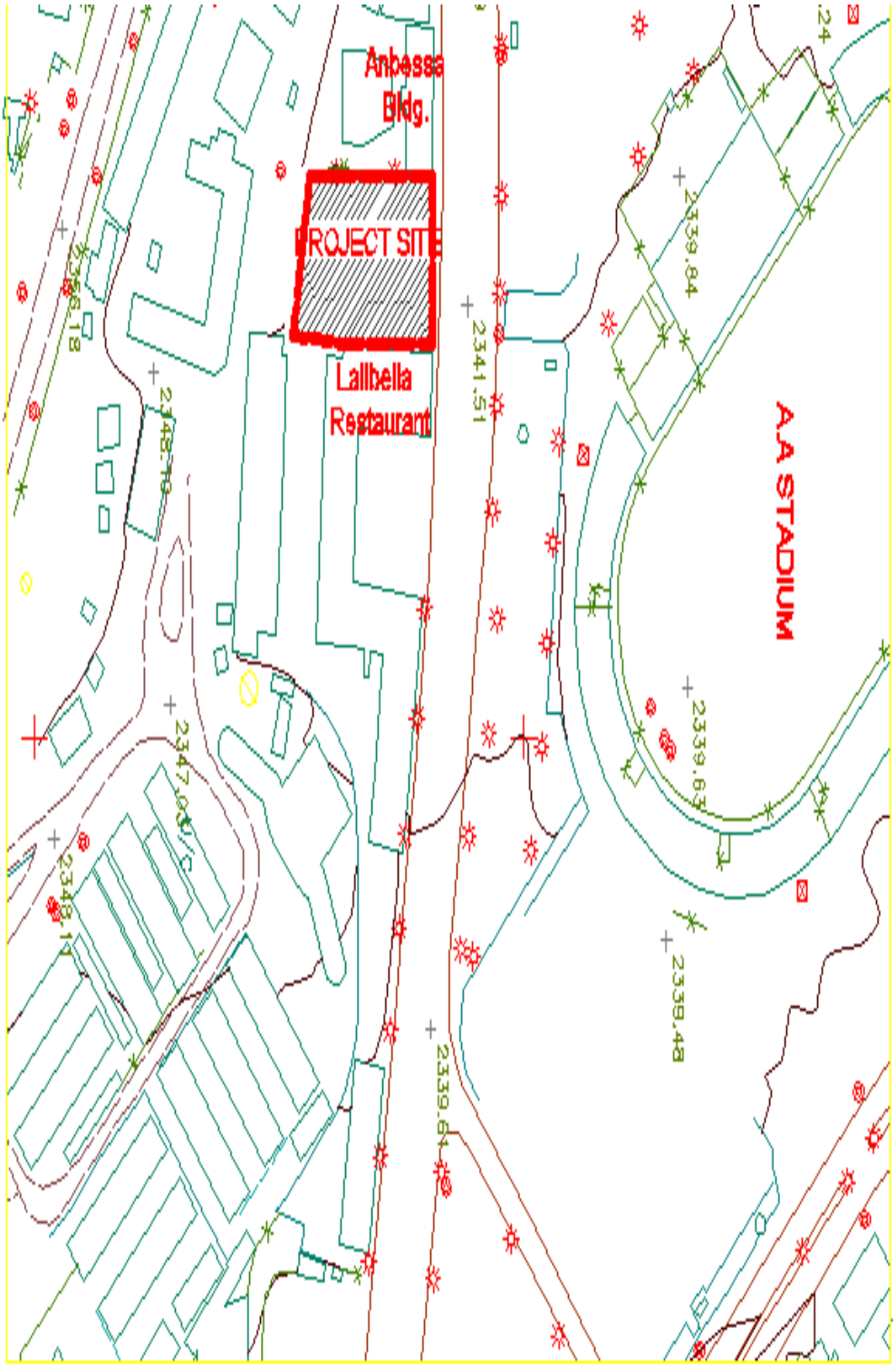

LOCATION MAP

GIS MAP OF KIRKOSE KEFLE KETEMA

Appendix 2- Borehole Location

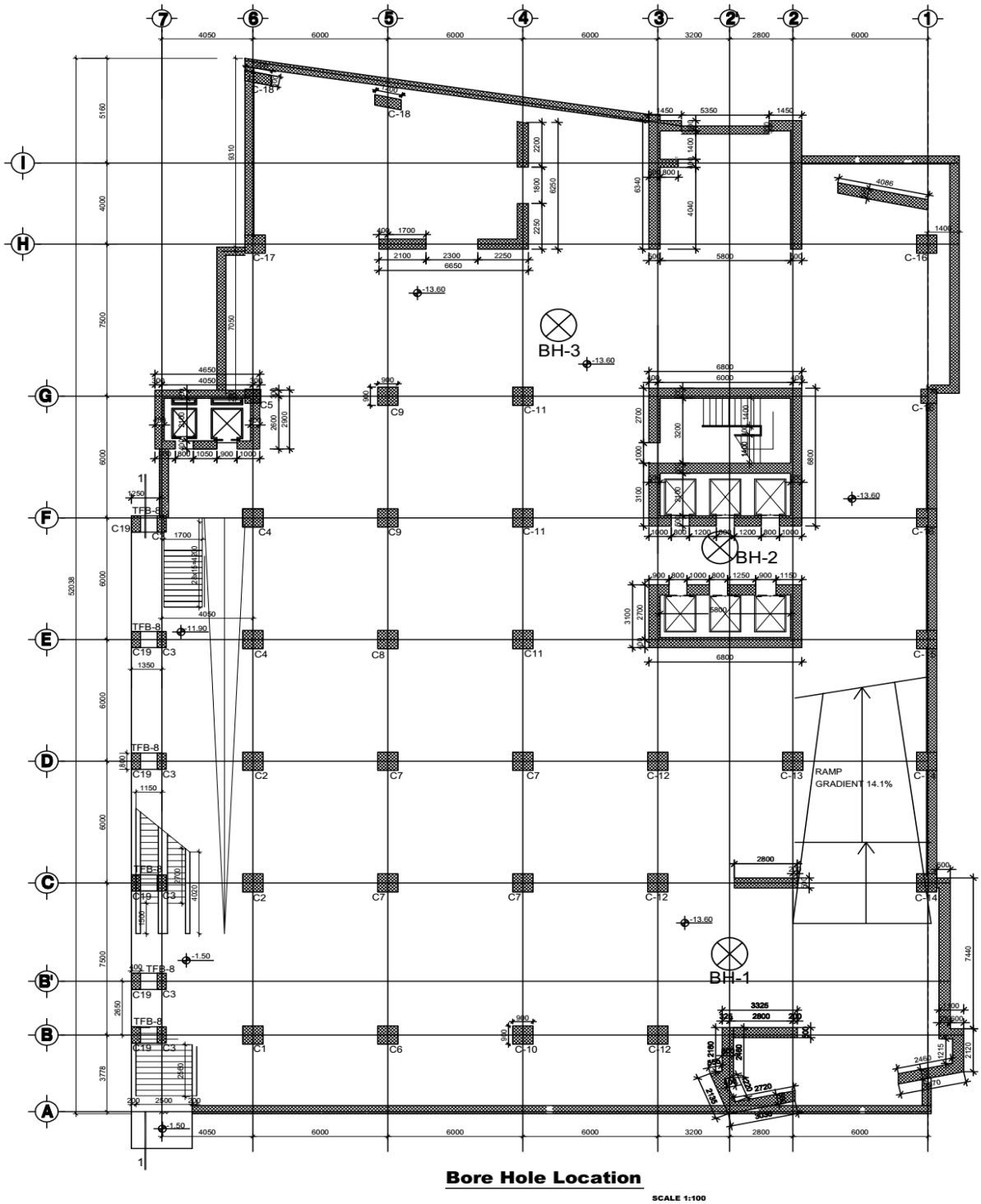

Borehole Location per the Floor Plan by ETG Designers and Consultants.

Appendix 3-Borehole Logs

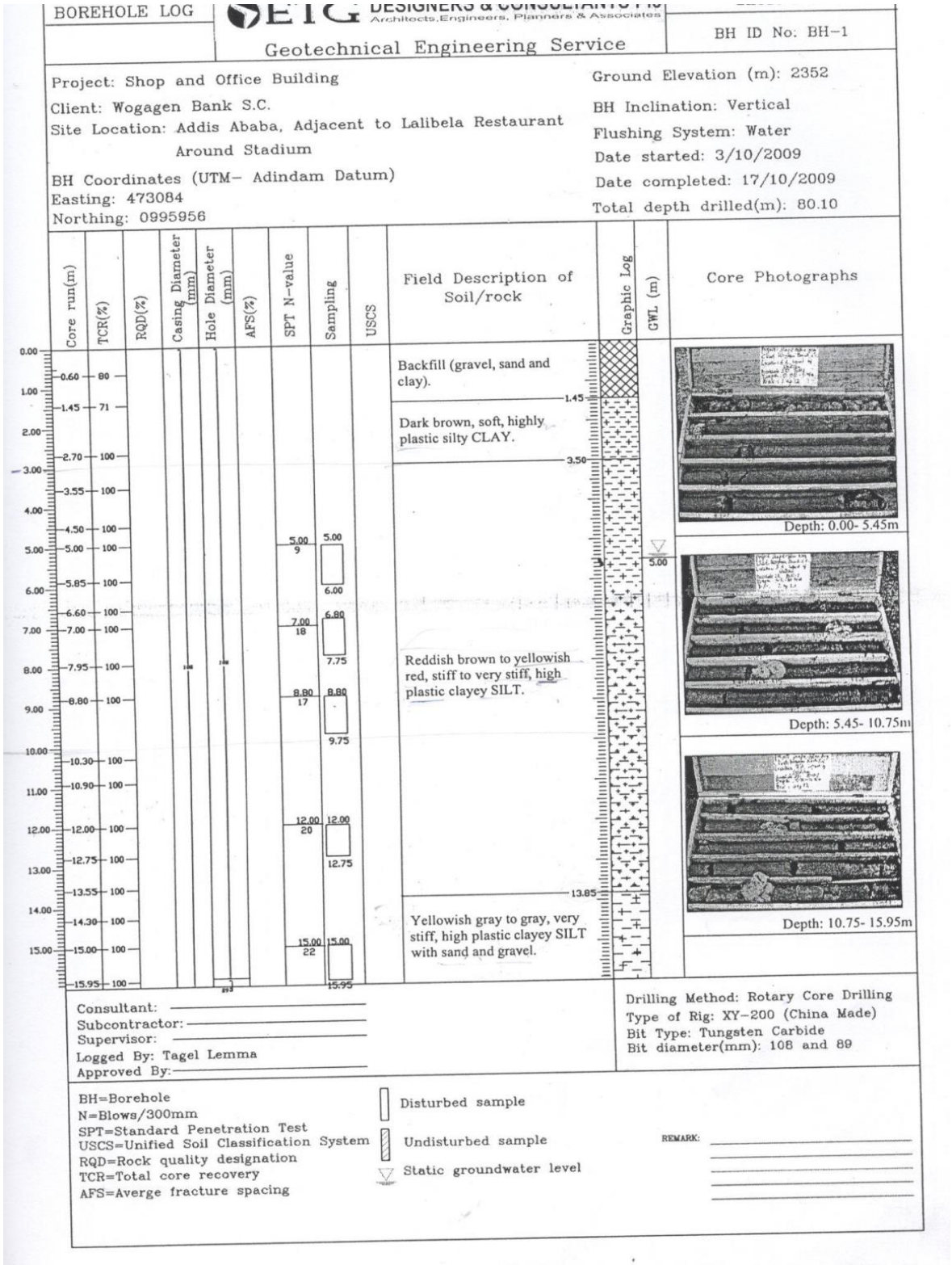

BOREHOLE LOG

DESIGNERS & CONSULTANTS PLC
Architects, Engineers, Planners & Associates

Geotechnical Engineering Service

BH ID No: BH-1

Project: Shop and Office Building
Client: Wogagen Bank S.C.
Site Location: Addis Ababa, Adjacent to Lalibela Restaurant Around Stadium
BH Coordinates (UTM- Adindam Datum)
Easting: 473084
Northing: 0995956

Ground Elevation (m): 2352
BH Inclination: Vertical
Flushing System: Water
Date started: 3/10/2009
Date completed: 17/10/2009
Total depth drilled(m): 80.10

Core run(m)	TCR(%)	RQD(%)	Casing Diameter (mm)	Hole Diameter (mm)	AFS(%)	SPT N-value	Sampling	USCS	Field Description of Soil/rock	Graphic Log	GWL (m)	Core Photographs
0.00									Backfill (gravel, sand and clay).			
0.60	80											
1.45	71											
									Dark brown, soft, highly plastic silty CLAY.			
2.70	100											
3.50												
3.55	100											
4.50	100											
5.00	100					5.00 9	5.00 6.00				5.00	Depth: 0.00- 5.45m
5.85	100											
6.60	100											
7.00	100					7.00 18	6.80 7.75					Depth: 5.45- 10.75m
7.95	100								Reddish brown to yellowish red, stiff to very stiff, high plastic clayey SILT.			
8.80	100					8.80 17	8.80 9.75					
10.30	100											
10.90	100											Depth: 10.75- 15.95m
12.00	100					12.00 20	12.00 12.75					
12.75	100											
13.55	100											
13.85												
14.30	100								Yellowish gray to gray, very stiff, high plastic clayey SILT with sand and gravel.			
15.00	100					15.00 22	15.00 15.95					
15.95	100											

Consultant:
Subcontractor:
Supervisor:
Logged By: Tagel Lemma
Approved By:

Drilling Method: Rotary Core Drilling
Type of Rig: XY-200 (China Made)
Bit Type: Tungsten Carbide
Bit diameter(mm): 108 and 89

BH=Borehole
N=Blows/300mm
SPT=Standard Penetration Test
USCS=Unified Soil Classification System
RQD=Rock quality designation
TCR=Total core recovery
AFS=Averge fracture spacing

Disturbed sample
Undisturbed sample
Static groundwater level

REMARK:

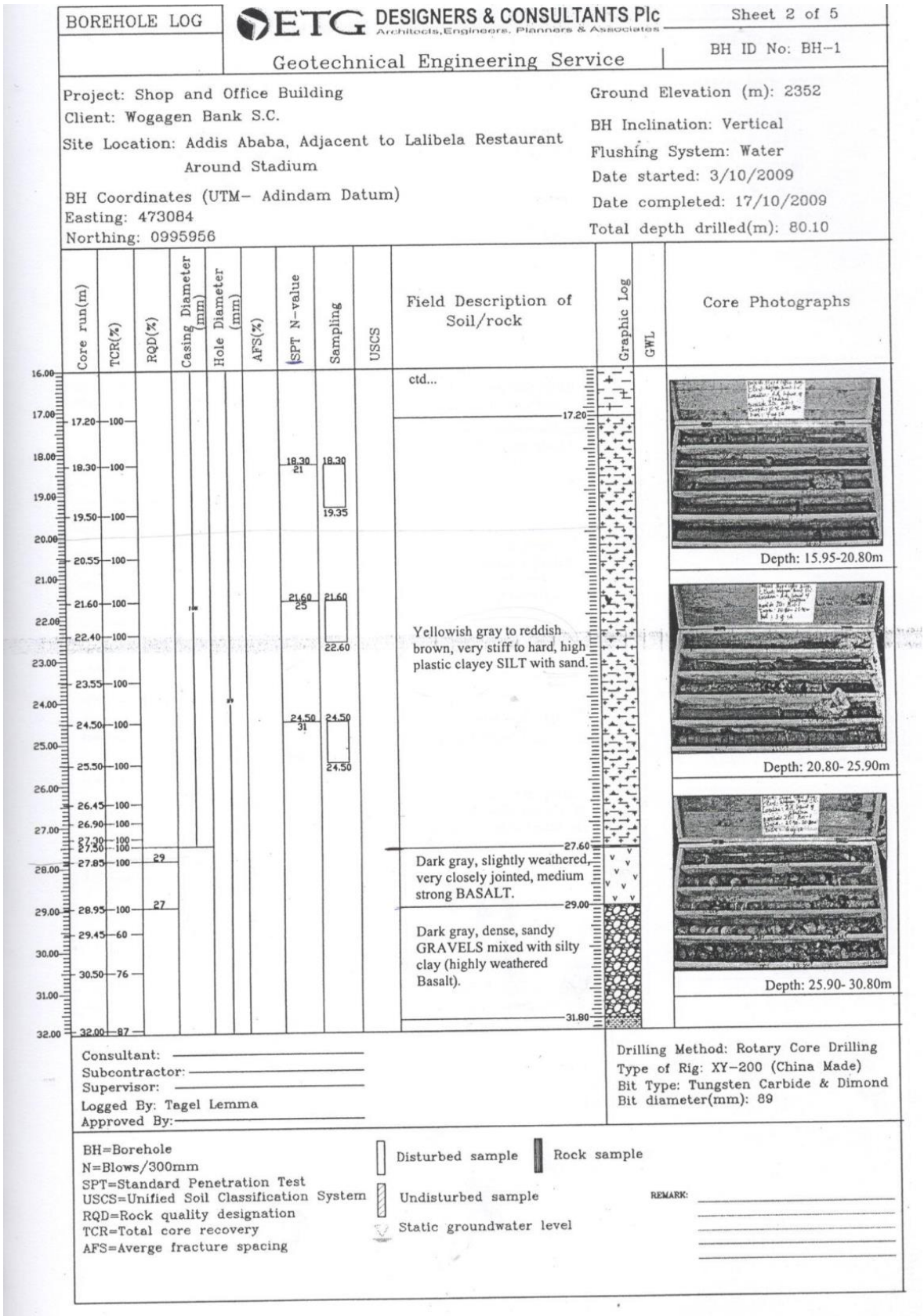

Appendix 4-Laboratory Test Results

SUMMARY OF LABORATORY TEST RESULTS

Sr. No.	Station	Depth(m)	Soil Discription	ARTICLE SIZE DISTRIBUTION(% PASSING)								Atterberg Limits AASHTO T 89-90		Free Swell, %	Soil Classification		% GRAVEL	% SAND	%FINE
				25.0 (mm)	19.0 (mm)	12.5 (mm)	9.5 (mm)	4.75 (mm)	2.0 (mm)	0.425 (mm)	0.075 (mm)	LL (%)	PI (%)		AASHTO	USCS			
1	BH1	4.00 - 5.00	Low plastic sandy silty CLAY	-	-	100.0	99.9	99.0	96.0	94.1	81.7	39	17	-	A - 6(11)	CL	0.0	17.0	82.0
2	BH1	6.80 - 7.75	High plastic clayey SILT	-	-	-	100.0	99.6	99.3	99.2	97.8	66	27	-	A - 7 - 6(19)	MH	0.4	1.8	97.8
3	BH1	8.80 - 9.75	High plastic clayey SILT	-	-	100.0	99.5	99.0	98.5	98.3	95.8	64	22	-	A - 7 - 5(17)	MH	1.5	2.7	95.8
4	BH1	12.00 - 12.75	High plastic clayey SILT	-	-	-	100.0	99.6	98.9	98.6	96.5	64	28	-	A - 7 - 5(19)	MH	0.4	3.1	96.5
5	BH1	15.00 - 15.95	High plastic clayey SILT with few gravel & sand	100.0	99.6	98.9	97.1	94.7	91.9	90.6	83.5	55	18	-	A - 7 - 5(14)	MH	9.8	6.7	83.5
6	BH1	18.30 - 19.35	High plastic clayey SILT	-	-	-	100.0	99.9	99.8	99.7	97.5	65	31	110	A - 7 - 5(20)	MH	0.1	2.4	97.5
7	BH1	21.60 - 22.60	High plastic clayey SILT with sand	-	-	100.0	99.8	99.6	96.6	94.4	86.4	65	23	-	A - 7 - 5(17)	MH	0.6	13.0	86.4
8	BH1	24.50 - 25.50	High plastic clayey SILT	-	-	-	-	-	100.0	99.9	97.4	69	26	-	A - 7 - 5(18)	MH	0.0	2.6	97.4
9	BH2	5.25 - 6.70	High plastic clayey SILT	-	-	-	100.0	99.9	99.9	99.5	98.2	70	35	90	A - 7 - 5(20)	MH	0.1	1.7	98.2
10	BH2	6.75 - 7.85	High plastic clayey SILT	-	-	-	-	100.0	99.9	99.7	98.7	73	34	90	A - 7 - 5(20)	MH	0.0	1.3	98.7
11	BH2	9.45 - 10.50	High plastic clayey SILT	-	-	-	-	-	100.0	99.8	96.6	60	19	-	A - 7 - 5(16)	MH	0.0	3.4	96.6
12	BH2	12.85 - 14.00	High plastic clayey SILT	-	-	-	100.0	99.9	99.3	97.5	93.9	60	19	-	A - 7 - 5(18)	MH	0.1	6.0	93.9
13	BH2	15.10 - 16.75	Low plastic clayey SILT with sand	-	-	-	100.0	99.8	98.5	95.9	83.2	46	13	-	A - 7 - 5(10)	ML	0.2	16.6	83.2
14	BH2	17.80 - 18.90	Low plastic clayey SILT with sand	-	-	-	-	100.0	99.3	97.2	88.8	44	11	-	A - 7 - 5(9)	ML	0.0	11.2	88.8
15	BH2	20.80 - 21.80	High plastic clayey SILT	-	-	-	-	-	100.0	99.8	97.1	51	17	-	A - 7 - 5(13)	MH	0.0	3.9	97.1
16	BH2	24.35 - 25.50	High plastic clayey SILT with sand	-	-	-	-	100.0	99.9	96.1	87.2	61	24	-	A - 7 - 5(17)	MH	0.0	12.8	87.2
17	BH2	27.35 - 28.50	High plastic clayey SILT	-	-	-	-	-	100.0	99.4	97.3	77	31	100	A - 7 - 5(20)	MH	0.0	2.7	97.3
18	BH3	6.20 - 7.45	High plastic clayey SILT	-	-	-	-	-	100.0	99.8	98.6	63	26	-	A - 7 - 5(18)	MH	0.0	1.4	98.6
19	BH3	7.80 - 8.85	High plastic clayey SILT	-	-	-	-	-	100.0	99.8	98.8	64	24	-	A - 7 - 5(17)	MH	0.8	1.2	98.8
20	BH3	10.10 - 11.30	High plastic clayey SILT	-	-	-	-	-	100.0	99.7	97.2	64	25	-	A - 7 - 5(18)	MH	0.0	2.8	97.2

PARTICLE SIZE DISTRIBUTION REPORT

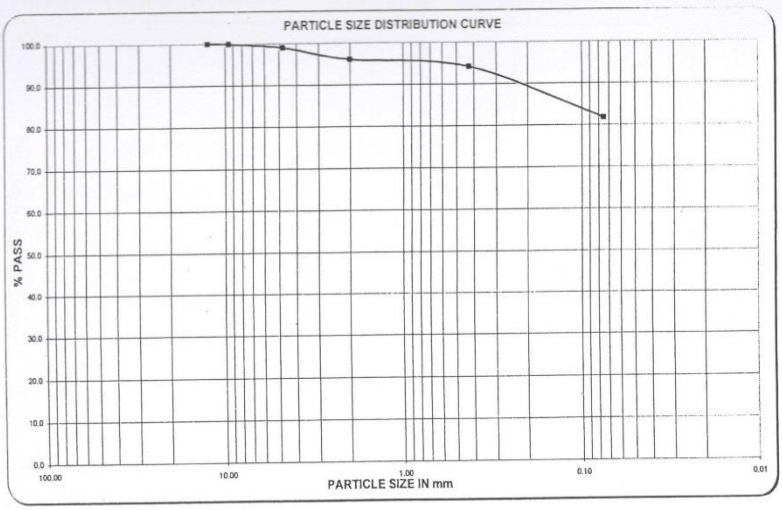

SIEVE SIZE (MM.)	% PASSED
12.50	100.0
9.50	99.9
4.75	99.0
2.00	96.0
0.425	94.1
0.075	81.7

Soil Description

Low plastic sandy silty CLAY

Atterberg Limit

LL 39

PI 17

Classification

USCS CL

AASHTO A - 6(11)

% COBBLE	% GRAVEL	% SAND	% FINE
-	1.1	17.2	81.7

REPORTED BY :

APPROVED BY :

ETG DESIGNERS & CONSULTANTS Plc
Architects,Engineers, Planners & Associates

GEOTECHNICAL ENGINEERING SERVICE

P.O.Box 110246, Addis Ababa Ethiopia
Tel., +251 11 860 36 99, +251 11 860 37 83/84, Fax: +251 860 36 99
E-mail: ar-con@ethionet.et

CLIENT	Wegagen Bank S.C
PROJECT	Shop and Office Building
LAB. NO.	007/09
SAMPLE SOURCE :	BH1
DEPTH (m):	5.00 - 6.00
REPORTED ON :	19/11/09

G BH1 , 5.00 - 6.00

LIQUID AND PLASTIC LIMITS TEST REPORT

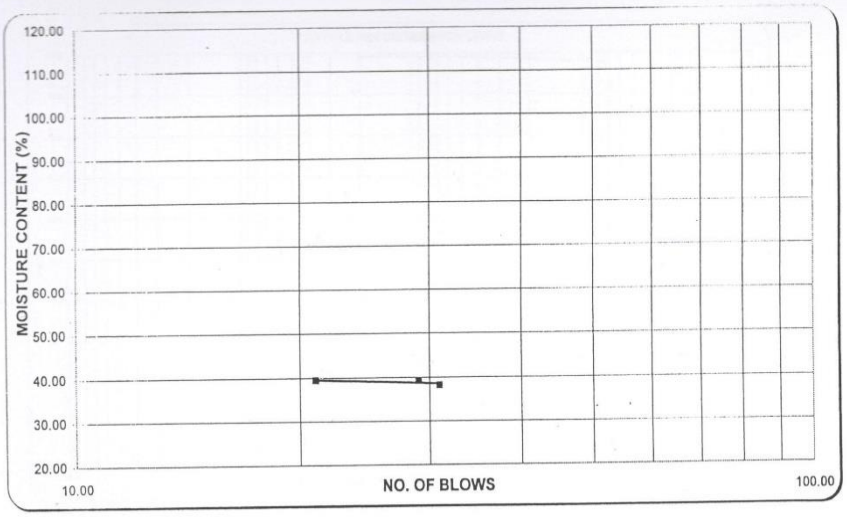

	LIQUID LIMIT			PLASTIC LIMIT	
No. Blows	31	29	21		
Wt. wet soil (g.)	24.60	25.20	24.40	7.40	7.20
Wt. dry soil (g.)	17.80	18.10	17.50	6.10	5.90
Moisture content (%)	38.20	39.23	39.43	21.31	22.03
				AV. PL (%)	21.7

Liquid Limit LL(%)	Plastic Limit PL(%)	Plasticity Index PI	WET SEIVE ANALYSIS, % PASS		
			2mm	0.425mm	0.075mm
39	22	17	96.0	94.1	81.7

REPORTED BY

APROVED BY

ETG DESIGNERS & CONSULTANTS Plc
Architects,Engineers, Planners & Associates

GEOTECHNICAL ENGINEERING SERVICE

P.O.Box 110246, Addis Ababa Ethiopia
Tel., +251 11 860 36 99, +251 11 860 37 83/84, Fax: +251 860 36 99
E-mail: ar-con@ethionet.et

CLIENT : Wegagen Bank S.C
PROJECT : Shop and Office Building
LAB. NO. 007/09
SAMPLE SOURCE : BH1
DEPTH(m) : 5.00 - 6.00
REPORTED ON : 19/11/09

L BH1 5.00 - 6.00

ETG Designers & Consultants

PARTICLE SIZE DISTRIBUTION REPORT

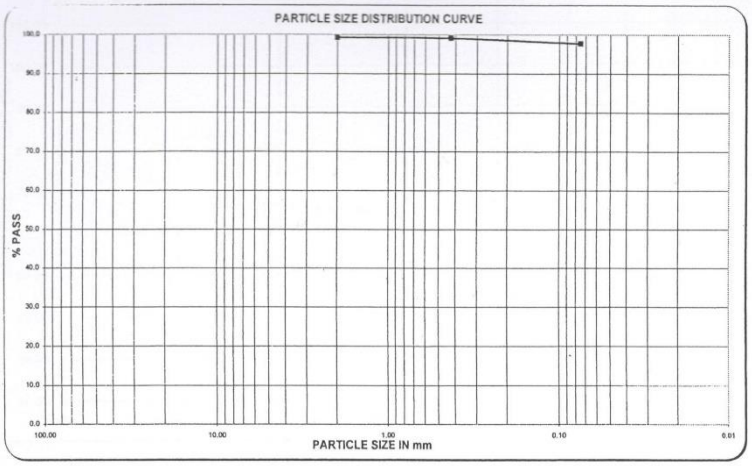

SIEVE SIZE (MM.)	% PASSED
9.50	100.0
4.75	99.6
2.00	99.3
0.425	99.2
0.075	97.8

Soil Description
High plastic clayey SILT

Atterberg Limit
LL 66
PI 27

Classification
USCS MH
AASHTO A - 7 - 5(19)

% COBBLE	% GRAVEL	% SAND	% FINE
-	0.4	1.8	97.8

REPORTED BY :

APPROVED BY :

ETG DESIGNERS & CONSULTANTS Plc
Architects,Engineers, Planners & Associates
GEOTECHNICAL ENGINEERING SERVICE
P.O.Box 110246, Addis Ababa Ethiopia
Tel., +251 11 860 36 99, +251 11 860 37 83/84, Fax: +251 860 36 99
E-mail: ar-con@ethionet.et

CLIENT	Wegagen Bank S.C
PROJECT	Shop and Office Building
LAB. NO.	007/09
SAMPLE SOURCE :	BH1
DEPTH (m):	6.80 - 7.75
REPORTED ON :	19/11/09

G BH1, 6.80 - 7.75

LIQUID AND PLASTIC LIMITS TEST REPORT

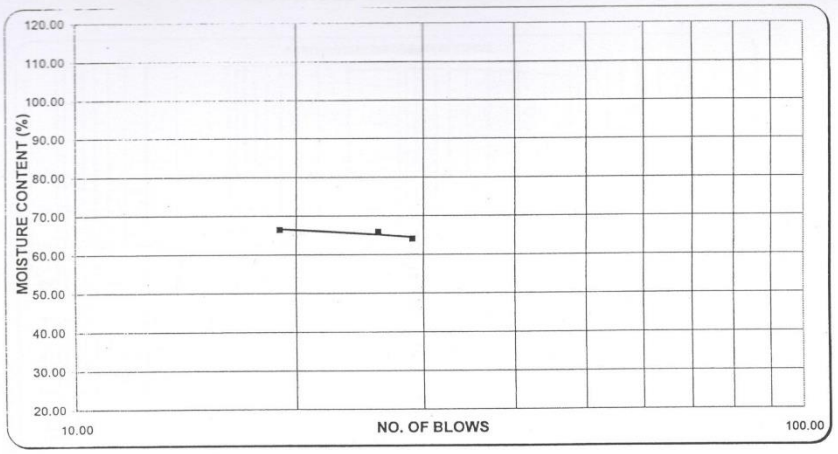

	LIQUID LIMIT			PLASTIC LIMIT	
No. Blows	29	26	19		
Wt. wet soil (g.)	27.40	26.20	26.30	7.10	6.50
Wt. dry soil (g.)	16.70	15.80	15.80	5.12	4.68
Moisture content (%)	64.07	65.82	66.46	38.67	38.89
				AV. PL (%)	38.8

Liquid Limit LL(%)	Plastic Limit PL(%)	Plasticity Index PI	WET SEIVE ANALYSIS, % PASS		
			2mm	0.425mm	0.075mm
66	39	27	99	99	98

REPORTED BY

APROVED BY

ETG DESIGNERS & CONSULTANTS Plc
Architects,Engineers, Planners & Associates

GEOTECHNICAL ENGINEERING SERVICE

P.O.Box 110246, Addis Ababa Ethiopia
Tel., +251 11 860 36 99, +251 11 860 37 83/84, Fax: +251 860 36 99
E-mail: ar-con@ethionet.et

CLIENT : Wegagen Bank S.C
PROJEC : Shop and Office Building
LAB. NO. 007/09
SAMPLE SOURCE : BH1
DEPTH(m) : 6.80 - 7.75
REPORTED ON : 19/11/09

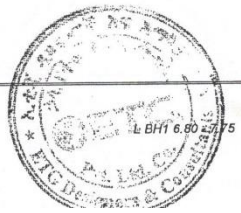

PARTICLE SIZE DISTRIBUTION REPORT

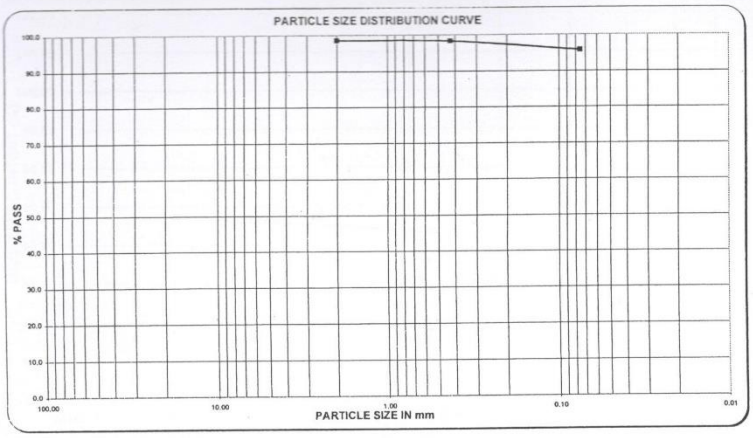

SIEVE SIZE (MM.)	% PASSED
12.50	100.0
9.50	99.5
4.75	99.0
2.00	98.5
0.425	98.3
0.075	95.8

Soil Description
High plastic clayey SILT
Atterberg Limit
LL 64
PI 22
Classification
USCS MH
AASHTO A - 7 - 5(17)

% COBBLE	% GRAVEL	% SAND	% FINE
-	1.5	2.7	95.8

REPORTED BY :

APPROVED BY :

ETG DESIGNERS & CONSULTANTS Plc
Architects,Engineers, Planners & Associates

GEOTECHNICAL ENGINEERING SERVICE

P.O.Box 110246, Addis Ababa Ethiopia
Tel., +251 11 860 36 99, +251 11 860 37 83/84, Fax: +251 860 36 99
E-mail: ar-con@ethionet.et

CLIENT: Wegagen Bank S.C
PROJECT: Shop and Office Building
LAB. NO.: 007/09
SAMPLE SOURCE : BH1
DEPTH (m): 8.80 - 9.75
REPORTED ON : 19/11/09

G BH1 8.80 - 9.75

LIQUID AND PLASTIC LIMITS TEST REPORT

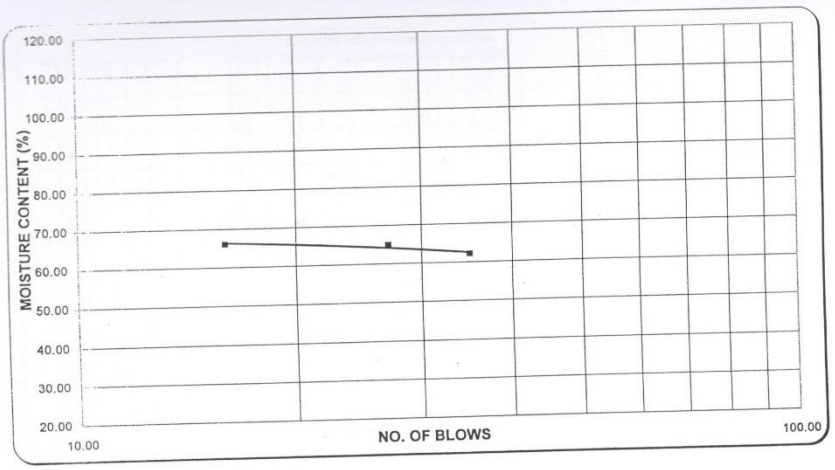

	LIQUID LIMIT			PLASTIC LIMIT	
No. Blows	35	27	16		
Wt. wet soil (g.)	22.70	24.20	22.50	6.70	6.80
Wt. dry soil (g.)	14.00	14.68	13.55	4.70	4.80
Moisture content (%)	62.14	64.85	66.05	42.55	41.67
				AV. PL (%)	42.1

Liquid Limit LL(%)	Plastic Limit PL(%)	Plasticity Index PI	WET SEIVE ANALYSIS, % PASS		
			2mm	0.425mm	0.075mm
64	42	22	98.5	98.3	95.8

REPORTED BY

APROVED BY

ETG DESIGNERS & CONSULTANTS Plc
Architects,Engineers, Planners & Associates

GEOTECHNICAL ENGINEERING SERVICE

P.O.Box 110246, Addis Ababa Ethiopia
Tel., +251 11 860 36 99, +251 11 860 37 83/84, Fax: +251 860 36 99
E-mail: ar-con@ethionet.et

CLIENT : Wegagen Bank S.C
PROJEC : Shop and Office Building
LAB. NO. 007/09
SAMPLE SOURCE : BH1
DEPTH(m) : 8.80 - 9.75
REPORTED ON : 19/11/09

PARTICLE SIZE DISTRIBUTION REPORT

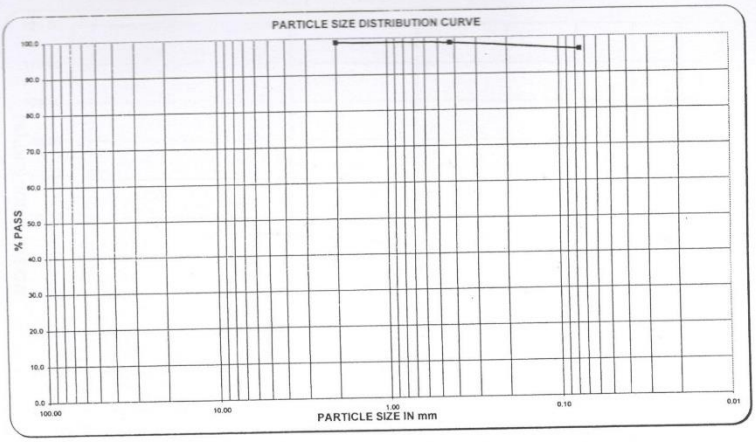

SIEVE SIZE (MM.)	% PASSED
9.50	100.0
4.75	99.6
2.00	98.9
0.425	98.6
0.075	96.5

Soil Description
High plastic clayey SILT

Atterberg Limit
LL 64
PI 28

Classification
USCS MH
AASHTO A - 7 - 5(19)

% COBBLE	% GRAVEL	% SAND	% FINE
-	0.4	3.1	96.5

REPORTED BY :

APPROVED BY :

ETG DESIGNERS & CONSULTANTS Plc
Architects,Engineers, Planners & Associates

GEOTECHNICAL ENGINEERING SERVICE

P.O.Box 110246, Addis Ababa Ethiopia
Tel., +251 11 860 36 99, +251 11 860 37 83/84, Fax: +251 860 36 99
E-mail: ar-con@ethionet.et

CLIENT	Wegagen Bank S.C
PROJECT	Shop and Office Building
LAB. NO.	007/09
SAMPLE SOURCE :	BH1
DEPTH (m):	12.00 - 12.75
REPORTED ON :	19/11/09

G BH1, 12.00 - 12.75

ETG Designers & Consultants

LIQUID AND PLASTIC LIMITS TEST REPORT

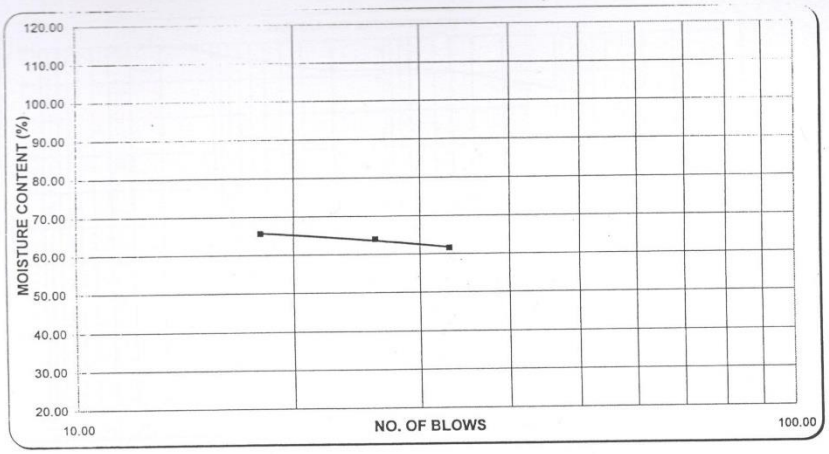

	LIQUID LIMIT			PLASTIC LIMIT	
No. Blows	33	26	18		
Wt. wet soil (g.)	27.30	26.40	26.00	6.90	7.10
Wt. dry soil (g.)	16.90	16.10	15.70	5.10	5.20
Moisture content (%)	61.54	63.98	65.61	35.29	36.54
				AV. PL (%)	35.9

Liquid Limit LL(%)	Plastic Limit PL(%)	Plasticity Index PI	WET SEIVE ANALYSIS, % PASS		
			2mm	0.425mm	0.075mm
64	36	28	98.9	98.6	96.5

REPORTED BY

APROVED BY

ETG DESIGNERS & CONSULTANTS Plc
Architects,Engineers, Planners & Associates

GEOTECHNICAL ENGINEERING SERVICE

P.O.Box 110246, Addis Ababa Ethiopia
Tel., +251 11 860 36 99, +251 11 860 37 83/84, Fax: +251 860 36 99
E-mail: ar-con@ethionet.et

CLIENT : Wegagen Bank S.C
PROJEC : Shop and Office Building
LAB. NO. 007/09
SAMPLE SOURCE : BH1
DEPTH(m) : 12.00 - 12.75
REPORTED ON : 19/11/09

BH1 12.00 - 12.75

PARTICLE SIZE DISTRIBUTION REPORT

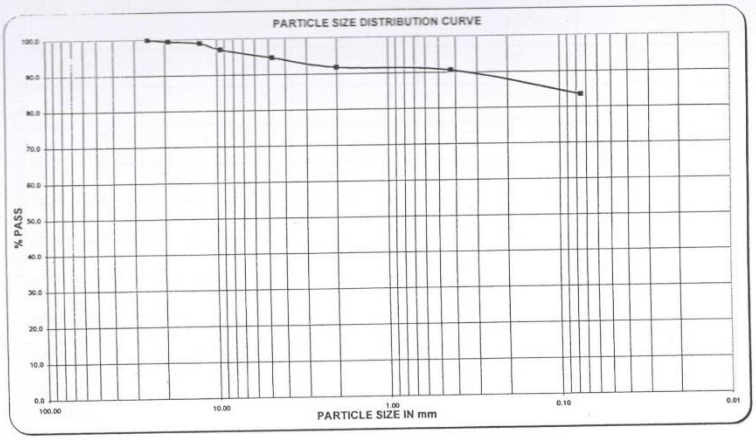

SIEVE SIZE (MM.)	% PASSED
25.00	100.0
19.00	99.5
12.50	98.9
9.50	97.1
4.75	94.7
2.00	91.9
0.425	90.6
0.075	83.5

Soil Description
High plastic clayey SILTwith few gravel and sand
Atterberg Limit
LL 55
PI 18
Classification
USCS MH
AASHTO A - 7 - 5(14)

% COBBLE	% GRAVEL	% SAND	% FINE
-	9.8	6.7	83.5

REPORTED BY :

APPROVED BY :

ETG DESIGNERS & CONSULTANTS Plc
Architects,Engineers, Planners & Associates

GEOTECHNICAL ENGINEERING SERVICE

P.O.Box 110246, Addis Ababa Ethiopia
Tel., +251 11 860 36 99, +251 11 860 37 83/84, Fax: +251 860 36 99
E-mail: ar-con@ethionet.et

CLIENT: Wegagen Bank S.C
PROJECT: Shop and Office Building
LAB. NO.: 007/09
SAMPLE SOURCE : BH1
DEPTH (m): 15.00 - 15.95
REPORTED ON : 19/11/09

G BH1, 15.00 - 15.95

LIQUID AND PLASTIC LIMITS TEST REPORT

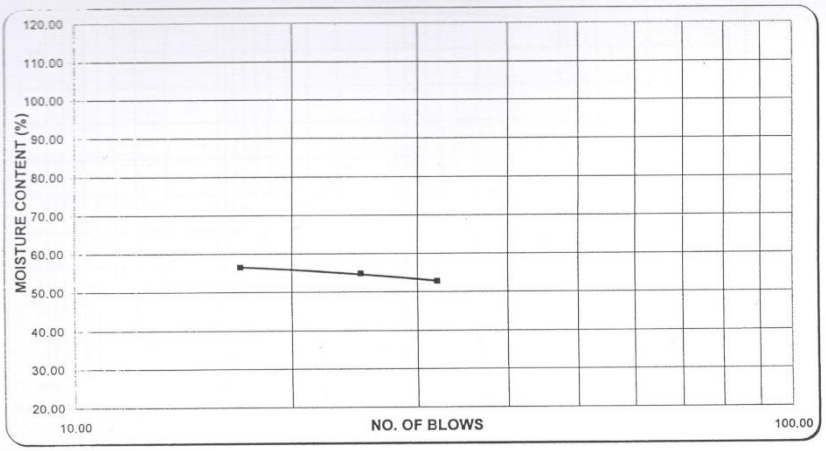

	LIQUID LIMIT			PLASTIC LIMIT	
No. Blows	32	25	17		
Wt. wet soil (g.)	27.80	27.70	27.70	4.80	5.10
Wt. dry soil (g.)	18.20	17.90	17.70	3.50	3.70
Moisture content (%)	52.75	54.75	56.50	37.14	37.84
				AV. PL (%)	37.5

Liquid Limit LL(%)	Plastic Limit PL(%)	Plasticity Index PI	WET SEIVE ANALYSIS, % PASS		
			2mm	0.425mm	0.075mm
55	37	18	91.9	90.6	83.5

REPORTED BY

APROVED BY

ETG DESIGNERS & CONSULTANTS Plc
Architects,Engineers, Planners & Associates

GEOTECHNICAL ENGINEERING SERVICE

P.O.Box 110246, Addis Ababa Ethiopia
Tel., +251 11 860 36 99, +251 11 860 37 83/84, Fax: +251 860 36 99
E-mail: ar-con@ethionet.et

CLIENT : Wegagen Bank S.C
PROJEC' : Shop and Office Building
LAB. NO. 007/09
SAMPLE SOURCE : BH1
DEPTH(m) : 15.00 - 15.95
REPORTED ON : 19/11/09

L BH1 15.00 - 5.35

PARTICLE SIZE DISTRIBUTION REPORT

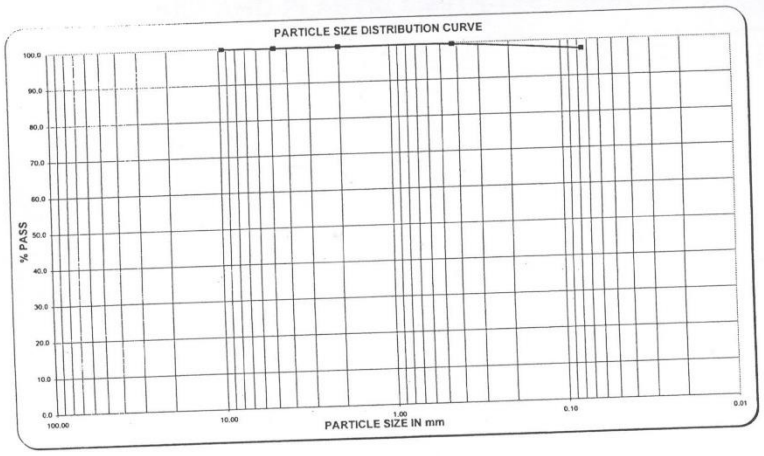

SIEVE SIZE (MM.)	% PASSED
9.50	100.0
4.75	99.9
2.00	99.8
0.425	99.7
0.075	97.5

Soil Description
High plastic clayey SILT
Atterberg Limit
LL 65
PI 31
Classification
USCS MH
AASHTO A - 7 - 5(20)

% COBBLE	% GRAVEL	% SAND	% FINE
-	0.1	2.4	97.5

REPORTED BY :

APPROVED BY :

ETG DESIGNERS & CONSULTANTS Plc
Architects,Engineers, Planners & Associates

GEOTECHNICAL ENGINEERING SERVICE

P.O.Box 110246, Addis Ababa Ethiopia
Tel., +251 11 860 36 99, +251 11 860 37 83/84, Fax: +251 860 36 99
E-mail: ar-con@ethionet.et

CLIENT	Wegagen Bank S.C
PROJECT	Shop and Office Building
LAB. NO.	007/09
SAMPLE SOURCE :	BH1
DEPTH (m):	18.30 - 19.35
REPORTED ON :	19/11/09

@ BH1 , 18.30 - 19.35

ETG Designers & Consultants

LIQUID AND PLASTIC LIMITS TEST REPORT

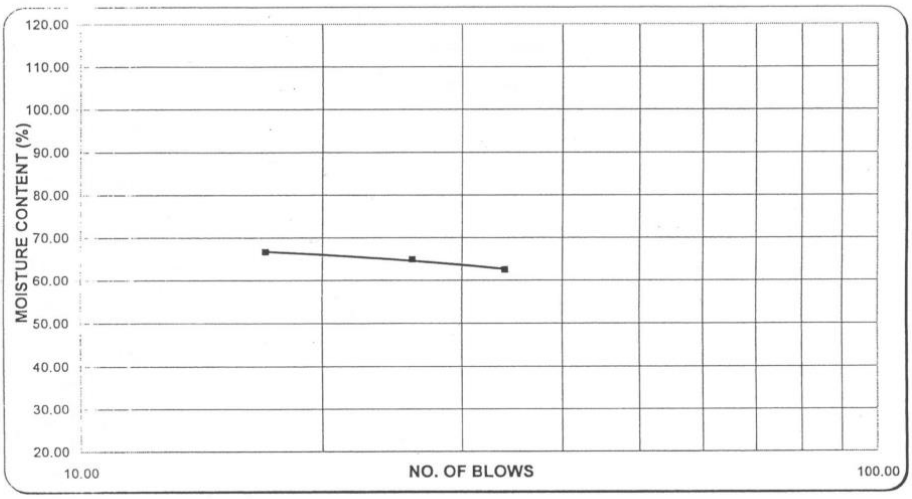

	LIQUID LIMIT			PLASTIC LIMIT	
No. Blows	34	26	17		
Wt. wet soil (g.)	27.30	26.30	26.00	4.90	6.30
Wt. dry soil (g.)	16.80	15.95	15.60	3.65	4.70
Moisture content (%)	62.50	64.89	66.67	34.25	34.04
				AV. PL (%)	34.1

Liquid Limit LL(%)	Plastic Limit PL(%)	Plasticity Index PI	WET SEIVE ANALYSIS, % PASS		
			2mm	0.425mm	0.075mm
65	34	31	99.8	99.7	97.5

REPORTED BY

APROVED BY

ETG DESIGNERS & CONSULTANTS Plc
Architects,Engineers, Planners & Associates

GEOTECHNICAL ENGINEERING SERVICE

P.O.Box 110246, Addis Ababa Ethiopia
Tel., +251 11 860 36 99, +251 11 860 37 83/84, Fax: +251 860 36 99
E-mail: ar-con@ethionet.et

CLIENT : Wegagen Bank S.C
PROJEC : Shop and Office Building
LAB. NO. 007/09
SAMPLE SOURCE : BH1
DEPTH(m) : 18.30 - 19.35
REPORTED ON : 19/11/09

BH1 18.30 - 19.35

PARTICLE SIZE DISTRIBUTION REPORT

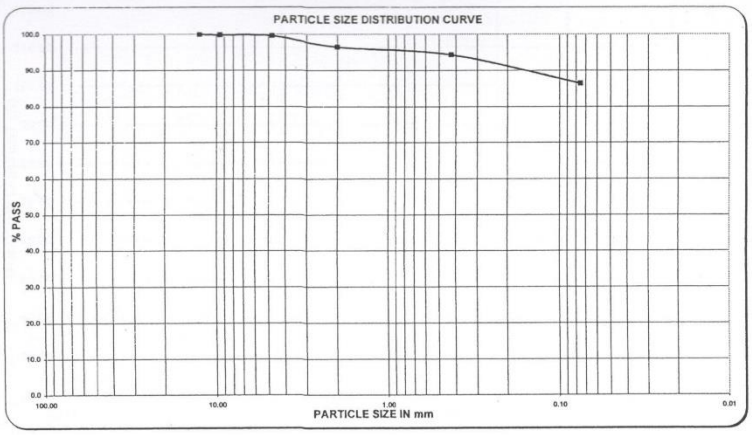

SIEVE SIZE (MM.)	% PASSED
12.50	100.0
9.50	99.8
4.75	99.6
2.00	96.6
0.425	94.4
0.075	86.4

Soil Description
High plastic clayey SILT with sand
Atterberg Limit
LL 65
PI 23
Classification
USCS MH
AASHTO A - 7 - 5(17)

% COBBLE	% GRAVEL	% SAND	% FINE
-	0.6	13.0	86.4

REPORTED BY :

APPROVED BY :

ETG DESIGNERS & CONSULTANTS Plc
Architects, Engineers, Planners & Associates
GEOTECHNICAL ENGINEERING SERVICE
P.O.Box 110246, Addis Ababa Ethiopia
Tel., +251 11 860 36 99, +251 11 860 37 83/84, Fax: +251 860 36 99
E-mail: ar-con@ethionet.et

CLIENT	Wegagen Bank S.C
PROJECT	Shop and Office Building
LAB. NO.	007/09
SAMPLE SOURCE :	BH1
DEPTH (m):	21.60 - 22.60
REPORTED ON :	19/11/09

G BH1, 21.60 - 22.60

LIQUID AND PLASTIC LIMITS TEST REPORT

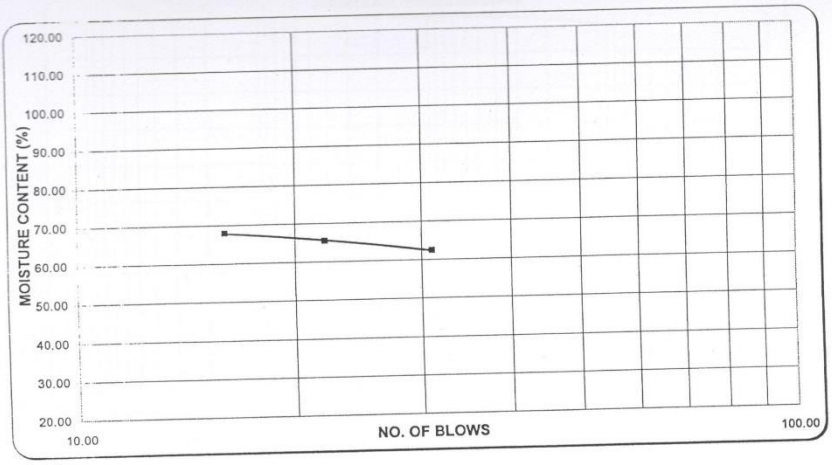

	LIQUID LIMIT			PLASTIC LIMIT	
No. Blows	31	22	16		
Wt. wet soil (g.)	21.60	23.00	21.50	9.80	8.80
Wt. dry soil (g.)	13.30	13.90	12.80	6.90	6.20
Moisture content (%)	62.41	65.47	67.97	42.03	41.94
				AV. PL (%)	42.0

Liquid Limit LL(%)	Plastic Limit PL(%)	Plasticity Index PI	WET SEIVE ANALYSIS, % PASS		
			2mm	0.425mm	0.075mm
65	42	23	96.6	94.4	86.4

REPORTED BY

APROVED BY

ETG DESIGNERS & CONSULTANTS Plc
Architects,Engineers, Planners & Associates

GEOTECHNICAL ENGINEERING SERVICE

P.O.Box 110246, Addis Ababa Ethiopia
Tel., +251 11 860 36 99, +251 11 860 37 83/84, Fax: +251 860 36 99
E-mail: ar-con@ethionet.et

CLIENT :	Wegagen Bank S.C
PROJEC' :	Shop and Office Building
LAB. NO.	007/09
SAMPLE SOURCE :	BH1
DEPTH(m) :	21.60 - 22.60
REPORTED ON :	19/11/09

ETG Designers & Consultants Pvt. Ltd. BH1 21.60

PARTICLE SIZE DISTRIBUTION REPORT

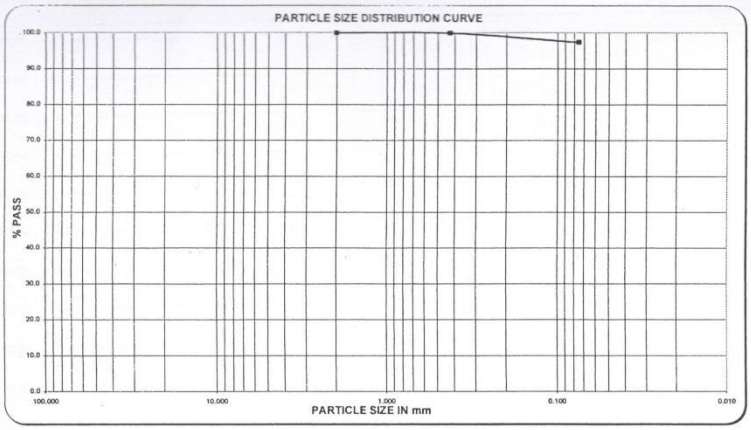

SIEVE SIZE (MM.)	% PASSED
2.000	100.0
0.425	99.9
0.075	97.4

Soil Description
High plastic clayey SILT
Atterberg Limit
LL 69
PI 26
Classification
USCS MH
AASHTO A - 7 - 5(18)

% COBBLE	% GRAVEL	% SAND	% FINE
-	0.4	3.0	97.0

REPORTED BY :

APPROVED BY :

ETG DESIGNERS & CONSULTANTS Plc
Architects,Engineers, Planners & Associates
GEOTECHNICAL ENGINEERING SERVICE
P.O.Box 110246, Addis Ababa Ethiopia
Tel., +251 11 860 36 99, +251 11 860 37 83/84, Fax: +251 860 36 99
E-mail: ar-con@ethionet.et

CLIENT	Wegagen Bank .SC
PROJECT	Shop and Office Building
LAB. NO.	007/09
SAMPLE SOURCE :	BH1
DEPTH (m):	24.50 - 25.5
REPORTED ON :	19/11/09

G BH1, 24.50 - 25.50

ETG Designers & Consultants Pvt. Ltd. Co.

LIQUID AND PLASTIC LIMITS TEST REPORT

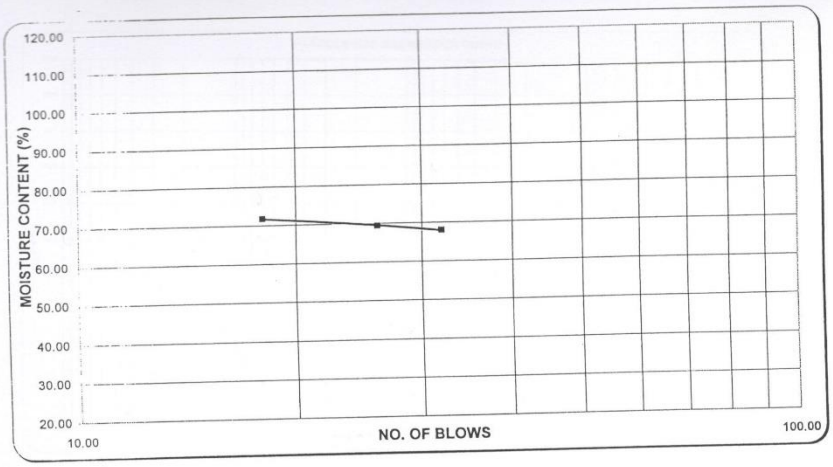

	LIQUID LIMIT			PLASTIC LIMIT	
No. Blows	32	26	18		
Wt. wet soil (g.)	25.20	24.40	26.10	4.70	4.50
Wt. dry soil (g.)	15.00	14.40	15.20	3.30	3.15
Moisture content (%)	68.00	69.44	71.71	42.42	42.86
				AV. PL (%)	42.6

Liquid Limit LL(%)	Plastic Limit PL(%)	Plasticity Index PI	WET SEIVE ANALYSIS, % PASS		
			2mm	0.425mm	0.075mm
69	43	26	100	99.9	97.4

REPORTED BY

APROVED BY

ETG DESIGNERS & CONSULTANTS Plc
Architects,Engineers, Planners & Associates

GEOTECHNICAL ENGINEERING SERVICE

P.O.Box 110246, Addis Ababa Ethiopia
Tel., +251 11 860 36 99, +251 11 860 37 83/84, Fax: +251 860 36 99
E-mail: ar-con@ethionet.et

CLIENT : Wegagen Bank S.C
PROJEC : Shop and Office Building
LAB. NO. 007/09
SAMPLE SOURCE : BH1
DEPTH(m) : 24.50 - 25.50
REPORTED ON : 19/11/09

ETG Designers & Consultants P.L.C.

1 BH1 24.50 - 25.50 CK

Appendix 5-Plates of Core Boxes

Plate 1: BH-1;

Depth: 0.00-5.45m

Plate 2: BH-1,

Depth: 5.45-10.75m

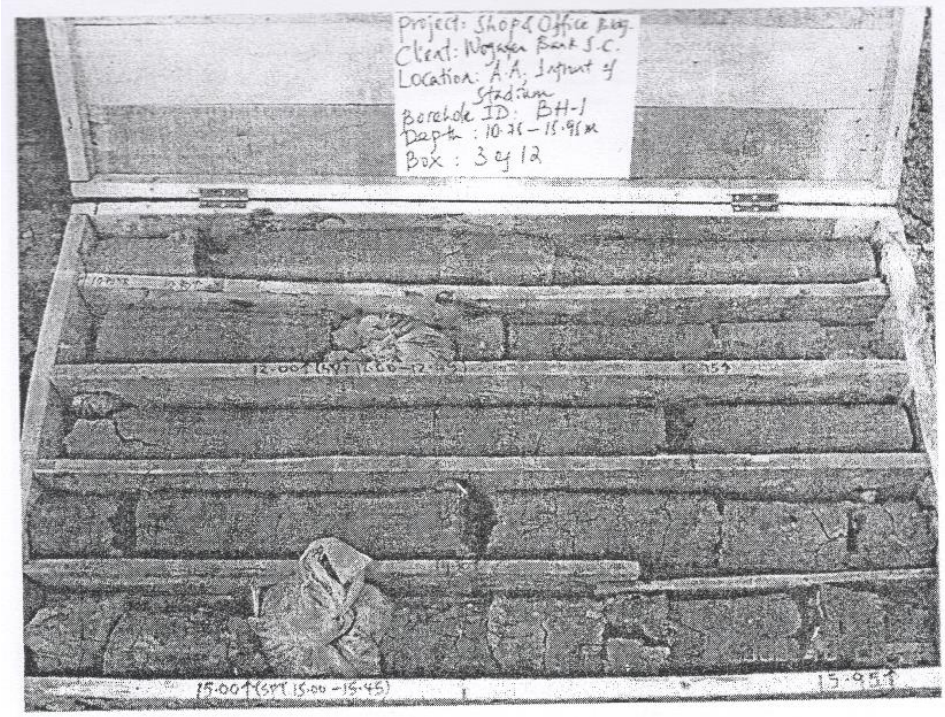

Plate 3: BH-1,

Depth: 10.75-15.95m

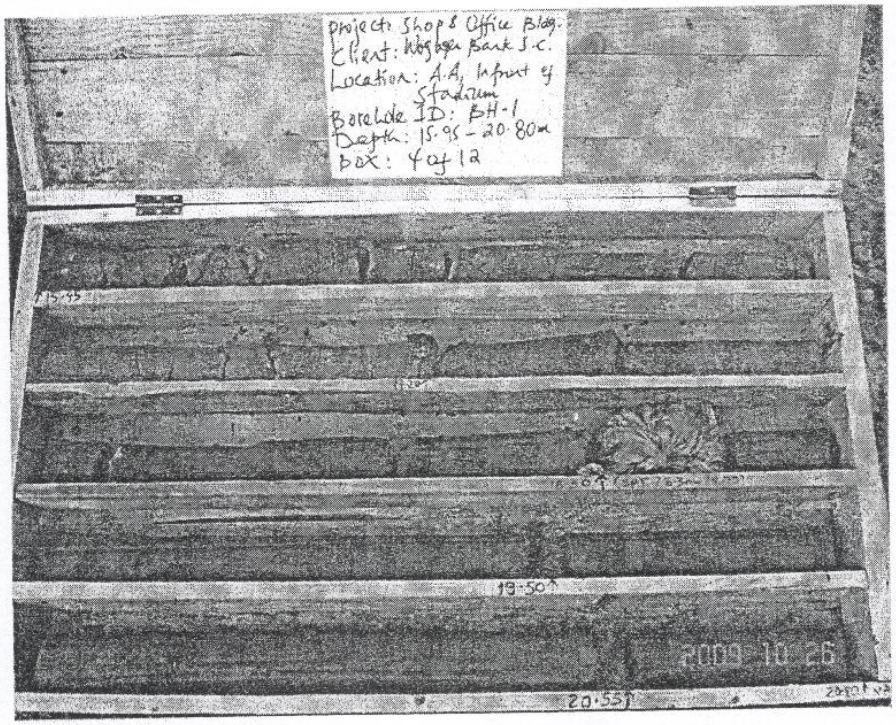

Plate: 4, BH-1,

Depth: 15.95-20.80m

Plate 5: BH-1;

Depth: 20.80-25.90m

Plate 6: BH-1;

Depth: 25.90-30.80m

Appendix 6-Model of Pile and Soil in Plaxis 3D Foundation

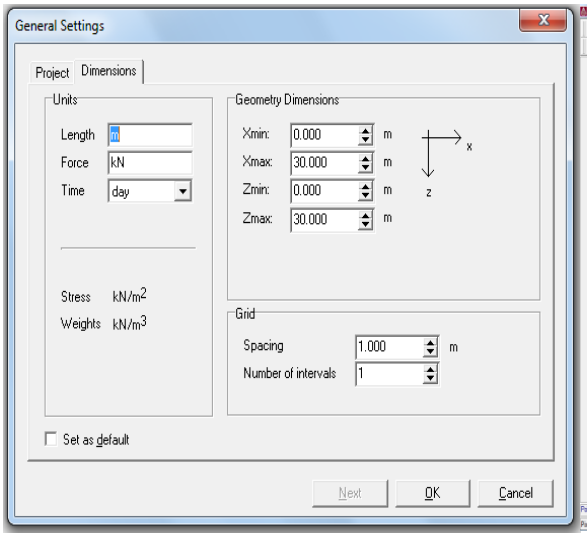

a) setting project name and units

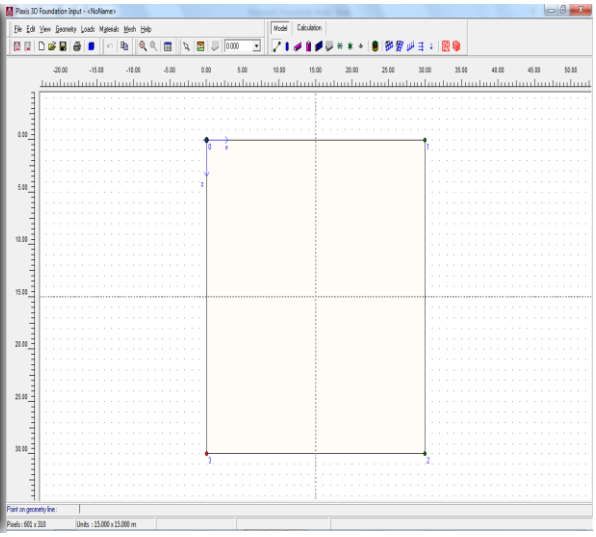

b) geometrical limit of soil in horizontal plane

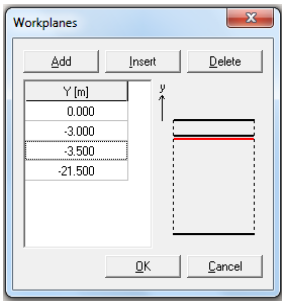

c) defining work planes

Plaxis Output Version 2.1.0.308

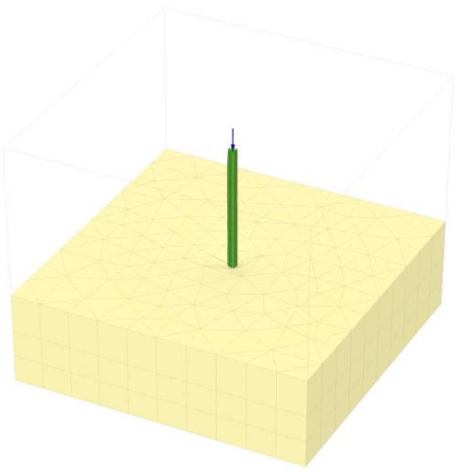

Deformed Mesh (scaled up 50.00 times)
Maximum Value = $29.58*10^{-3}$ m
Minimum Value = 0.00 m

PLAXIS Finite Element Code for Soil and Rock Analyses	Project description FP-600mm		Date 17/08/2017
	Project filename FP-600mm	Step 6	User name Construction Design S. Co.

Plaxis Output Version 2.1.0.308

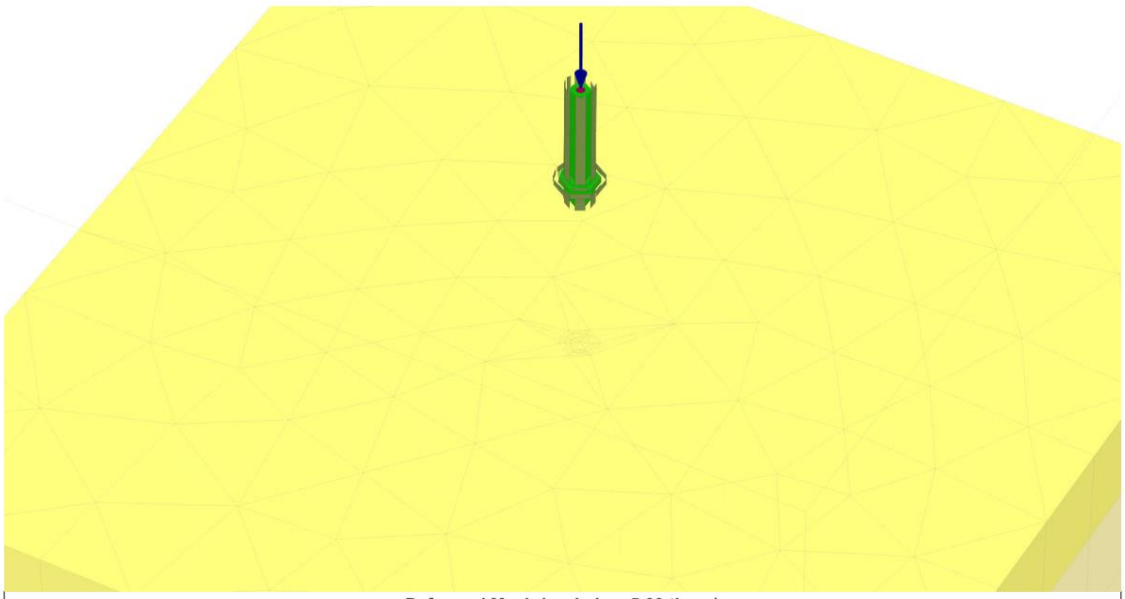

Deformed Mesh (scaled up 5.00 times)
Maximum Value = $177.72*10^{-3}$ m
Minimum Value = 0.00 m

PLAXIS Finite Element Code for Soil and Rock Analyses	Project description URP DIA 600mm		Date 17/08/2017
	Project filename URP DIA 600mm	Step 22	User name Construction Design S. Co.

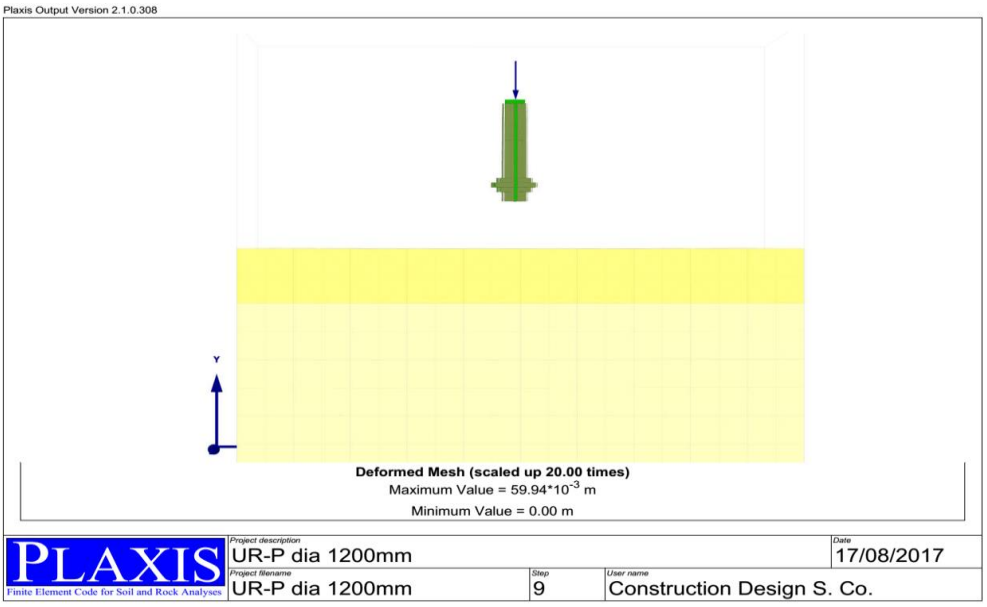

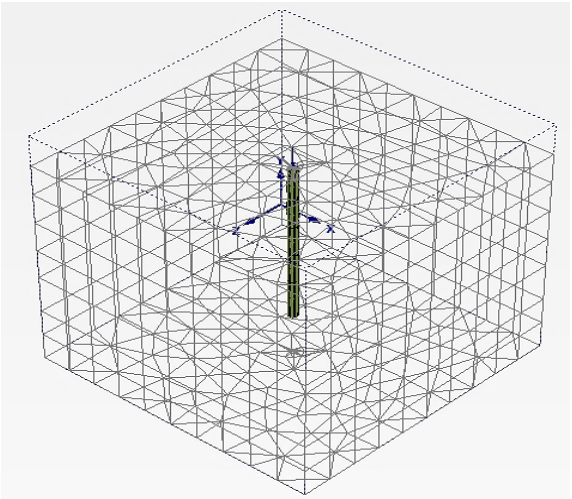

a) friction pile diameter 600mm

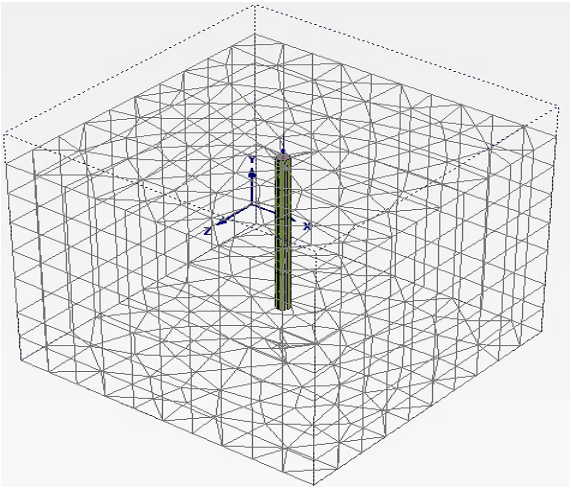

b) friction pile diameter 900mm

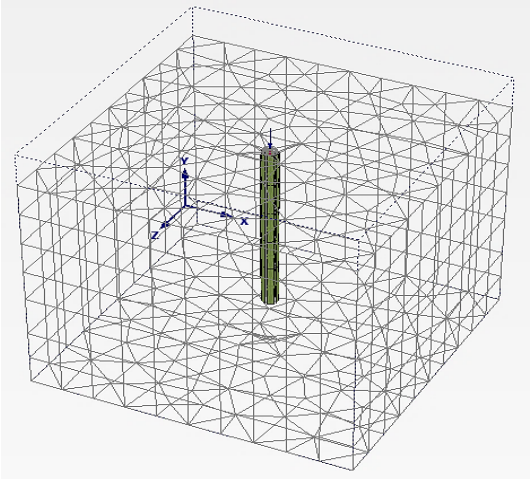

c) friction pile diameter 1200mm

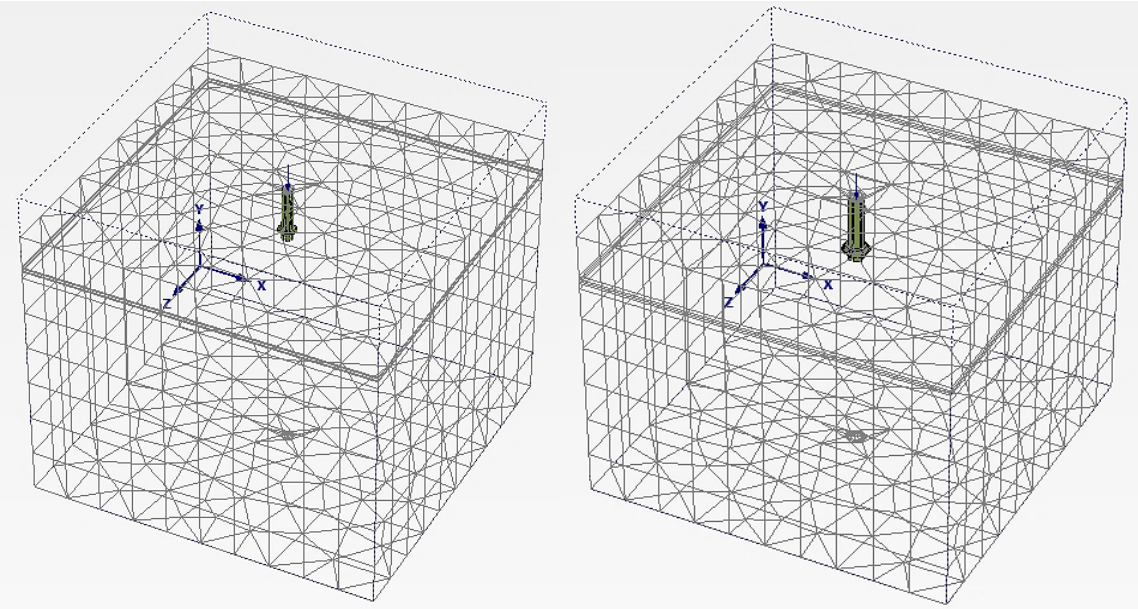

a) Under-reamed pile diameter 600mm b) Under-reamed pile diameter 900mm

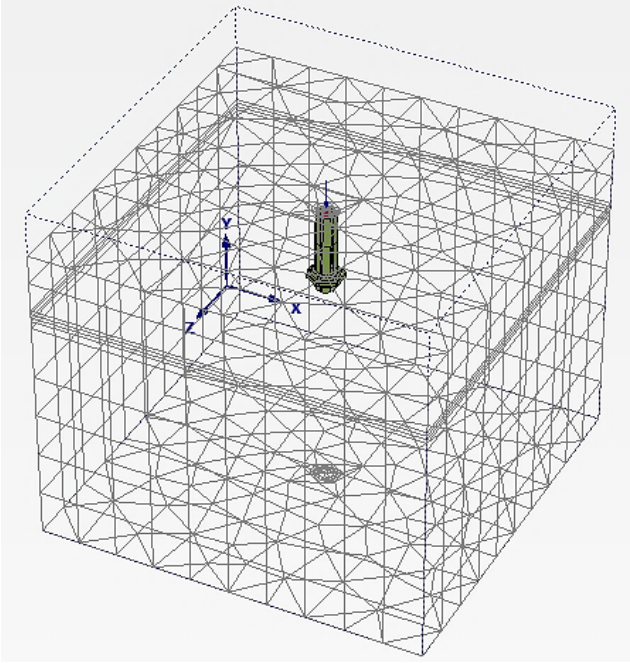

b) Under-reamed pile diameter 1200mm

Appendix 7-Soil Young's Modulus Used in PLAXIS 3D Foundation